A Reproduced Copy

OF

Reproduced for NASA

by the

NASA Scientific and Technical Information Facility

5

CR-128937

(NASA-CR-128937) A STUDY OF SPACE SHUTTLE ENERGY MANAGEMENT, APPROACH AND LANDING ANALYSIS Final Report (Intermetrics, Inc.) 166 p HC $10.50 CSCL 22A G3/30

N73-24830

Unclas

04306

INTERMETRICS

A STUDY OF SPACE SHUTTLE ENERGY MANAGEMENT, APPROACH AND LANDING ANALYSIS

by

Raymond Morth

Final Report

9 April 1973

Prepared for:

NASA Manned Spacecraft Center
Houston Texas

Under Contract NAS9-12578

INTERMETRICS INCORPORATED · 701 CONCORD AVENUE · CAMBRIDGE, MASSACHUSETTS 02138 · (617) 661-1840

FOREWORD

This report has been prepared for NASA Manned Spacecraft Center under Contract NAS9-12578. The technical monitor of this effort has been Claude A Graves of the MSC Mission Planning and Analysis Division.

The principal investigator for this effort has been Raymond Morth. Neal Carlson, Richard Ku, and William Widnall consulted on the navigation study.

INTERMETRICS INCORPORATED • 701 CONCORD AVENUE • CAMBRIDGE, MASSACHUSETTS 02138 • (617) 661-1840

CONTENTS

INTERMETRICS INCORPORATED • 701 CONCORD AVENUE • CAMBRIDGE, MASSACHUSETTS 02138 • (617) 661-1840

CHAPTER 1

INTRODUCTION AND SUMMARY

1.1 Study Objectives

This report is concerned with the steering of the Shuttle vehicle in the final several hundred miles prior to landing. The steering starts just prior to the transition maneuver from high to low angle-of-attack and ends with the touch-down of the vehicle on the landing strip.

The objective of this study is to extend and complete the analytic design that was made as part of the Phase B effort [1]. Here simple formulae were used to represent the vehicle performance characteristics. These formulae were used in a guidance scheme that is characterised by a spiral turn to dissipate the excess potential energy (altitude) prior to a standard straight-in final approach That study was fairly complete but several issues that were not resolved due to lack of time are the subject of this report.

Most important of these improvements and extensions are:

1. Tailor the steering with a view to pilot desires and capabilities
2. Add a flare maneuver logic
3. Design steering logic for transition phase
4. Incorporate phugoid damping
5. Decouple the center-of-curvature control from ranging control
6. Incorporate the use of drag brakes

As a second part of this study, this improved logic is to be used to define targeting procedures for the nominal Shuttle trajectory.

Thirdly, the logic is to be stressed by both variation in key parameters and by realistic system errors. These include:

1. Aerodynamic parameters

2. Atmospheric variations

3. Winds (both steady and gusts)

4. Initial condition variations

The error performance is to be characteristic of a navigation system which includes an inertial measurement unit and an on-board navigation computer. This on-board system is to be updated by both conventional landing aids, i.e.,

1. barometric and radar altimeters

2. VOR and DME of a TACAN type system

3. ILS system, both glide slope and localizer

and also precision DME equipment as characterized by the Cubic CR 100.

1.2 Key Design Considerations

Several design considerations were listed at the start of the study. They are for the most part met naturally by the analytic nature of the guidance design. These considerations as numerated by the contract monitor are:

1. Must be capable of using all the vehicle ranging ability

2. Compatible with manual procedures

3. Compatible with ground control procedures and monitoring

4. Capable of converging in final approach target

5. Maintain an energy reserve for the nominal case

6. Maintain the ability to compensate for winds

7. Use minimum navigation aids in contingency cases.

8. Targeting flexible to permit landing at alternate runways

9. Capable of performing category III landings

10. Maintain subsonic velocities

11. Constrained to alleviate over-pressure during transitions

1.3 Background, Other Design Approaches

There have been a large number of guidance schemes proposed for approach and landing phase of the Space Shuttle, and for all other guidance phases for that matter. In fact, there are so many that it will be difficult to select the primary system from all the candidates. On the other hand, this decision may not be too difficult because all the guidance schemes "work" and any one that is used will do the job. It is only in the way the different schemes will handle the many contraints and adapt to system errors that one system may show superior performance over the others.

The many schemes are roughly divided into two categories; non-turning and turning approach patterns. The Bell system [2] is characterized by a single turn on to final approach. Detailed calculations based on poorly defined system parameters are characteristic of this system. The Draper Lab [3] defines a system with no turns relying on drag brakes to dissipate the excess energy. If the drag brakes do not have sufficient power such a mode is not possible. But direct control of the kinetic plus potential energy as proposed in this system seems to have some merit, particularly in the presence of large disturbing winds.

The turning approach can further be divided into three categories. There is a two-turn or so called "racetrack" system as proposed by several investigators at MSC [4,5]. Here there is a turn on to a down-wind leg away from the runway until sufficient altitude is lost so that the second turn on to final approach is appropriate. Then there is the so called cone cylinder approach of MACDAC [6], in which the vehicle dissipates the energy by first flying about a large radius circle, then at the appropriate time changes the flight to a small circle tangent to the final approach path.

Finally, there is the spiral descent path which is the subject of this report and also of earlier work by Sperry Rand [7]. The difference in the two spiral guidance techniques is that this approach is characterized by simple analytic formulae which are used to represent the vehicle characteristics and the guidance loop is then closed using these formulae. It is of interest to note

that the first flight tests of the Sperry Rand system look very similar to the two-turn system [8]. It is also significant to note that this system has demonstrated automatic landings to touchdown on a real aircraft (a CV 990 modified to fly like the Space Shuttle) using real equipment (an inertial measurement unit (IMU), an airborne computer, a radar altimeter, and other conventional landing aids).

In the original work for this study [1], the North American vehicle had a much lower wing loading. With the resultant lower velocity at altitude, sometimes up to 5 turns would be required. Here, as with similar studies on the Grumman Phase B vehicle, no more than two turns is observed and it is usually one. But should this capability return (it never does as projects evolve) the present logic as developed in this report will call for a many turn spiral approach.

1.4 Importance of Analytic Approach

This system has as its central feature a turn capability prediction based on a simple analytic formula. That is, based on the present state of the vehicle and an estimate of the vehicle lift-to-drag ratio, L/D, a turn capability of say 2 1/2 revolutions is predicted at the start of circling flight. The guidance will then choose a commanded bank angle based on the nominal value such that desired number of, say two, revolutions result; and this computation is repeated every cycle. Subsequent analysis will show quite close agreement between the actual and predicted turn capability.

This analytic type approach is important for several reasons. First, a natural type trajectory results. That is, the vehicle is not commanded into any extreme maneuvers by the very fact that the guidance is based on its predicted capability. Second, the simple nature of this approach allows a flexibility to adapt to changing constraints that always appear as the program matures. This is particularly important in the early stages of the program. Third, the simple nature of the program accelerates the check-out and debugging time and also does not over-tax the airborne computer storage or duty cycle. This last feature is of course quite secondary in view of the vast computer capability proposed for the Space Shuttle.

It will be demonstrated in section 4 the analytic techniques are possible for both the transition and flare maneuvers as well as the energy dissipating turn. Further, it will be shown that several approach geometrics are possible with this analytic technique even though it was

primarily designed for circling flight.

1.5 Important Conclusions

The most important lesson that will be demonstrated in subsequent chapters is that simple analytic formulae will meet all mission requirements. Moreover, this type approach is highly desirable since new requirements can be easily adapted by the analytic nature as they may arise. The guidance permits ranging to all points within the vehicle capability. Since important disturbances such as winds are compensated directly, there is a high tolerance to disturbances.

Key vehicle parameters such as L/D need not be estimated in flight except perhaps for the final flare maneuver. Since this estimation is an easy task, there is little reason for not doing it.

The large initial navigation errors are resolved within the first few measurements and there is weak coupling between the navigation errors and the steering. However, large cross-track errors can lead to navigation filter divergence if measurements are not available to resolve these type difficulties. That is, there is a real danger of underspecifying the navigation equipment to the point of failing the mission.

CHAPTER 2

VEHICLE CHARACTERISTICS AND CAPABILITY

2.1 The 040a Vehicle

The Shuttle vehicle for this study is the 040a model which was the baseline model for many MSC studies in this period. The aerodynamic characteristics are defined in ref.[10]. The computer model based on this reference is found in Appendix D. Typical L/D values are shown in Figure 2.1 and more detailed characteristics (C_L C_D & L/D) for the subsonic flight are shown in Appendix F.

It is seen that the "clean" vehicle has a maximum L/D of 7.6 occurring at an angle-of-attack of 8 degrees. Note also that the speed brake has a profound effect decreasing the L/D almost in half when fully deflected.

The nominal vehicle has these other significant characteristics:

WT	140000 lb.
Ref Area	3130 ft^2
Mean Chord	51 ft.

The ground effect from ref. [10] is also simulated.

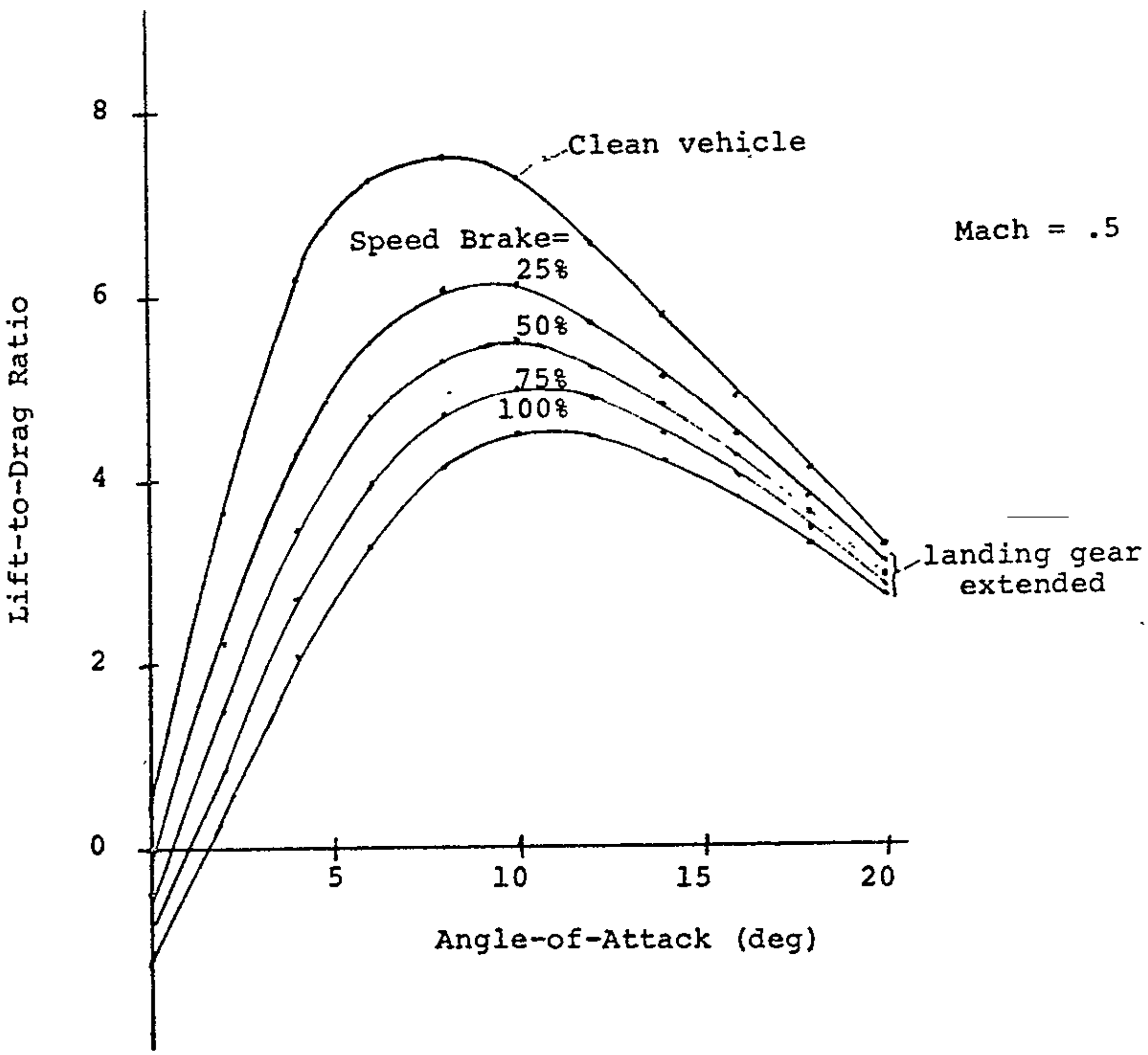

Fig. 2.1: 040a L/D Characteristics at Mach .5

2.2 Footprints

The subsonic ranging capability has been defined in Ref. [1]. This capability is shown in the form of the footprints in Fig. 2.2. Here are shown range capability for a vehicle with L/D=8, starting at various initial altitudes. The negative down range direction is smaller because two 180 degree turns are required to attain this point. The first changes the heading to the negative direction. The second changes the heading back to aline with the runway direction. It is seen that near 80 nm are possible in the forward direction, with 50 nm in the negative direction if one starts at a nominal 60,000 ft.

The supersonic ranging capability is considerably less because the maximum L/D is only 2. That is to say variations in range are less pronounced because there is less possible variation in L/D. It is of interest that the glide slope is not even close to $1/(\frac{L}{D})$ at this low L/D. The altitude rate can be found by using the results of Appendix A by first noting that $\frac{V^2\beta}{2g}$ is much greater than 1 in Eq. (A.13) so that assuming $\phi = 0$, we have

$$\frac{dV}{dt} \approx - \frac{g}{(\frac{L}{D})} \qquad (2.1)$$

Then Eq. (A.4) gives for $\frac{dH}{dt}$

$$\frac{dH}{dt} = - \frac{2g}{(\frac{L}{D})V\beta} \qquad (2.2)$$

Altitude rate thus varies from -120 fps when V = 6000 fps to -720 fps when V = 1000 fps.

The constant deceleration Eq. (2.1) of about 1/2 g is appropriate to generate the supersonic range as has been done in the transition ranging logic (Section 3.2, Eq. 3.2). Applying Eq. (2.1) into Eq. (3.2), gives a maximum range of 180 nm for the supersonic phase, assuming an $\frac{L}{D}$ of 2.

No supersonic footprints have been generated here. This footprint capability is rather shown in the performance data of Section 4.3, where the guidance achieves edges of the footprint by flying at maximum L/D.

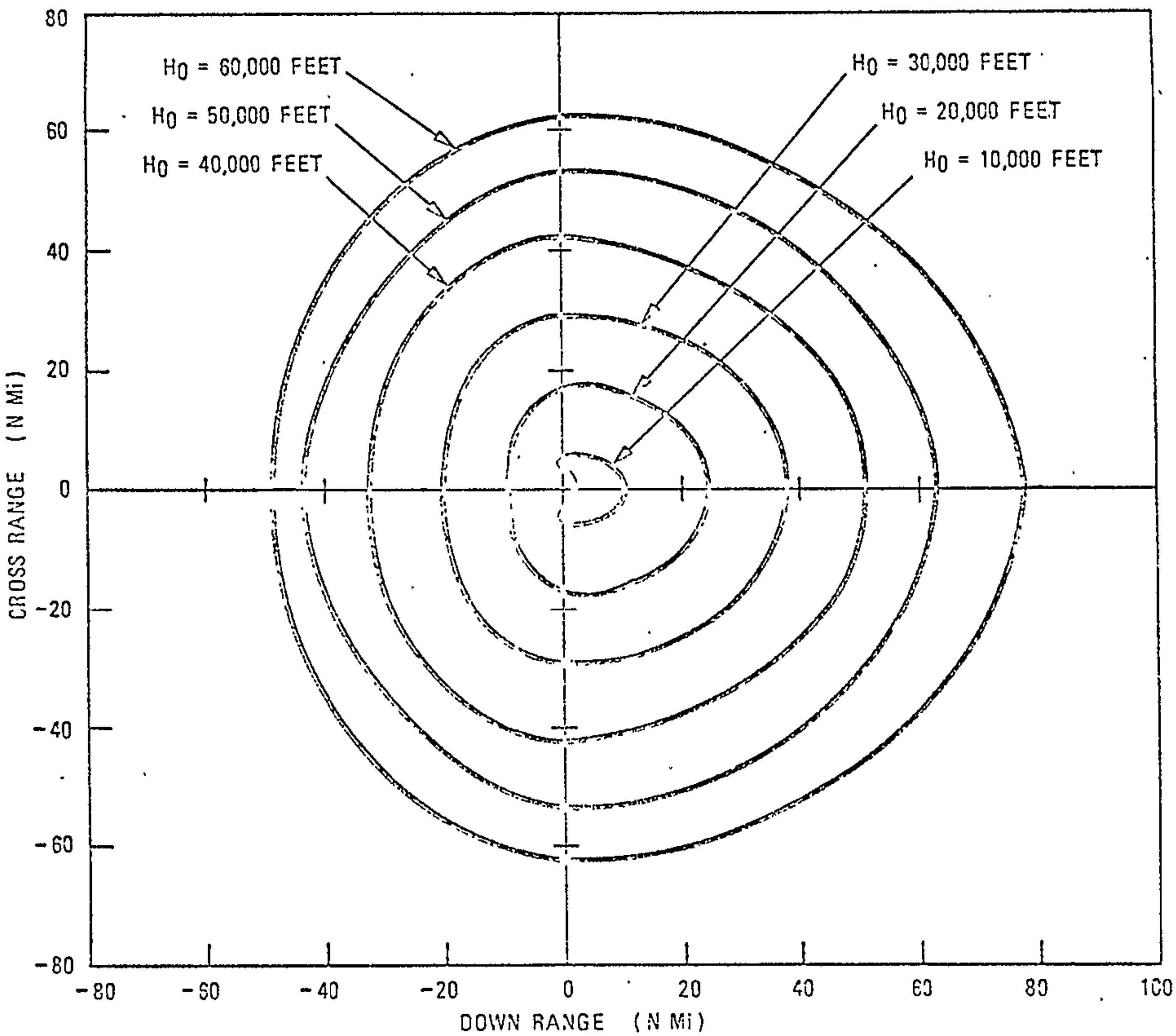

Fig. 2.2: Subsonic Range Capability of Shuttle Orbiter (L/D=8)

CHAPTER 3

GUIDANCE DESIGN

3.1 Guidance Phases

The guidance designed here was essentially completed as part of the Phase B effort [1]. Several improvements and additions were made since that time including transition logic, improved targeting, damping terms added and flare logic. Also, a major effort was made in testing the guidance in a realistic navigation environment. For sake of completeness, the total guidance logic is described here.

The trajectory starts at about 150,000 feet with the vehicle at Mach 6, having just emerged from radio blackout. There is then a transition maneuver from high angle-of-attack of 30 degrees to a low value of about 8 degrees. During this transition maneuver, there is some ranging also performed though only a limited amount is possible. Next there is a glide to the pre aim-point before the runway, performed at maximum L/D. Circling flight is next initiated with one or two revolutions possible. The next phase is the final approach starting at 10,000 feet altitude and ten miles before the runway threshold. A first flare maneuver starts at roughly 700 feet altitude to reduce the glide slope from 10 to 3 degrees. Finally, a second flare is initiated at about 50 feet altitude to reduce to sink rate to a nominal 4 feet/sec.

3.2 Transition Logic

There are two functions accomplished during the transition phase: 1) a change in angle-of-attack, 2) ranging to an aim point near the landing site.

The change in angle-of-attack can be accomplished with a pitch over rate of between .05 and .2 deg/sec without either exceeding the g limits on one hand and not accomplishing the maneuver in time on the other. There is therefore, established a velocity at which to start the maneuver, designated VLM2. There after, the angle-of-attack is commanded as a function of velocity by:

$$\alpha = \alpha_o - \mathrm{KTR}\ (\mathrm{VLM2} - \mathrm{VA}) \qquad (3.1)$$

where

α = angle-of-attack

α_o = initial value

KTR = Pitch over gain nominally .0075

VA = velocity relative to the ground

The ranging portion of the transition maneuver is targeted to a point 30 nm before the runway with an arrival velocity of 1000 ft/sec. This point is roughly centered within the remaining ranging capability of the vehicle. The roll angle is commanded to accomplish this ranging by first calculating a nominal range based on an assumed constant rate of change of velocity. This constant deceleration has been observed over a large class of transition maneuvers and leads to a simple range calculation:

$$RTOGON = (VA^2 - VF^2)/2ACTR \tag{3.2}$$

where

RTOGON = nominal range

VF = final velocity = 1000 fps

ACTR = nominal deceleration

= 15 ft/sec^2

The roll angle is then commanded by

$$\phi = \cos^{-1} (RTOGO/RTOGON) \tag{3.3}$$

where

RTOGO = range to initial target from Eq. (3.6)

ϕ = commanded magnitude of roll angle

The roll command is modified with a lateral logic which will allow only one roll reversal and turn-rate limiter which limits the azimuth rate so as not to aggravate the effect on the sonic over pressure ("sonic boom"). The roll angle is initially commanded in the direction so as to decrease the heading error. (Or it would be initially commanded in the same direction as in the previous entry guidance phase). This roll direction is maintained until the heading error, DEL, exceeds a threshold value, DELTR. Then, the opposite direction of roll is commanded.

The turn rate limiting is not started until velocity is less than 3000 fps, (VLM3). Excessive turn rates are not possible at higher velocities. At this time, the turn rate at nominal roll angle is calculated by:

$$\Omega = g \tan(\frac{RLB}{VA}) \tag{3.4}$$

where

$$\Omega = \text{turn rate}$$
$$RLB = \text{nominal bank angle}$$
$$g = 32.2 \text{ ft/sec}^2$$

If the turn rate exceeds the limit value, OMLM, the roll is commanded to achieve this limited value by:

$$\phi = \tan^{-1} \left(\frac{OMLM\ VA}{g}\right) \tag{3.5}$$

Also, the roll angle is commanded to drive the heading angle to zero in the next interval if this is possible and no limits are exceeded.

3.3 Landing Pattern Targeting

When the velocity is less than VLM1 (1200 fps), the start of the circling flight mode is initiated. An aim-point is selected to start the turning flight so as to arrive at the final approach with no lateral offset by the following two step procedure: First, the target vector, $\overline{URT}$, located at the edge of the landing field is projected backward a fixed bias distance, to $\overline{URT2}$. Figure 3-1 is appropriate. Ten miles has been selected for this bias distance in the initial studies. This bias corresponds to an altitude of 10,000 feet at the start of the final glide and a nominal L/D of 5 for the final glide. Then using the heading of the vehicle to this initial aim point, an offset aim point is calculated, see Figure 3-2. Two circles are calculated. The circle of radius R corresponds to circling flight at the velocity V_1 which is the arrival velocity at $\overline{URT2}$. The circle of radius r corresponds to circling flight at V_2, the equilibrium velocity at the final altitude, H_f. The calculation follows. First calculate the range from the vehicle to $\overline{URT2}$:

$$RTOGO = \cos^{-1} (\overline{UR}.\overline{URT2})SF \tag{3.6}$$

where

$RTOGO$ = range to offset target, feet

$\overline{UR}$ = unit vector at present position

$\overline{URT2}$ = initial target unit vector

SF = scale factor converting earth central angle to feet

Then calculating the altitude loss δH in this segment assuming flight at a known maximum L/D, $(L/D)_m$

$$\delta H = RTOGO/(L/D)_m \tag{3.7}$$

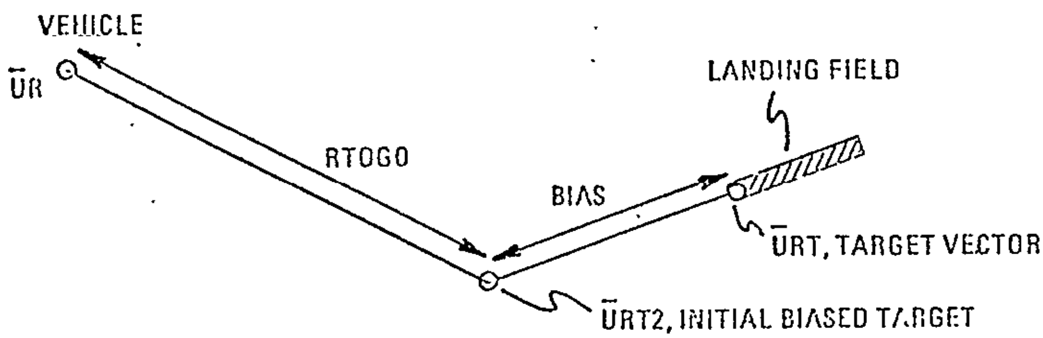

Fig. 3-1 Initial Target Calculation

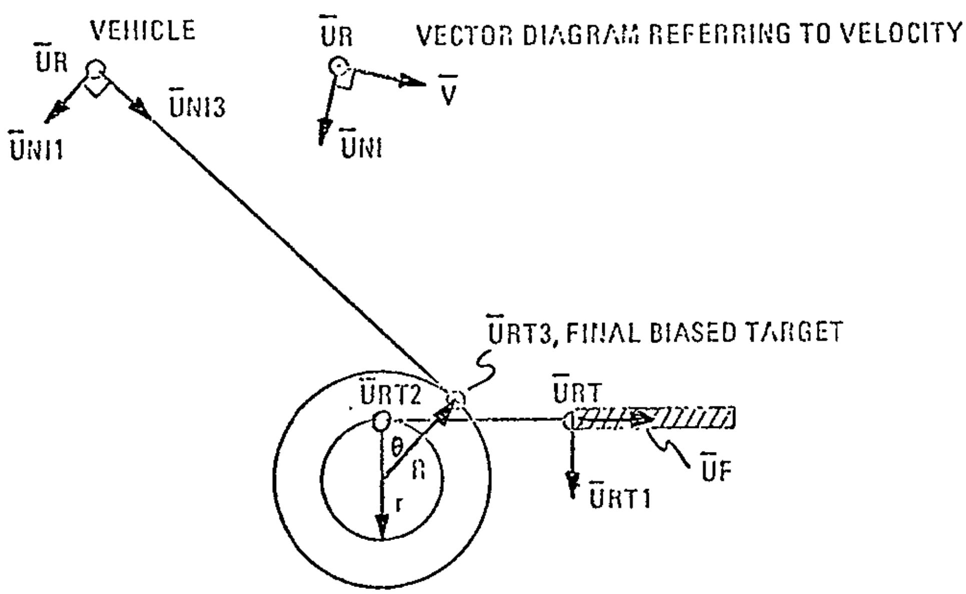

Fig. 3 -2 Final Target Calculation

The velocity at $\bar{U}RT2$, V_1, is then assuming equilibrium at both the initial and final points.

$$V_1 = VA1\ e^{-(\beta\ \delta H/2)} \tag{3.8}$$

where

$$VA1 = \text{present velocity corrected for roll angle}$$
$$= VA\sqrt{g/AMAG\ \cos\ (\phi)}$$
$$\beta = \text{reciprocal of atmospheric scale height}$$
$$= 1/25000$$
$$AMAG = \text{total acceleration, fpss}$$

Similarly the velocity at the start of the final glide, V_2, is related to the altitude at the start of final glide, H_f, by

$$V_2 = VA1\ e^{-\ \beta(H-H_f)/2} \tag{3.9}$$

The initial and final turn radii (R,r) are then calculated using the commanded bank angle ϕ.

$$R = V_1{}^2/(g\ \tan\ \phi\ ) \tag{3.10}$$

$$r = V_2{}^2/(g\ \tan\ \phi\ ) \tag{3.11}$$

where

$$g = \text{gravitational acceleration} = 32.2\ \text{ft/sec}^2$$
$$\phi = \phi n \text{ initially, then defined by Eq. (3.22)}$$
$$\phi_n = \text{nominal bank angle, 30 deg.}$$

The final offset vector is then seen to be

$$\bar{U}RT3 = \bar{U}RT2 + (\frac{r-R\ \cos\ \theta}{RE})\ \bar{U}RT1 + \frac{R\ \sin\ \theta}{RE}\ \bar{U}F \tag{3.12}$$

where

$$\bar{U}RT3 = \text{final offset unit target vector}$$
$$\bar{U}RT1 = \bar{U}F \times \bar{U}RT$$
$$\bar{U}RT = \text{unit target vector at edge of runway}$$
$$\bar{U}F = \text{unit vector in direction of runway}$$

The radius of the earth, RE, is used to convert the offset distance into angles. The angle θ is not calculated explicitly, but the cosine and sine of θ are calculated by the vector relations

$$\cos\ \theta = \bar{U}NI1 \cdot \bar{U}RT1 \tag{3.13}$$

$$\sin\ \theta = -\sqrt{1 - \cos^2\ \theta}\ \text{SIGN}(\bar{U}NI1 \cdot \bar{U}F) \tag{3.14}$$

where

$$\overline{UNI1} = UNIT(\overline{URT2} \times \overline{UR}), \text{ for initial calculation;}$$
$$= UNIT(\overline{URT3} \times \overline{UR}), \text{ subsequently}$$

The appropriate vectors are shown in Figure 3-1 and SIGN is the sign function.

The above calculations are used for the initial calculation of the offset target vector, $\overline{URT3}$. A precise calculation would involve an iteration since the target vector is a function of the range-to-go, which is in turn a function of the target vector. This iteration is avoided by repeating the calculation of the offset target vector on subsequent guidance cycles replacing $\overline{URT2}$ with $\overline{URT3}$ in Eq. (3.6). The offset target calculation stops when the heading error, Del, is less than .01 radians.

3.4 Initial Turn

The initial turn is accomplished by banking at the nominal bank angle to drive the heading error toward zero until a calculated reduced bank angle will drive the error to zero in the next time interval.

The heading error Del is

$$Del = \cos^{-1} (\overline{UNI1} \cdot \overline{UNI}) \tag{3.15}$$

where

$$\overline{UNI} = UNIT (\overline{V} \times \overline{UR})$$

The bank angle command is

$$\phi = \phi n \; SIGN(\overline{UNI3} \cdot \overline{UNI})^{*} \tag{3.16}$$

where

$$\overline{UNI3} = \overline{UR} \times \overline{UNI1}$$

If Ωdt is less than DEL, the turning rate Ω is calculated by

$$\Omega = g \tan \phi n / V \tag{3.17}$$

and dt is the sampling interval. Five seconds are used in the simulations.

If Ωdt is greater than Del, the bank angle is commanded by

$$\phi = \tan^{-1} \left(\frac{Del \; V}{g \; dt}\right) SIGN(\overline{UNI3} \cdot \overline{UNI}) \tag{3.18}$$

* Note that positive bank directs a component of lift along $\overline{UNI}$.

Throughout the initial heading change the angle-of-attack is kept fixed near the value for maximum L/D.

The above steering logic neglects the dynamic response of the vehicle to the roll commands and no dynamic lag has been included in the simulations thus far. It is expected that the "dead beat" response described above can be extended to include these dynamics and would be superior to a constant gain feedback system type design. This is because more information is available on the vehicle characteristics and the implementation is more suited to the digital computer needed for guidance and navigation calculations.

3.5 Glide to First Aim Point

The glide to the pre-aim point is accomplished at maximum L/D. During this interval a calculation is made of the turn to lose altitude required during Phase 3. This turn angle is

$$D\theta = (L/D)_m \sin \phi n \; g \; HS\left(\frac{1}{V_2^2} - \frac{1}{V_1^2}\right)RTD + (L/D)_m \sin \phi n \; (H-H_f)RTD/2HS \tag{3.20}$$

This result is derived in Appendix A. Somewhere between 1 and 2 revolutions will be required depending on the range to the pre-aim point.

The next phase is entered when the vehicle arrives at $\overline{URT3}$. This is detected when the dot product, $\overline{UNI1} \cdot \overline{UNI}$, is negative.

3.6 Circling Descent

3.6.1 Turn Angle Control

The nominal circling descent is at constant bank angle ϕn. This angle has been set to 30 degrees for initial studies. The turn angle is calculated using Eq. (3.20) with V used in place of V1. The required turn angle is then calculated as

$$D\theta 1 = n\ 360 + Daz \tag{3.21}$$

where

$$Daz = Az - Azr$$

$$Az = \text{Azimuth} = \cos^{-1}(\overline{UE} \cdot \overline{UNI})RTD$$

if $\overline{V} \cdot \overline{UE}$ is negative, $Az = 360 - Az$

Azr = Azimuth of runway

n, chosen so that $|D\theta - D\theta 1| < 180$

RTD = factor to convert radians to degrees

$\overline{UE}$ = unit vector in easterly direction

An option to the logic allows n to be an input variable if desired. With this option, one can select the desired number of turns but only, of course, before the actual turn has started.

The number of revolutions, n, is further modified so that the value of Dθ1 does not differ by more than the 180 degrees from that of the previous computation cycle. Without this feature, an induced oscillation is possible as the desired turn angle changes back and forth to values near ± 180 degrees from the predicted turn angle. The bank angle is then

$$\phi = \sin^{-1}\left(\frac{D\theta 1}{D\theta} \sin \phi n\right) \qquad (3.22)$$

and the bank angle is limited to values less than ϕ_{max}, now chosen at 45°.

Thus, we see that the bank angle is continually adjusted so that the heading is the correct value at the final altitude. The initial targeting assured that the position relative to the runway is correct when this final heading is achieved.

A further modification of the turn logic allows for straight flight segment when the desired turn angle is 180 degrees. This logic is normally disabled because improved initial targeting does not require it. But it is included here to allow trajectory shaping as has been done in Chapter 4. This is done so that the predicted turn angle can decrease to the desired value. For example, the situation could arise where the desired turn angle was 180 degrees and the predicted turn angle, 360°. In this case the commanded bank angle would be 14.5 degrees and a much larger than nominal turn radius would result. The altitude loss during this straight flight segment is added to the final altitude, H_f. This is done to allow for the additional range needed in the final phase. Typically, one or two nautical miles will be flown in the straight-flight portion and correspondingly about 1,000 feet will be added to the final approach altitude, H_f. In this situation, however, the improved targeting would allow a 14.5 bank angle turn and no straight segment would be required.

3.6.2 Trajectory Damping

In the transition, the turn and the glide to the initial aim point, the phugoid motion is damped by commanding an incremental angle-of-attack.

$$D\alpha = KDMP\ (\dot{R}ref-\dot{R})$$

where

$D\alpha$ = incremental angle-of-attack

KDMP = constant damping gain

$\dot{R}$ = altitude rate

$\dot{R}ref$ = reference altitude rate

= - 250 fps in transition

= $-VA/(L/D)_m$, before turn

= $-VA/((L/D)_m \cos\phi)$, during turn

The angle-of-attack is further modified to anticipate the transient caused by changing angle-of-attack commands by

$$\alpha = \alpha\,\frac{(\cos\phi)_o}{\cos\phi}$$

where

$(\cos\phi)_o$ = $\cos\phi$ from last computation cycle

3.7 Center of Curvature Control

To make a positive control of position relative to the landing field during the turn, logic is written to control a specified center of curvature. This logic would be appropriate for the case of disturbances such as wind, improper navigation and unknown vehicle variations since the initial targeting assured proper positioning in the no disturbance case. The logic adds an incremental roll angle to the commanded roll angle so as to decrease distance between the instantaneous and desired center of curvature. Referring to Figure 3-3 a unit vector at the desired center of curvature, $\overline{U}c$, is described by

$$\overline{U}c = \text{UNIT}(\overline{U}RT2 + \frac{r}{RE}\,\overline{U}RT1) \qquad (3.23)$$

where r is defined by eq. (3.6).

The instantaneous center of curvature, $\overline{U}c1$, assumes turn at nominal bank angle

$$\overline{U}c1 = \text{UNIT}(\overline{U}R + \frac{R1}{RE}\,\overline{U}NI) \qquad (3.24)$$

where

$$R1 = V^2/(g\tan\phi)$$

The distance, Delc, between the desired and instantaneous centers of curvature is then

$$\text{Delc} = \cos^{-1}(\bar{U}c \cdot \bar{U}c1)\text{SF} \qquad (3.25)$$

The incremental roll angle, DRL, driving $\bar{U}c1$ toward $\bar{U}c$ is commanded by

$$\text{DRL} = -\text{KCN Delc SIGN (CTEST)} \qquad (3.26)$$

where

$$\text{KCN} = \text{constant gain} = .0003$$

$$\text{CTEST} = \bar{U}NI \cdot \bar{U}c2$$

$$\bar{U}c2 = \text{UNIT}(\bar{U}c \times \bar{U}c1)$$

$$= \text{normal to plane containing } \bar{U}c \text{ and } \bar{U}c1$$

Note that this incremental roll angle has the effect of increasing the turn radius if $\bar{U}c$ is ahead of $\bar{U}c1$ (As in Figure 3-3), and decreasing the turn radius of $\bar{U}c$ is behind $\bar{U}c1$. In both cases, the instantaneous center is driven toward the desired center.

3.8 Final Glide

The final glide starts when the indicated altitude is less than H_f. At this point the target is repositioned at the edge of the runway, at $\bar{U}RT$. Heading corrections are then made with logic identical to Eqs. (3.10, 3.11, 3.12) replacing only $\bar{U}RT3$ with $\bar{U}RT$.

An "s-turn" logic is exercied so that the lateral position as well as the heading is controlled. The lateral displacement accrued, d, in correcting the heading error is calculated by

$$d = 2 \text{ Rl} \sin^2\left(\frac{\text{Del}}{2}\right) \text{ SIGN (VLAT)} \qquad (3.27)$$

where

$$\text{Rl} = \text{turn radius at nominal bank angle}$$

$$= V^2/(g \tan \phi n)$$

$$d = \text{lateral displacement during turn (positive if along } \bar{U}RT1)$$

$$\text{VLAT} = \bar{V} \cdot \bar{U}RT1$$

The lateral error, Dl, is calculated by

$$\text{Dl} = (\bar{U}R \cdot \bar{U}RT1)\text{SF} \qquad (3.28)$$

If the total lateral error, Dl + d, is greater than a threshold value, the heading error is modified by

$$\text{Del} = \text{Del} - \text{Del}_3 \text{ SIGN}(d) \qquad (3.29)$$

where

Del_3 = 45 degrees nominally, but is varied by Eq. (3.32) to account for long range cases.

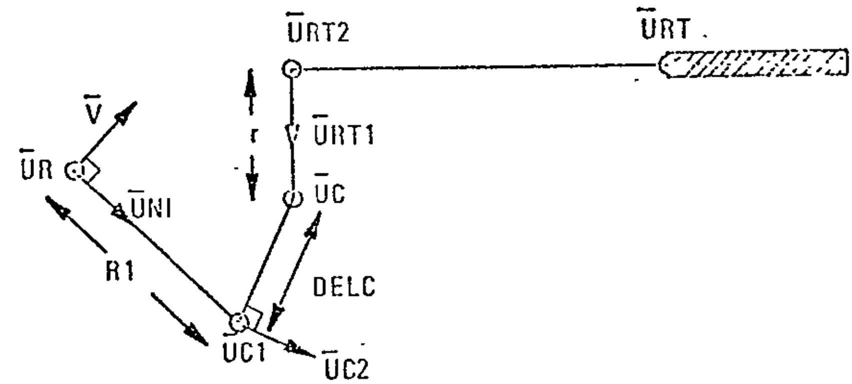

Fig. 3-3 Geometry for Center of Curvature Control

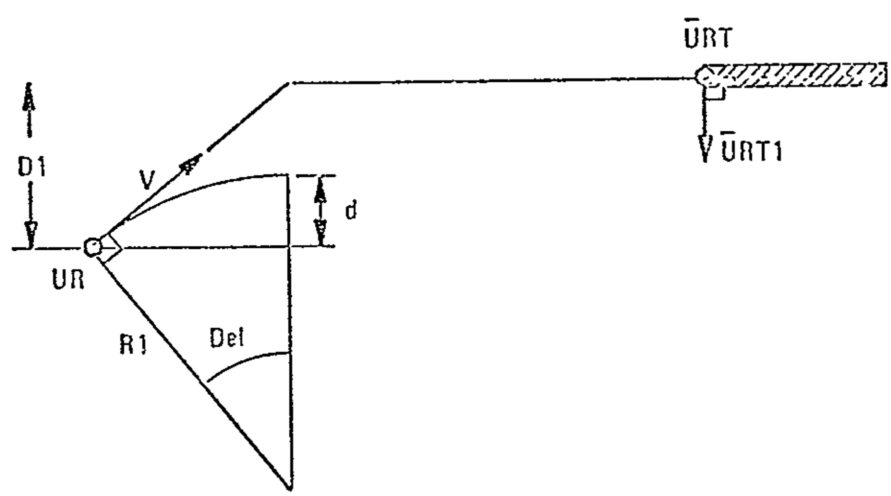

Fig. 3-4 Geometry for "s-turn" Logic

This logic has the effect of heading so as to close the lateral error and then reversing the bank angle to correct the heading error at a time when the lateral error will be zero when the heading is correct. Only one "s turn" is allowed in final glide. A standard linear feedback control on heading error and lateral displacement is then initiated after the initial "s-turn."

The law commands the bank angle by terms proportional to the lateral displacement and lateral velocity

$$\phi = \text{KDD D1} + \text{KVV VLAT} \tag{3.30}$$

where

KDD = -.07 = position gain

KVV = -.36 = damping gain

The gains have been chosen to provide a closed loop natural frequency of one minute and a damping ratio of .7.

At this point the angle-of-attack is modulated so that flight path intersects $\bar{\text{U}}$RT. This logic will be made with modulation on the "front-side" of the L/D curve. The angle of attack is commanded by the following equation:

$$\alpha = \alpha_o + \frac{K(L/D_c - L/D_o)}{\partial(L/D)/\partial\alpha} + \text{KDMP (Rref-R)} \tag{3.31}$$

where

α_o = 6 degrees

L/D_o = 5

$\partial(L/D)\partial\alpha$ = 1.4 deg^{-1}

K = 2

α is limited between 4 and 15 degrees

L/D_c = (RTOGO-BIAS1 6080)/H

Bias1 = Bias on final phase range = 1.8 n.m.

$\dot{\text{R}}$ref = Reference altitude rate = -VA/(L/D).

KDMP = damping gain = .01

3.8.1 Variable Lead Angle in S-Turn

Should the range to the landing site be so long that no turn is possible, special logic is in order. Because the conditions can arise that one turn is too much and a striaght-in approach is too little, an overshoot may result. In this case, the final phase is entered directly

if the predicted turn angle is less than 180 degrees, and the excess energy between one half turn and straight-in is dissipated by varying the lead angle DTH1 in the s turn logic.

$$Del_3 = Del_{30} \left(1 - \frac{L/D_c - L/D_o}{2}\right) \qquad (3.32)$$

where

$$Del_{30} = .75 \text{ rad.}$$

3.8.2 Speed Brake Law

The Speed brake is needed mainly to decrease the reference L/D during the final approach while still retaining a reasonable lift coefficient. Refering to Fig. 2-1, we see that L/D of (the reference value) 5 for the clean vehicle is at a 3 degree angle-of-attack. This low angle-of-attack would result in a high velocity to maintain equilibrium because the lift coefficient is so low, while a speed brake deflection of 25% doubles the anlge-of-attack for the reference L/D of 5.

The speed brake is used primarily to control velocity by defining a reference velocity as a function of altitude

$$VRSB = VR_o + KSBH\ H \qquad (3.33)$$

where

VR_o = reference velocity at zero altitude
= 425 fps

KSBH = speed brake gain = .003

The speed brake is then deflected to achieve this velocity by

$$SB = KSB(VA-VRSB) + SBO \qquad (3.34)$$

where

SB = speed deflection in per cent

KSB = speed brake gain = .5

SBO = bias setting = 20%

A limited amount of testing of an additional term to range with the speed brake showed little improvement and was discarded.

3.9 Flare Control

The flare maneuver is composed of two segments. The first flare reduces the flight path angle from about 10 to about 3 degrees. The second reduces the sink rate to a nominal 4 ft/sec. This logic commands a constant incremental normal acceleration to accomplish both flare maneuvers. The first flare is with an incremental g of nominally 0.3 g initiated so as to be completed at an altitutde of HF2 normally 600 feet. To do this, a threshold altitude is calculated at which to start the maneuver so as to be complete at HF2.

$$HTT = HF2 + (\dot{R}^2 - \dot{R}_2^{\,2})/2\ GF2 \qquad (3.35)$$

where

HTT = threshold altitude to start maneuver

$\dot{R}_2$ = final altitude rate = 18 fps

$GF2$ = incremental g = 10 fpss

$HF2$ = altitude at end of flare

When the altitude is less than HTT an incremental g is commanded by increasing the angle-of-attack

$$\alpha = \alpha \quad (GF1 + GS)/AMAG \qquad (3.36)$$

where

$$GF1 = (-\dot{R} + \dot{R}_2)/dt\text{, limited to } GF2$$

When H is less than the flare altitude, HF2, ranging is accomplished by commanding the altitude rate by

$$\dot{R}_2 = -\ VA\ H/(RTOGO - BIASFL) \qquad (3.37)$$

where

BIASFL = aim point before runway
= 2200 feet

Then angle-of-attack is commanded by Eq. (3.36).

The second flare is started when the altitude is less than the threshold value (HTT2 = 50 ft) and is accomplished by commanding angle-of-attack with Eq. (3.36) replacing the limit incremental g with GF3 = 6 fpss.

3.10 Left Hand Turn Logic

Originally, left hand turns were desired to possibly handle the long-range cases where no full turn was possible. But these possibilities were handled by the variable lead-angle logic of Section 3.7.1. However, other constraints may require this type turn so the modifications to the above logic are described here. There are four.

First, re-target the offset vector by modifying Eq. (3.12)

$$\overline{URT3} = \overline{URT2} - \left[\left(\frac{r - R\cos\theta}{RE}\right)\overline{URT1} + \frac{R\sin\theta}{RE}\,\overline{UF}\right] \qquad (3.12\ell)$$

Second, change the sign of the azimuth error

$$Daz = - (A_z - A_{zr}) \qquad (3.12\ell)$$

Third, command the opposite signs bank angle

$$\phi = - \sin^{-1}\left(\frac{D\theta 1}{D\theta}\right) \sin \phi n) \qquad (3.22\ell)$$

Finally, redefine the unit vector $\overline{Uc}$ by

$$\overline{Uc} = \text{UNIT}\left(\overline{URT2} - \frac{r}{RE}\overline{URT1}\right) \qquad (3.23\ell)$$

3.11 Concluding Remarks

The above guidance scheme can be found twice more in this report in increasing levels of detail. First, detailed flow graphs are presented in Appendix B. Second, a Fortran listing of this program is found in Appendix D.

CHAPTER 4

GUIDANCE PERFORMANCE

4.1 Nominal Case

The logic was tested with a variety of initial conditions and landing sites. The nominal trajectory is described first. This trajectory starts near 150,000 feet just prior to the transition maneuver. The landing site is chosen to be centered within the vehicle capability from this point. The vehicle initial state is summarized in Table 4-1.

V	= 6055 fps
H	= 143020 ft.
γ	= -1.9 deg
azimuth	= 45°
Mach	= 5.71
α	= 29°
latitude	= 0
longitude	= 0
Runway latitude	= 2.4 deg
Runway longitude	= 2.4 deg
Runway azimuth	= 75 deg

Table 4-1: Vehicle Initial State and Nominal Runway

The ground track for this trajctory is shown in Fig. 4.1. On this trajectory are shown tick marks for each minute of flight. Almost 17 1/2 minutes elapse (1040 sec). Shown also are the initial pre-aim, and the target for transition maneuver, as described in Section 3.2. The transition maneuver starts at about 90 seconds and ends at the six minute point. In this trajectory, a one-turn circling flight before the runway is performed.

An expanded view of the ground track and an elevation view of the last 10 minutes of flight are shown in Fig. 4.2. Shown here is the offset target and desired center of curvature.

In Fig. 4.3 are the altitude, velocity and altitude rate time histories. Altitude rate is seen to be about -250 feet/sec during the transition maneuver and shows small peaks at the start of both the turn and the final approach. Steps in altitude rate are also seen for each of the flare maneuvers. The altitude here shows a 2 Slope character: Steeper for the first 400 seconds due to the supersonic L/D or 2, and later shallower with the subsonic L/D of 7. The velocity decreases in a monotone fashion with the sharp decrease at 1000 seconds accompanying the flare maneuver.

The control variables in Fig. 4.4 show the roll angle, angle-of-attack and speed brake deflections. The roll angle shows the reversal at 150 seconds as part of the transition ranging. At 360 seconds there is an impulse of roll angle as the vehicle heads toward target 2. Circling flight begins at about 600 seconds with a near constant bank angle of 20 degrees. At 900 seconds the turn is complete and the final approach begins.

The angle-of-attack starts at 26 degrees (not 29) due to the phugoid damping which attempts to maintain an altitude rate of -250 ft/sec. At 90 seconds the pitch over is begun, though this is partially masked by the damper actions. The transition is complete at about 400 seconds arriving at an angle-of-attack of 7 degrees. The final approach shows an alpha of 6 1/2 degrees starting at about 900 seconds. Finally, the flare maneuvers show the double pulse character for the first and second flares and characteristic rise needed to maintain "equilibrium" as the vehicle slows down.

The speed brake shows a pulse to about 40% at the start of the final approach finally settling to a 20% deflection.

Not shown is the landing gear deflection which occurs at the start of the final approach.

The dynamic pressure in Fig. 4.5 is not constant during the turn as the turn angle prediction implicitly assumes. This is because of the model of the 040a vehicle which shows a slow decrease of C_L with Mach number. Dynamic pressure must therefore increase to maintain equilibrium. The characteric drop as seen in dynamic pressure at the end as the vehicle is pitched up on the flare maneuver.

The total acceleration, also in Fig. 4.5, does not stray far from the one g level. The peak is 1.25 g. The double pulse corresponding to the two flares is also seen in the acceleration trace as it was in the angle-of-attack trace.

The predicted and desired turn angles are shown in Fig. 4.6. It is seen that these two angles converge as driven by the 20 degree bank angle. A nonlinearity has been noted in the turn angle to bank angle. Namely, increasing the bank angle from the nominal 30 degree bank angle shows less of a change in turn angle than does decreasing the bank angle.

Details of the flare maneuver are seen in Fig. 4.6 showing altitude, altitude rate, velocity and angle-of-attack as a function of range-to-go to the landing site. The first flare shows an step in alpha of about 2 degrees lasting about 2 seconds. The second flare lasts only about 3 seconds. There is a characteristic drop in alpha just before touchdown as the ground-effect becomes effective.

The touch down velocity of 261 fps is low. This is made possible by using the ground effect which allows an early flare. This should probably be increased by delaying the first flare (decreasing HTT) and at the same time decreasing the bias on the final phase (BIAS1).

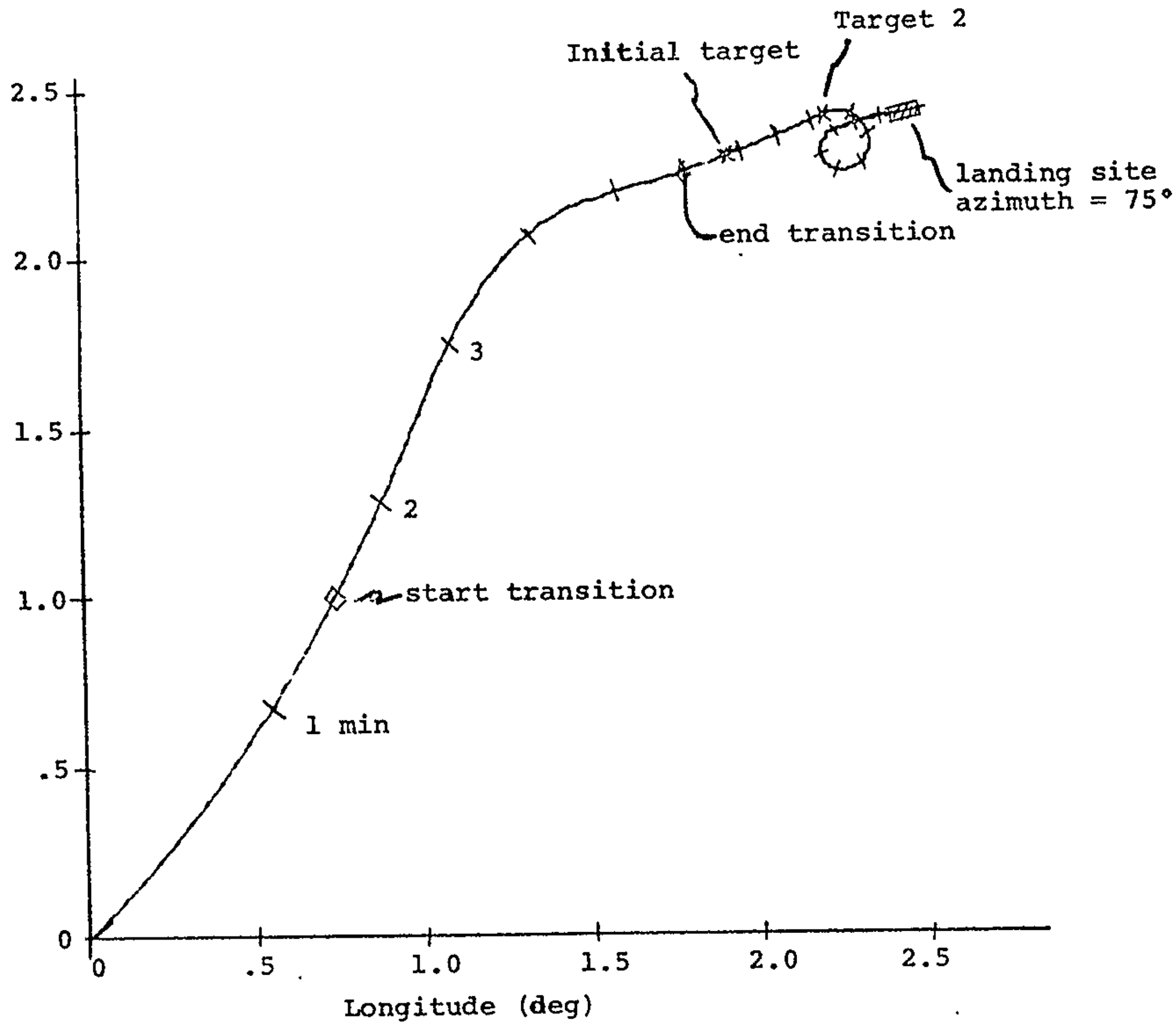

Fig. 4.1: Ground Track for Nominal Case

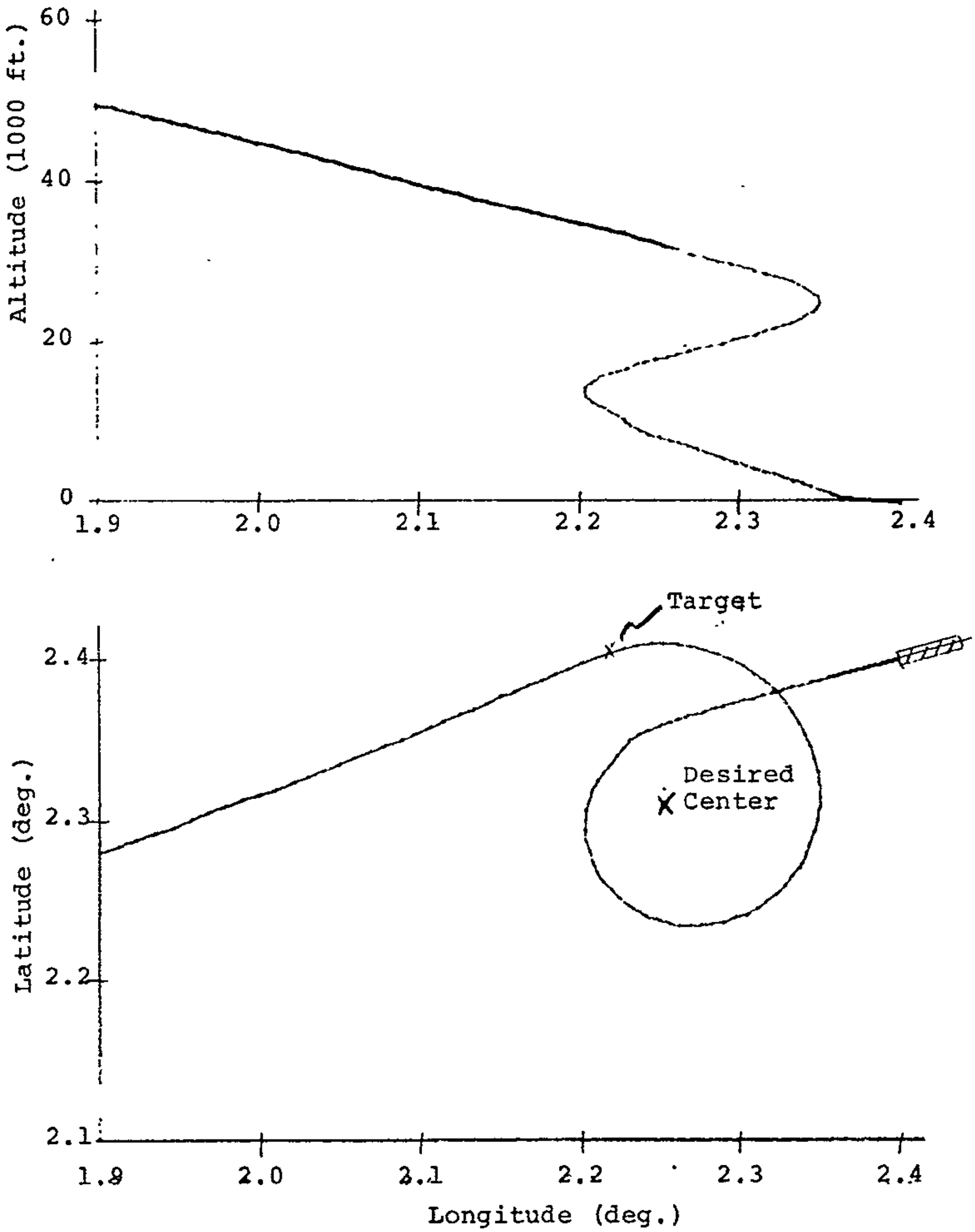

Fig. 4.2: Ground Track and Elevation Views for Nominal Case

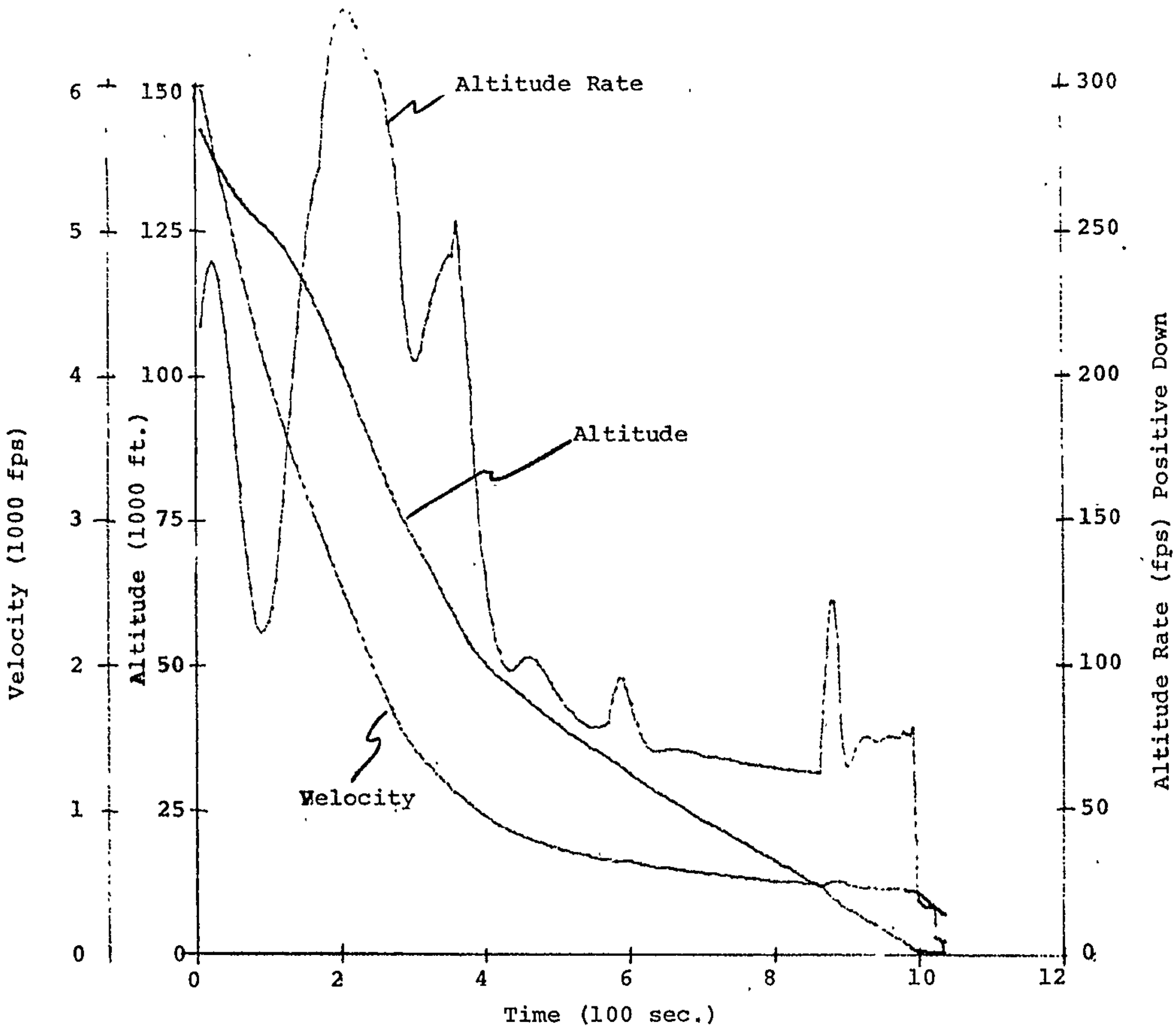

Fig. 4.3: Velocity, Altitude and Altitude Rate Time Histories for Nominal Case

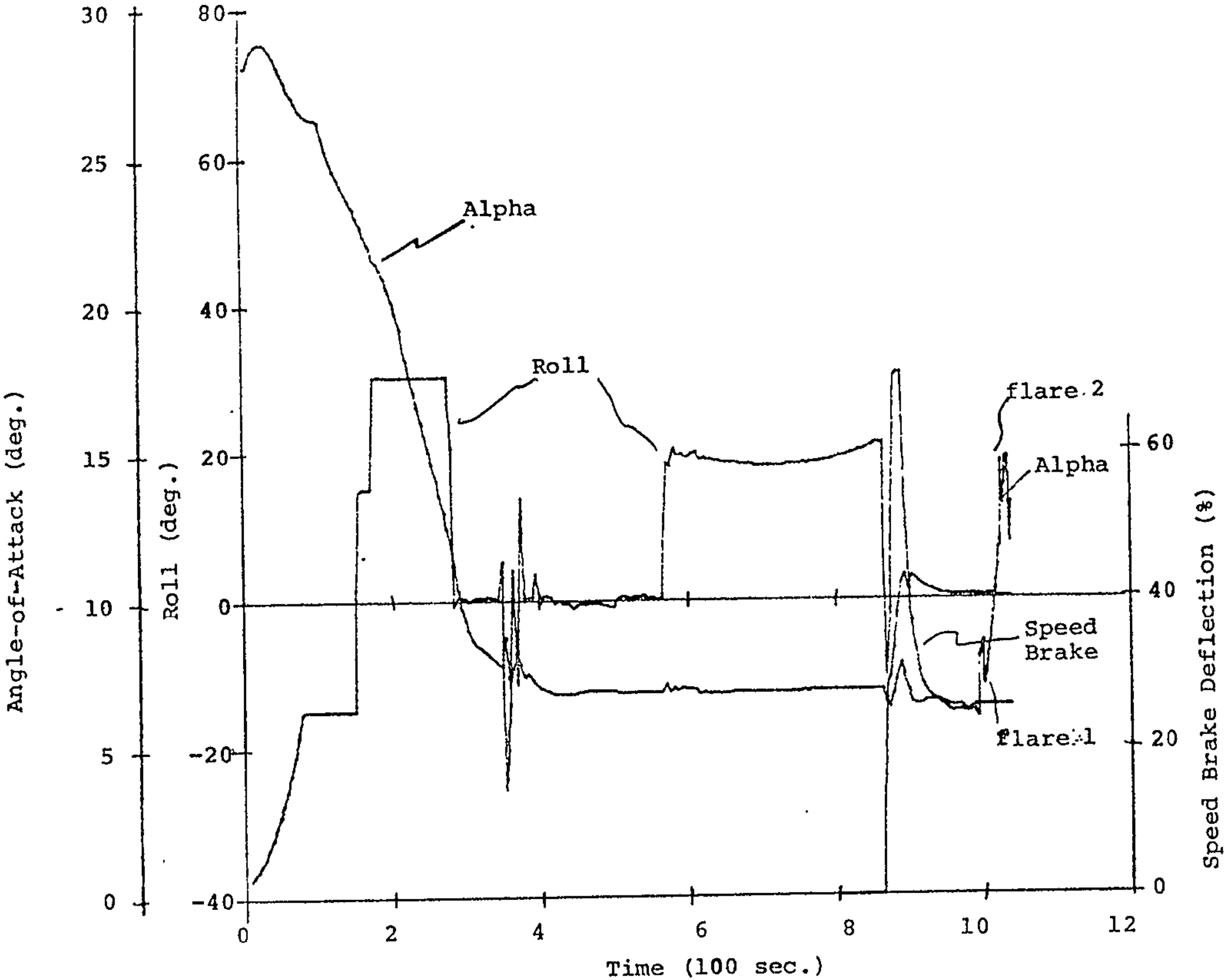

Fig. 4.4: Roll, Alpha and Speed Brake Time Histories for Nominal Case

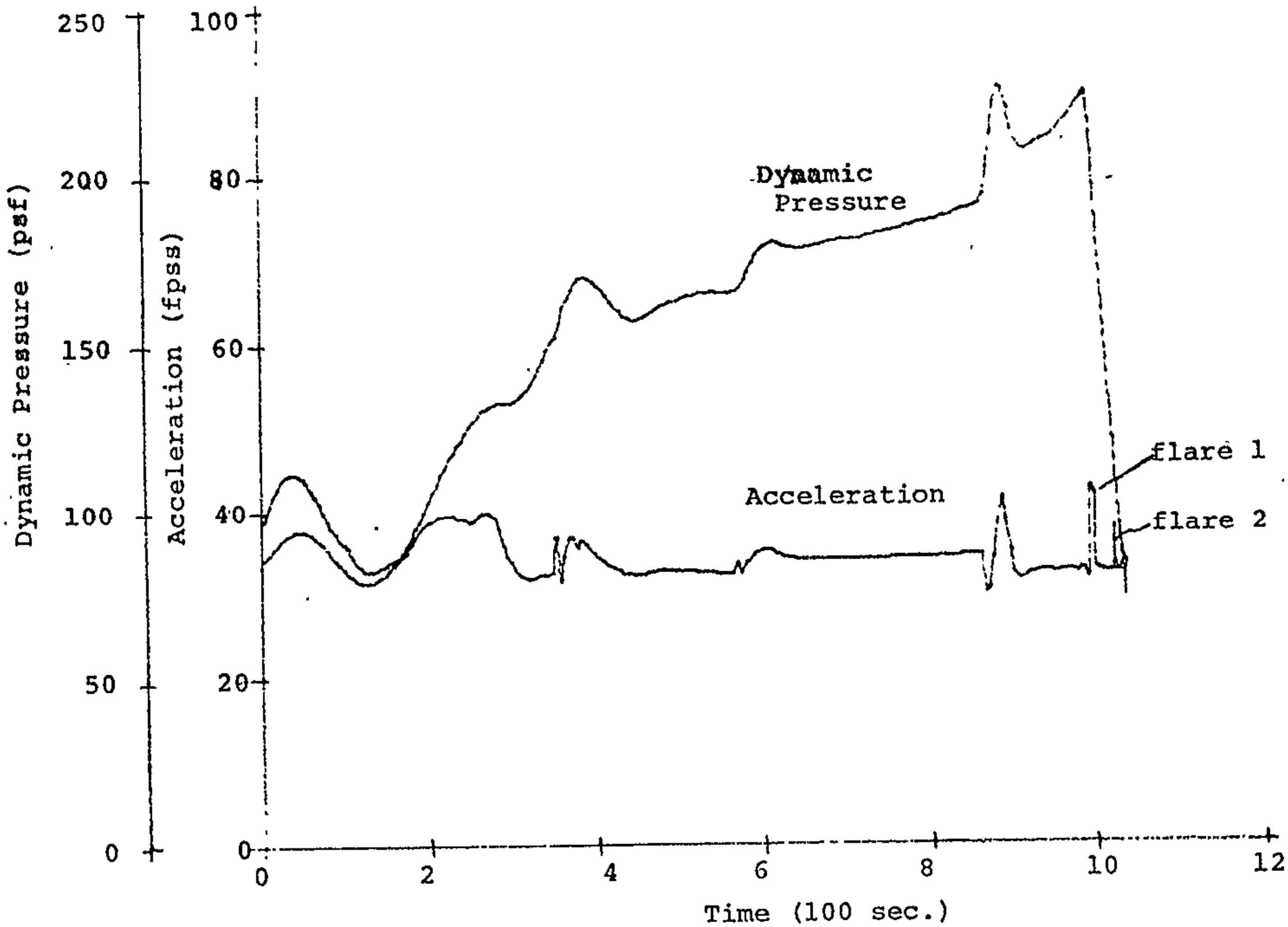

Fig. 4.5 : Acceleration and Dynamic Pressure Time Histories for Nominal Case

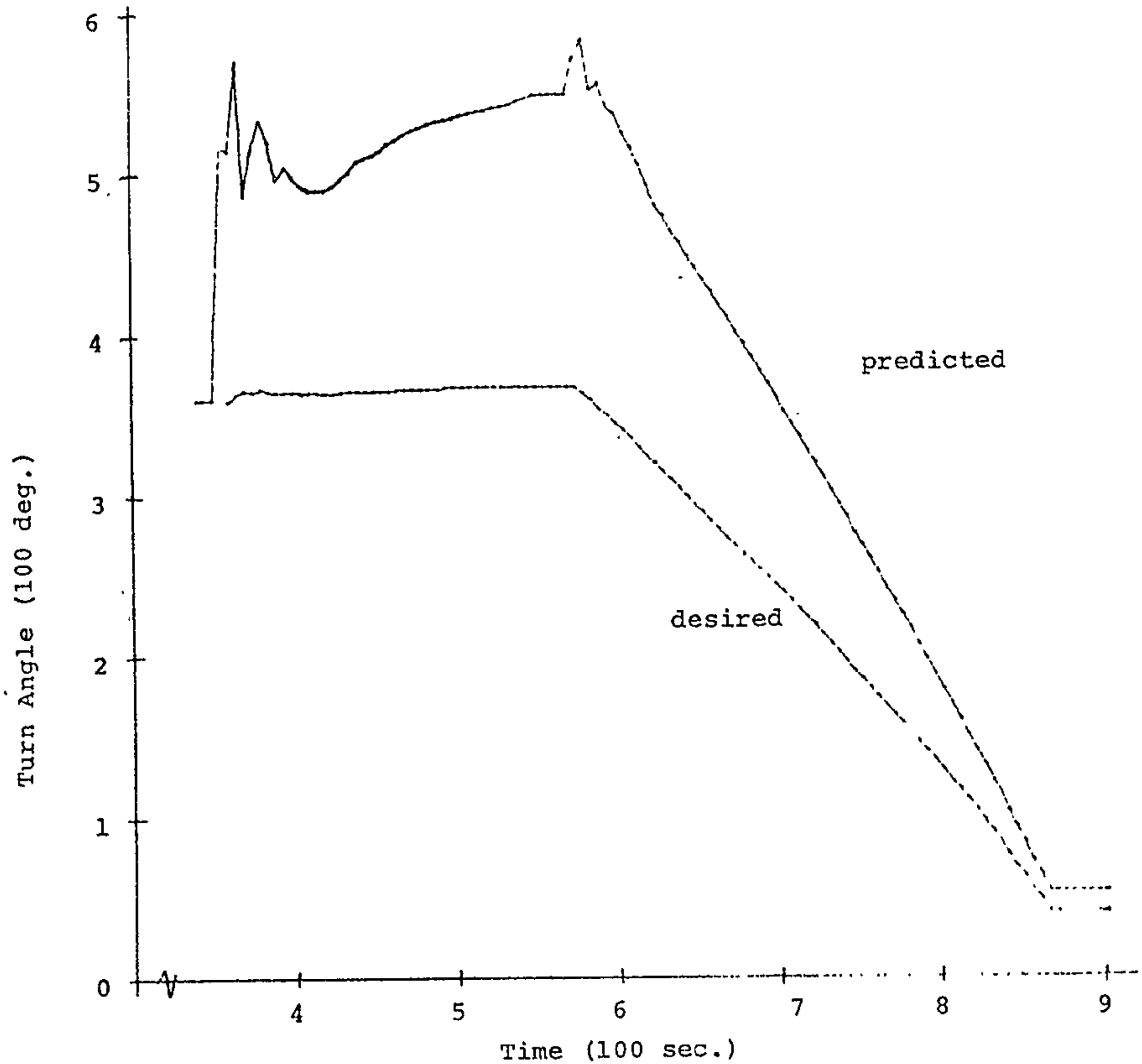

Fig. 4.6: Predicted and Desired Turn Angle for Nominal Case

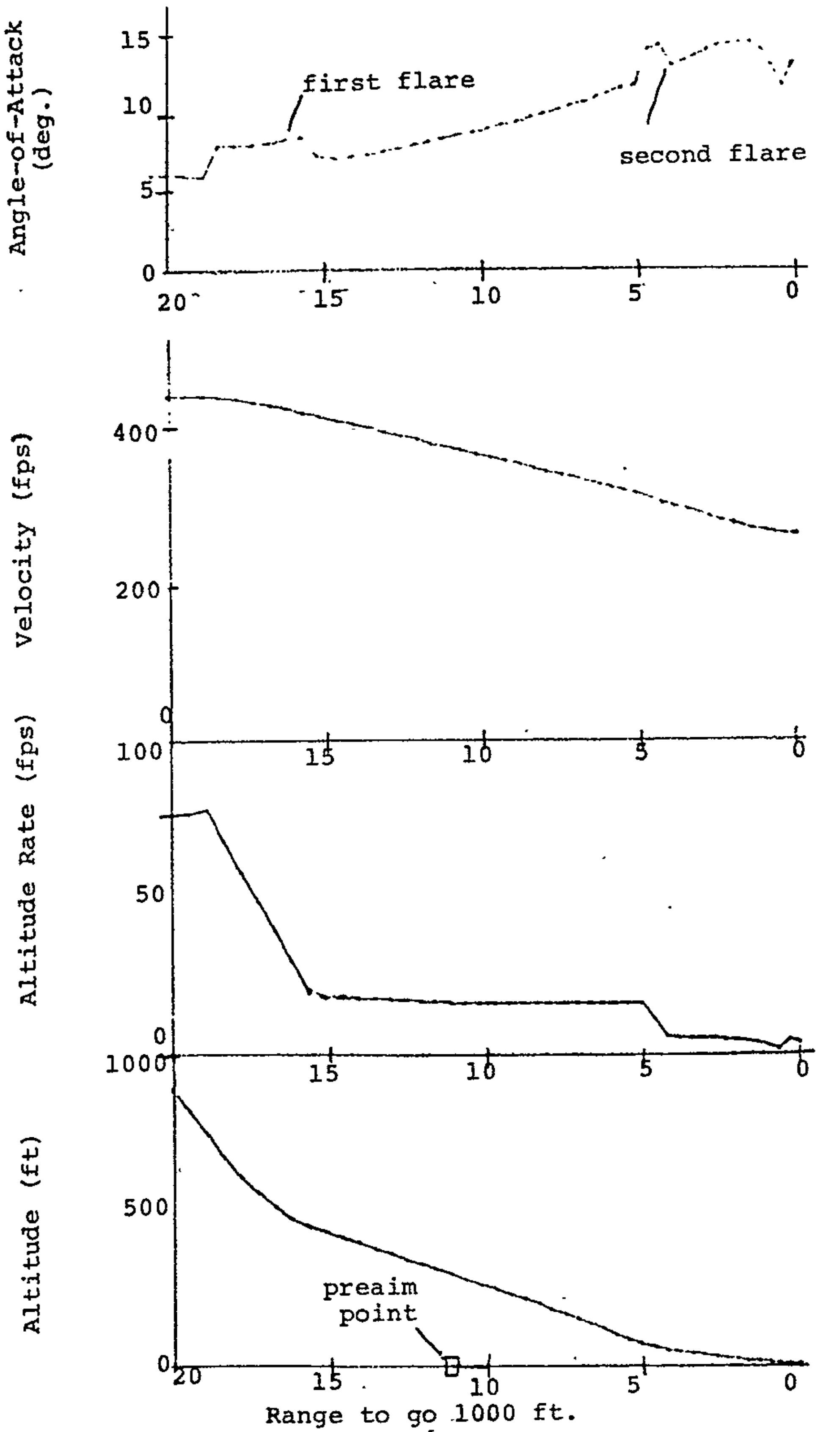

Fig. 4.7: Altitude, Altitude Rate, Velocity and Alpha as Function of Range to go During Flare for Nominal Case.

4.2 Variations on Nominal Case

4.2.1 Two Turn Case

A two turn case for the nominal target is shown in Figs. 4.8 - 4.11. This is the more natural mode for the nominal target centered in the footprint. It was generated by setting the angle-of-attack after transition to the max L/D value of 8 degrees and letting the steering equations choose the desired number of turns. Only the final part of the trajectory starting at 400 seconds is shown.

The ground track is in Fig. 4.8. There is a characteristic drift toward the landing site from the desired turn center. This is due in part to the increasing roll angle during the turn, but more directly it is caused by the fact that a higher velocity and slower turn rate at the start of the turn would naturally contribute to such a drift.

Altitude, altitude rate and velocity traces in Fig. 4.9 are very similar to the nominal case transients marking the beginnings and end of the turn segment are seen in altitude rate. Small transients at 700 and 750 seconds also mark the step changes in roll as the center control is exercised.

The control variables in Fig. 4.10 are also similar to the nominal case. Angle-of-attack is near constant near 8 degrees until the start of the final phase.

Roll angle starts near the nominal value of 30 degrees, but increases slowly as the initial turn angle predictions overpredicted the turn capability. A step down, then up, then down is seen in the roll angle as controlled by the center of curvature control logic.

The speed brake shows a nearly constant 30% deflection starting at 850 seconds, the beginning of the final phase.

The dynamic pressure in Fig. 4.11 again shows its characteristic rise, this time partly in response to the ever-increasing roll angle. The acceleration does not wander far from the 1 g level.

4.2.2 "Race Track"

In response to the discussion with pilots [5] and the results of other MSC investigations [4], a two turn trajectory was generated with this logic by changing certain control parameters. This would appear to be a back-up mode for this guidance should the pilot have to take-over from a primary system failure. The roll angle was constrained to 30 degrees and the target point was set at 5 nm before the runway and the corresponding final approach altitude set to 5000 feet. In this way, the vehicle would pass over the runway on the first turn.

The resulting trajectory is shown in Figs. (4.12) through (4.15). The ground track in Fig. (4.12) shows the characteristic down wind leg away from the runway. Though the runway is only about 20 nm away at most, this may not be desirable for the nominal landing. Note that the initial targeting provided an initial turn radius of the right value.

The altitude rate in Fig. (4.13) is "busier" in this trajectory as turns start and end. But this is not particularly objectionable.

The control variables shown in Fig. (4.14) show slightly more variation in angle-of-attack. The constant roll angle segments might be easier for a nominal mode.

The acceleration and dynamic pressure in Fig. 4.15 also show more variation than do the other two cases.

4.2.3 Left Turn Case

A left turn nominal case is illustrated in Fig. 4.15a. This is in response to the guidance changes described in Section 3.9. It is expected that right hand turns would be used universally. This would make the pilot monitor task easier. Only would an unusual mission constraint, not yet defined, call for a left hand turn.

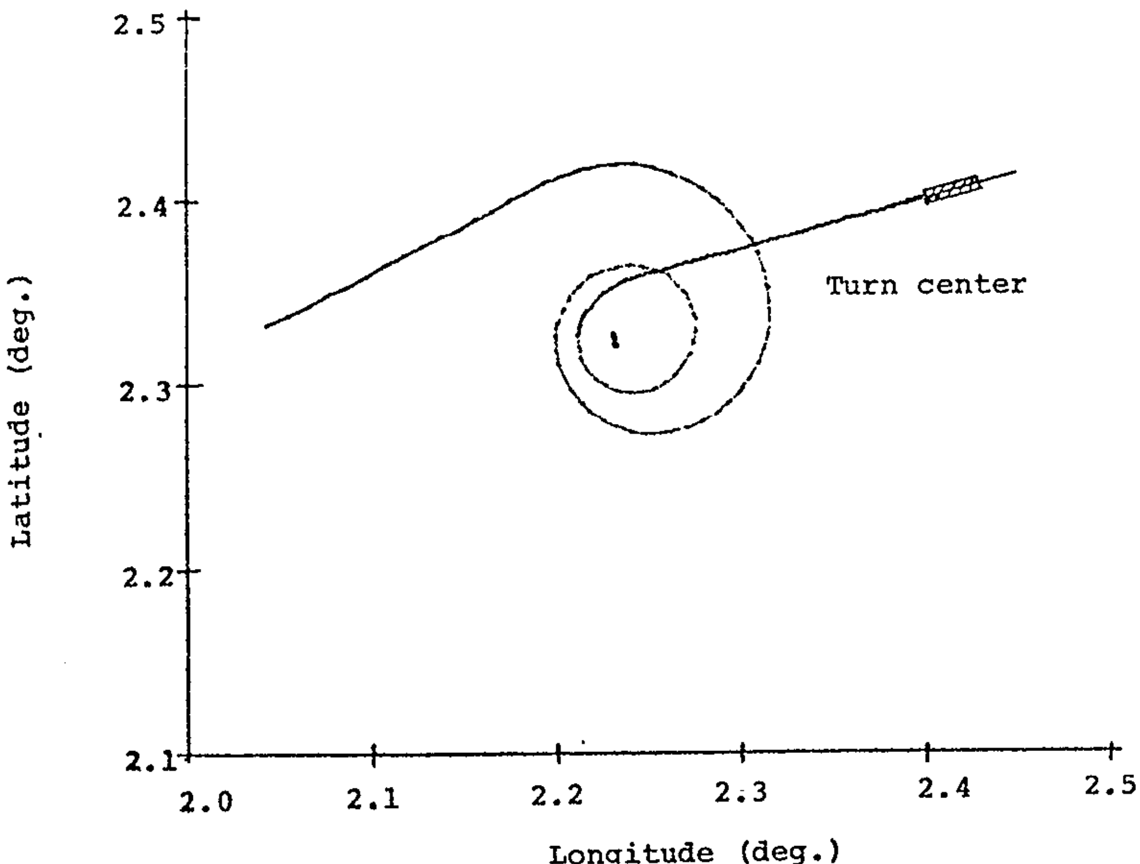

Figure 4.8 Ground Track For Two Turn Case

11/14/72

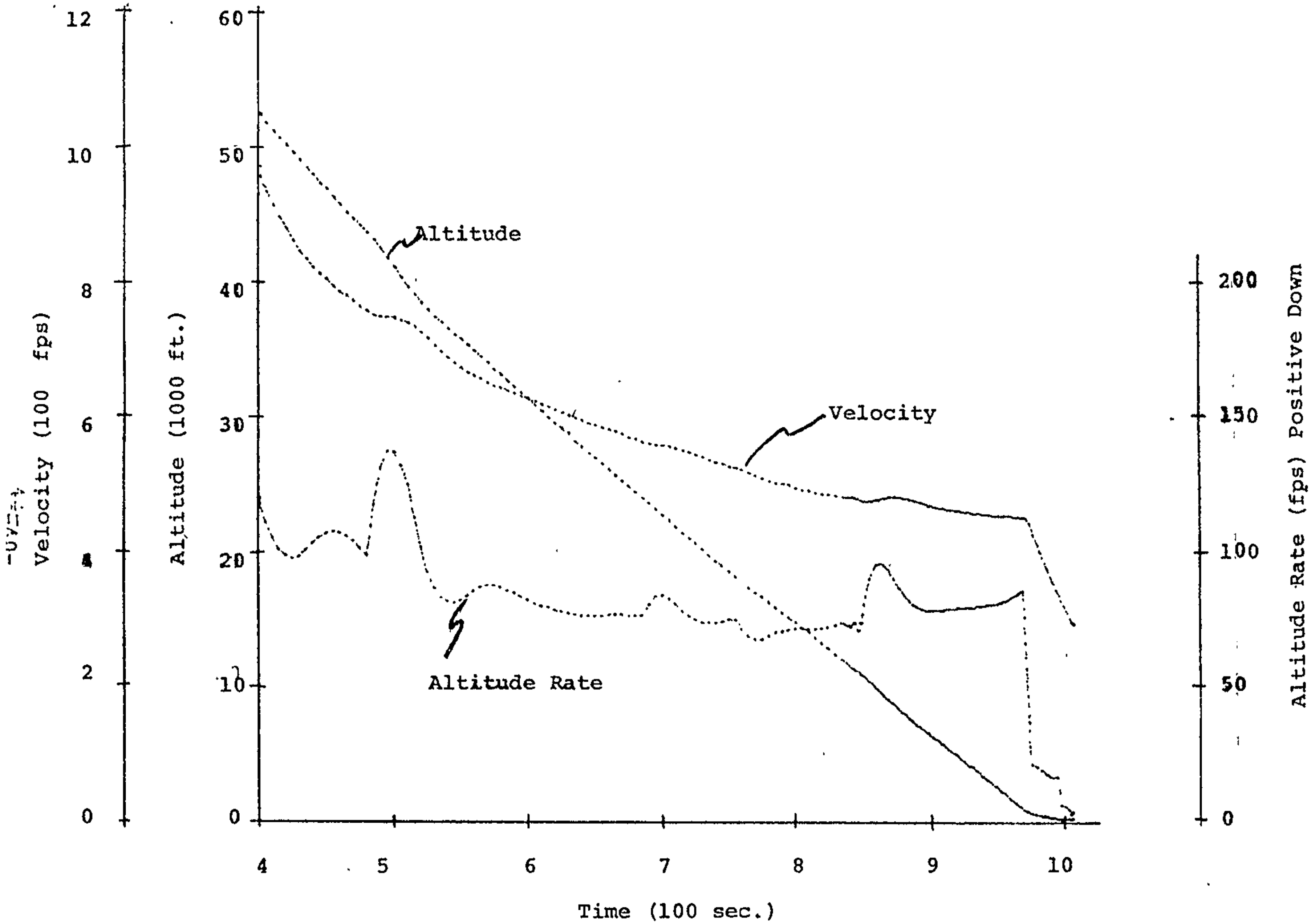

Figure A.9 Altitude Velocity & Altitude Rate Time Histories for .

11/14/72

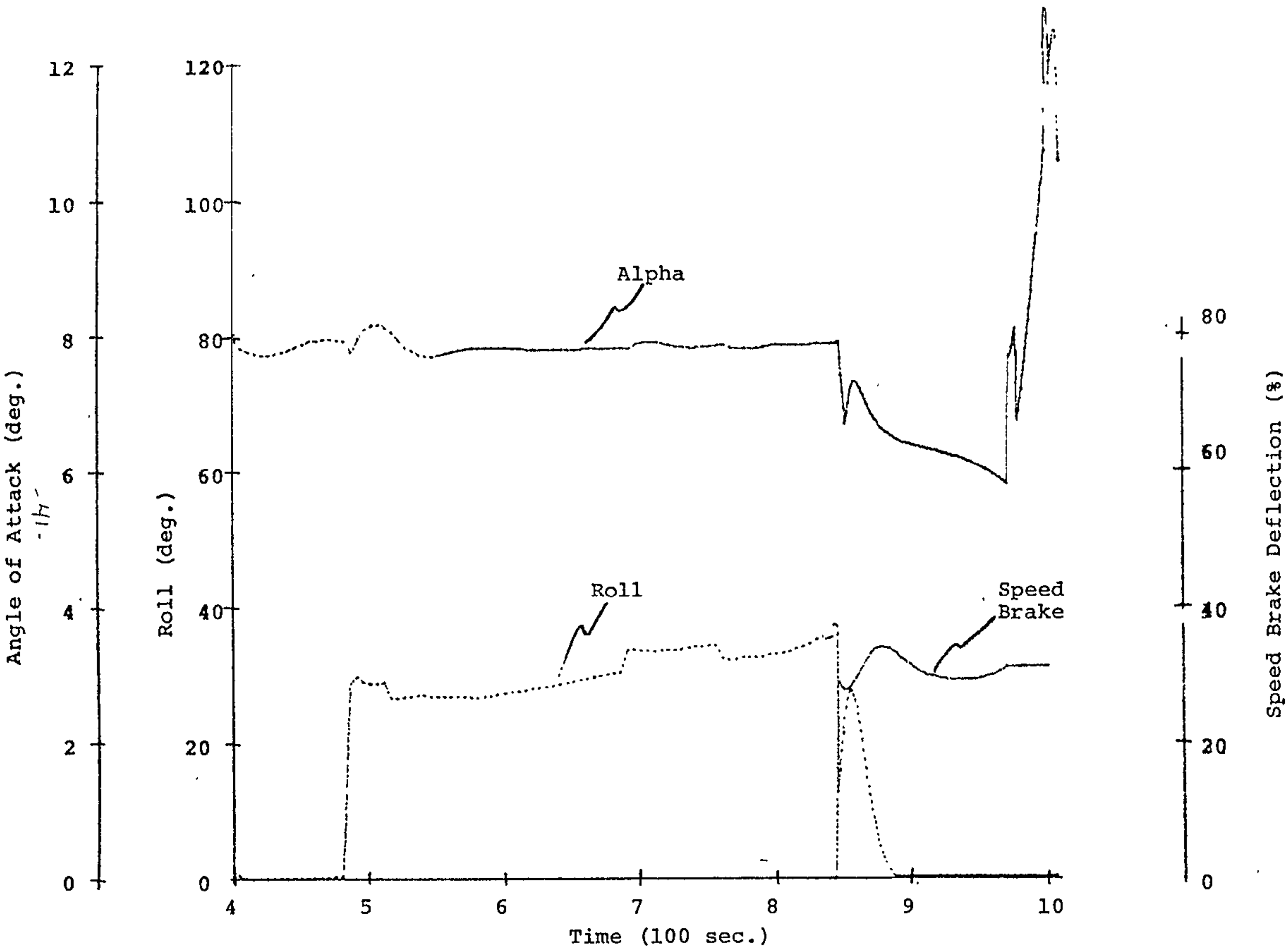

Figure 4.10, Roll, Alpha, Speed Brake Time Histories for Two Turn Case

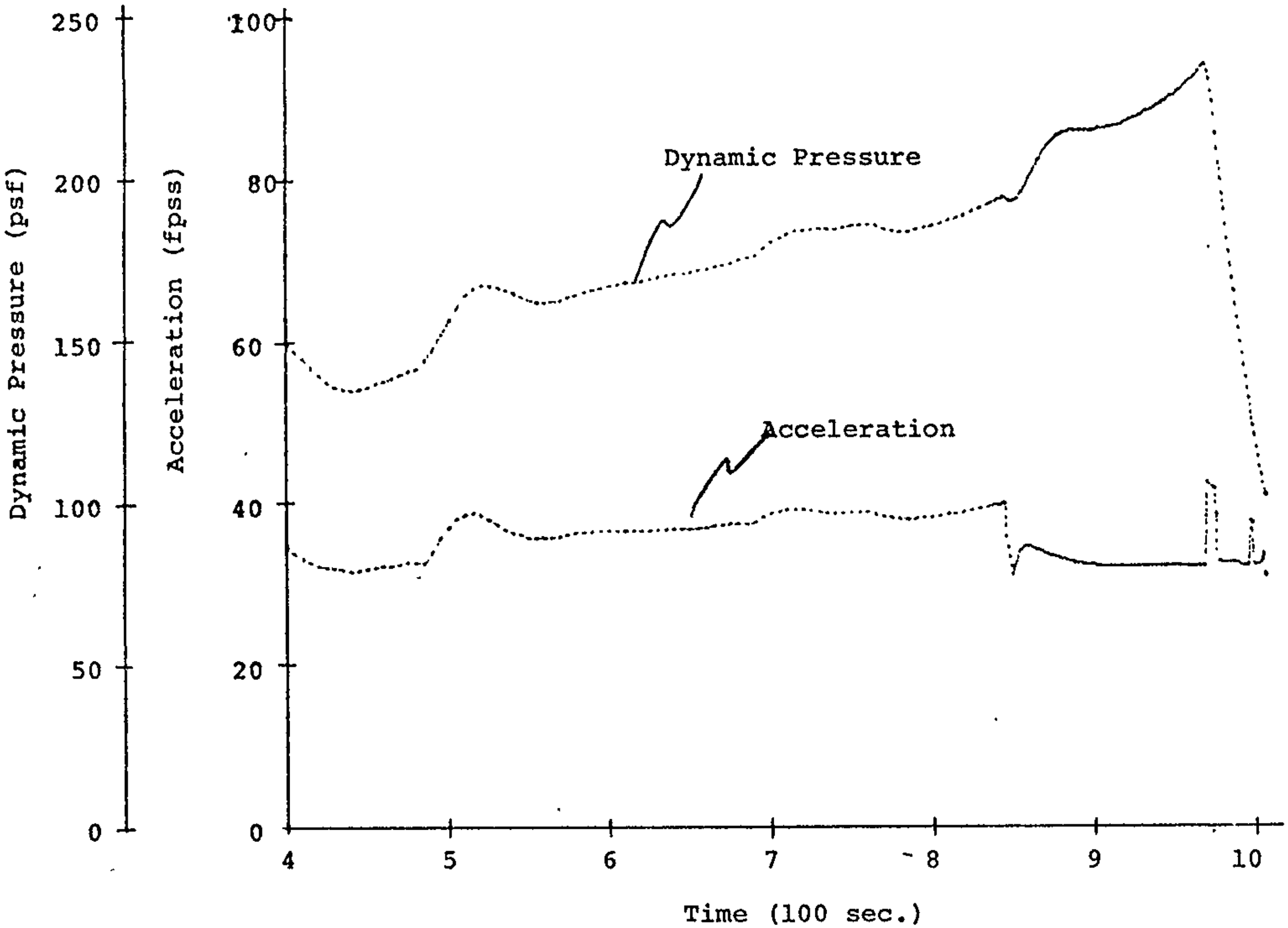

Figure 4.11: Acceleration and Dynamic Pressure Time Histories for Two Turn Case

11/14/72

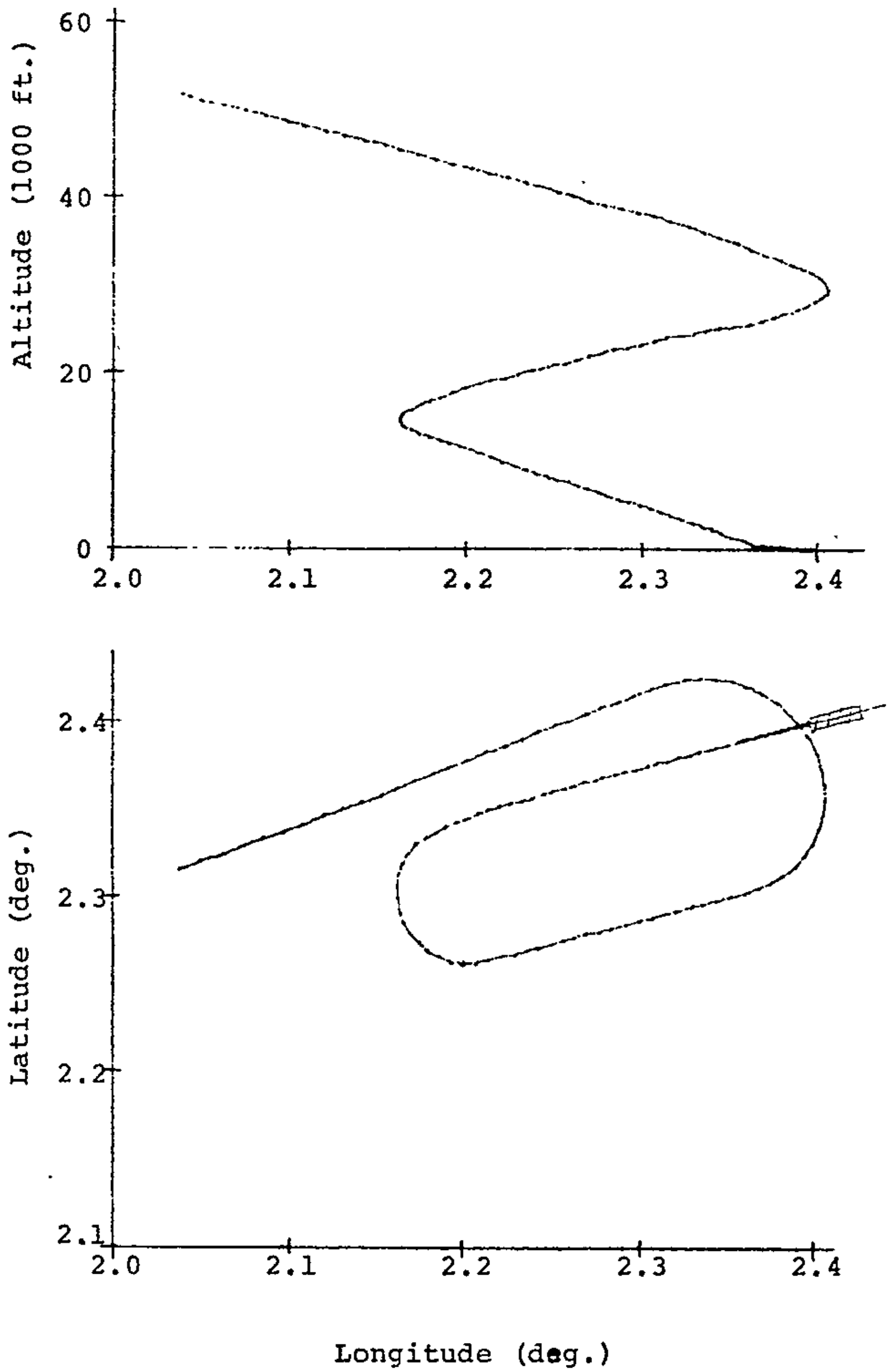

Figure 4.12 a; Ground Track & Elevation Views for Race Track Case

11/29/72

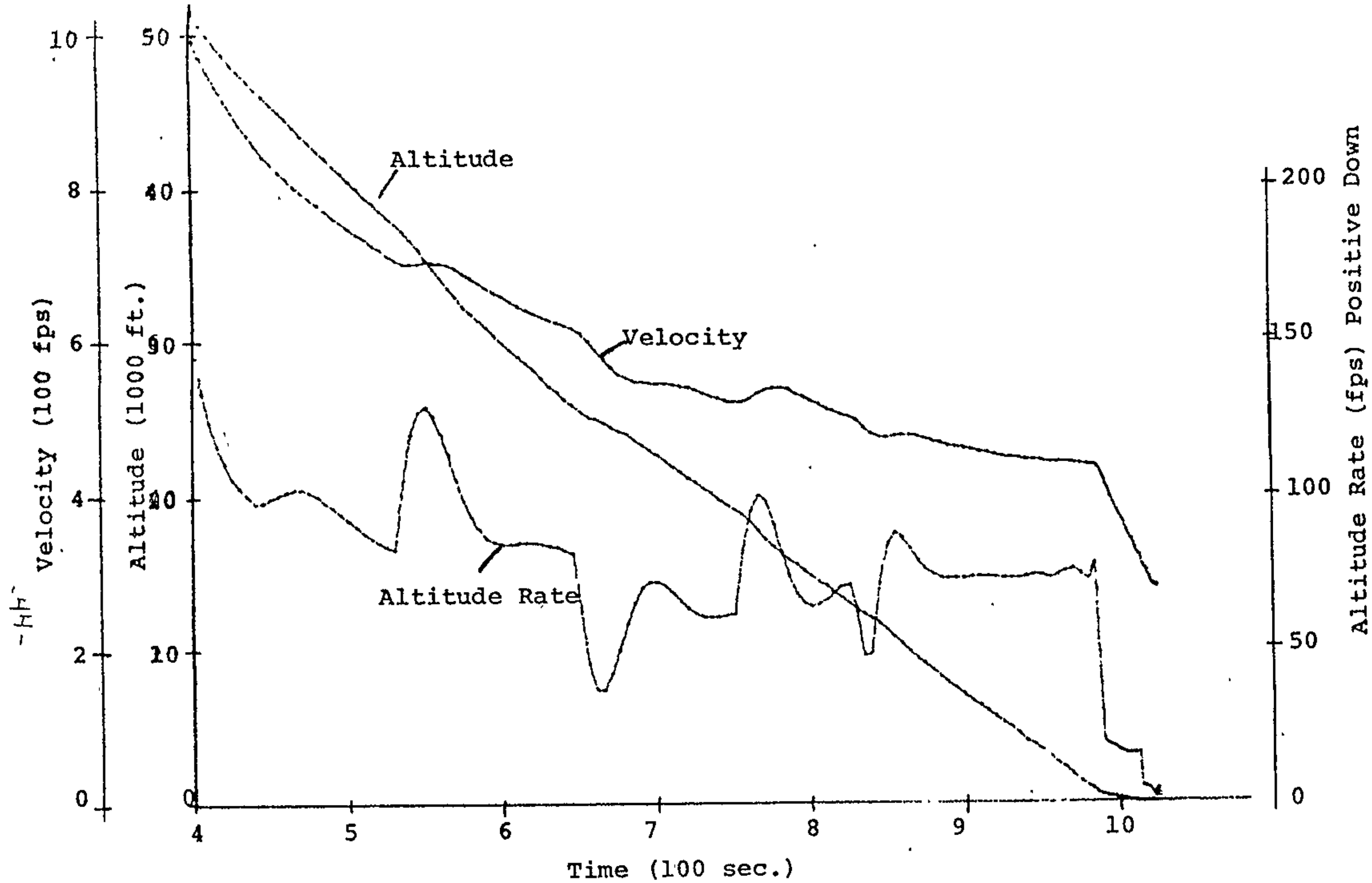

Figure 4.13: Altitude Velocity & Altitude Rate Time Histories for Race Track Case

11/29/72

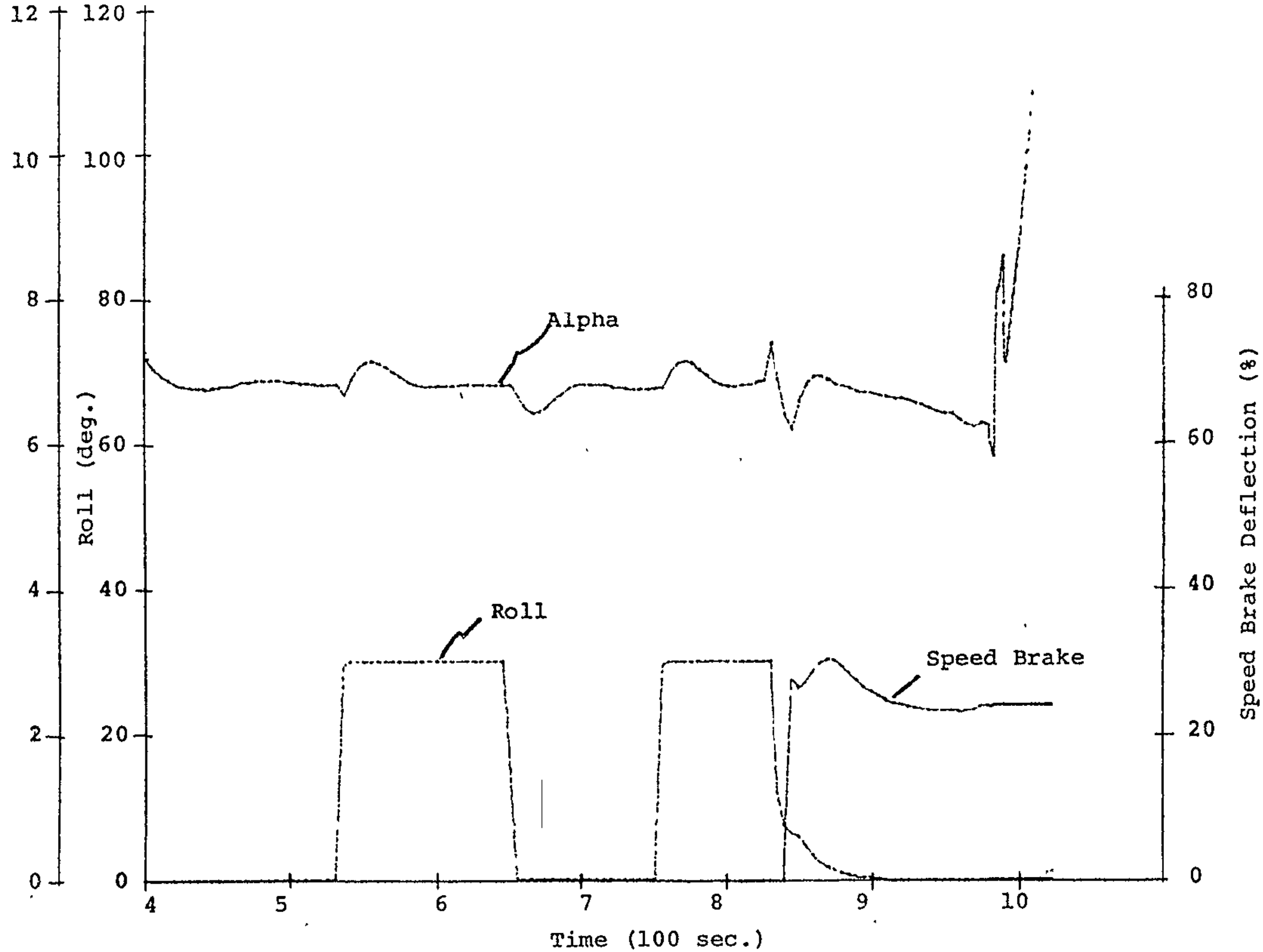

Figure 4.14: Roll, Alpha, Speed Brake Time Histories for the Race Track Case

11/29/72

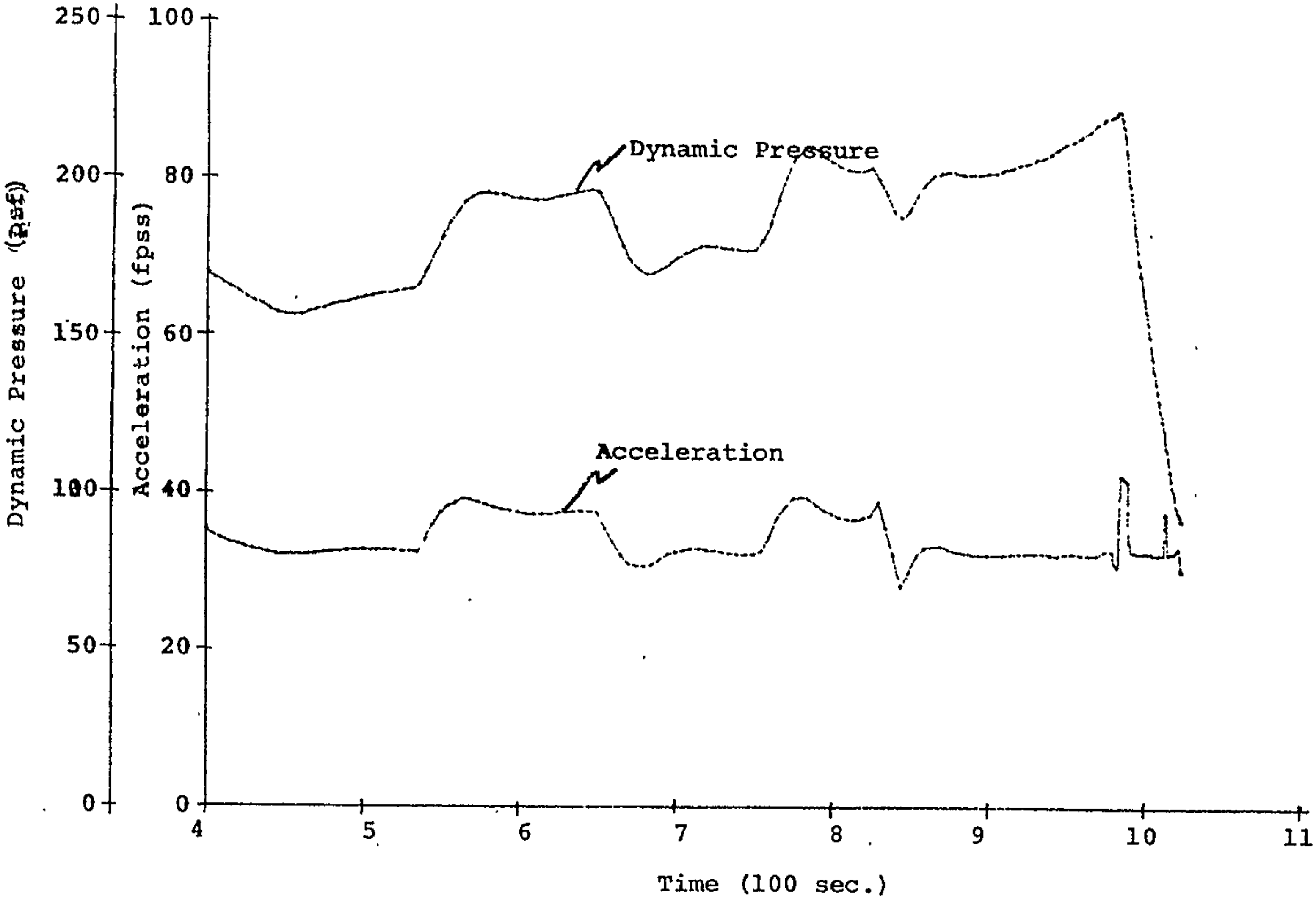

Figure 4.15: Acceleration and Dynamic Pressure Time Histories for Race Track Case

11/29/72

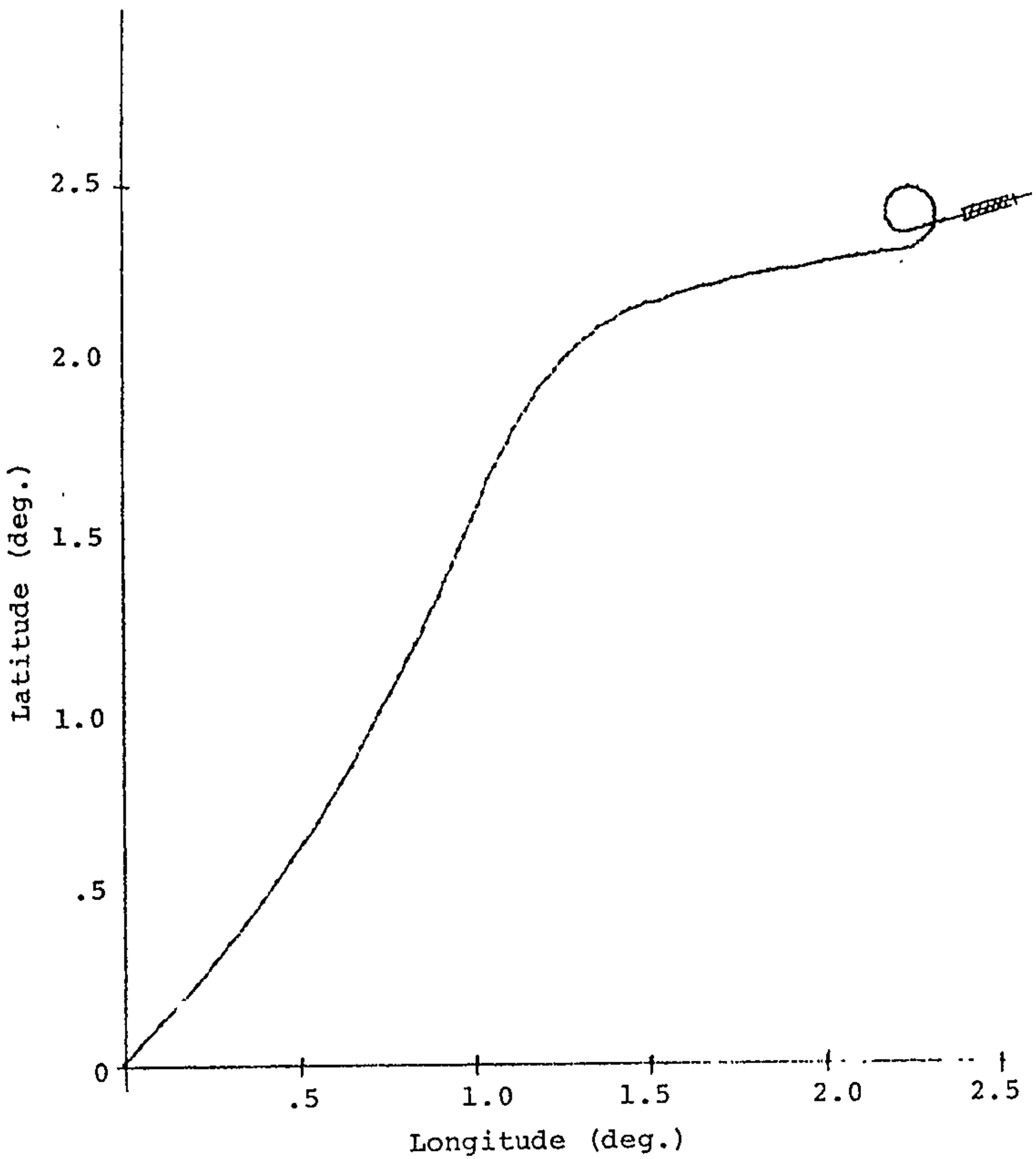

Fig. 4.15a: Ground Track for Nominal Target with Left Turn Logic

4.3 Different Landing Sites

Landing sites other than nominal were tested to see the capability of the guidance to range to the capability limits of the vehicle. This of course is the same as varying the initial position of the vehicle relative to a fixed landing site. Such variations might occur due to faulty navigation during the preceding trajectory segments. A once around abort mission with no navigation update has been seen to give particularly large initial errors. In this case, errors on the order of 30 nm are possible.

Ten different landing sites are shown in this section. In all cases, the vehicle starts in the same state as described in Table 4.1. The landing sites are in the order of decreasing range with two large cross range sites listed last.

Case	Landing Site Location		Comment
	Latitude (deg)	Longitude (deg)	
1	3.3	3.3	-
2	2.6	2.6	-
3	2.4	2.4	-
4	2.2	2.2	-
5	2.0	2.0	-
6	1.5	1.5	-
7	1.0	1.0	azimuth rate limit off
8	.5	.5	missed
9	1.5	3.5	large crossway
10	3.5	1.5	large crossway

Table 4.2 Landing Site Locations
Runway azimuth = 75°

In most cases, a two turn trajectory results because at this point a one turn trajectory had not been selected as nominal and a two turn trajectory was within the vehicle capability.

Case one, target at (3.3,3.3), shown in Fig. 4.16, represents the extreme long range case. An early transition starting point was even required to squeeze out the extra 10 nm that this allows.

The circles increase slightly in diameter as the range to target decreases from case to case until we come to the target at (1.5, 1.5). In this case, the guidance must try hard to get back to the final approach path and only a half turn on to final approach is possible.

The next case, target at (1.0,1.0) Fig. 4.22, is not possible with the azimuth limiter on. For that matter, it is near the minimum possible range. An approach from the other runway directions should be considered in this case. The effect of the variable lead angle logic, Section 3.8.1, is seen starting at 1.5 degrees latitude.

The landing site at (.5,.5), Fig. 4.23, is not attainable with this logic. It appears to be outside the vehicle capability.

The two large cross track landing sites are shown in Figs. 4.24 and 4.25. They are ± 85 nm from initial trajectory plane. Somewhat greater lateral range is possible but was not tested.

In all, landings are demonstrated within a band 195 nm in the down range direction and 170 nm in the cross range direction.

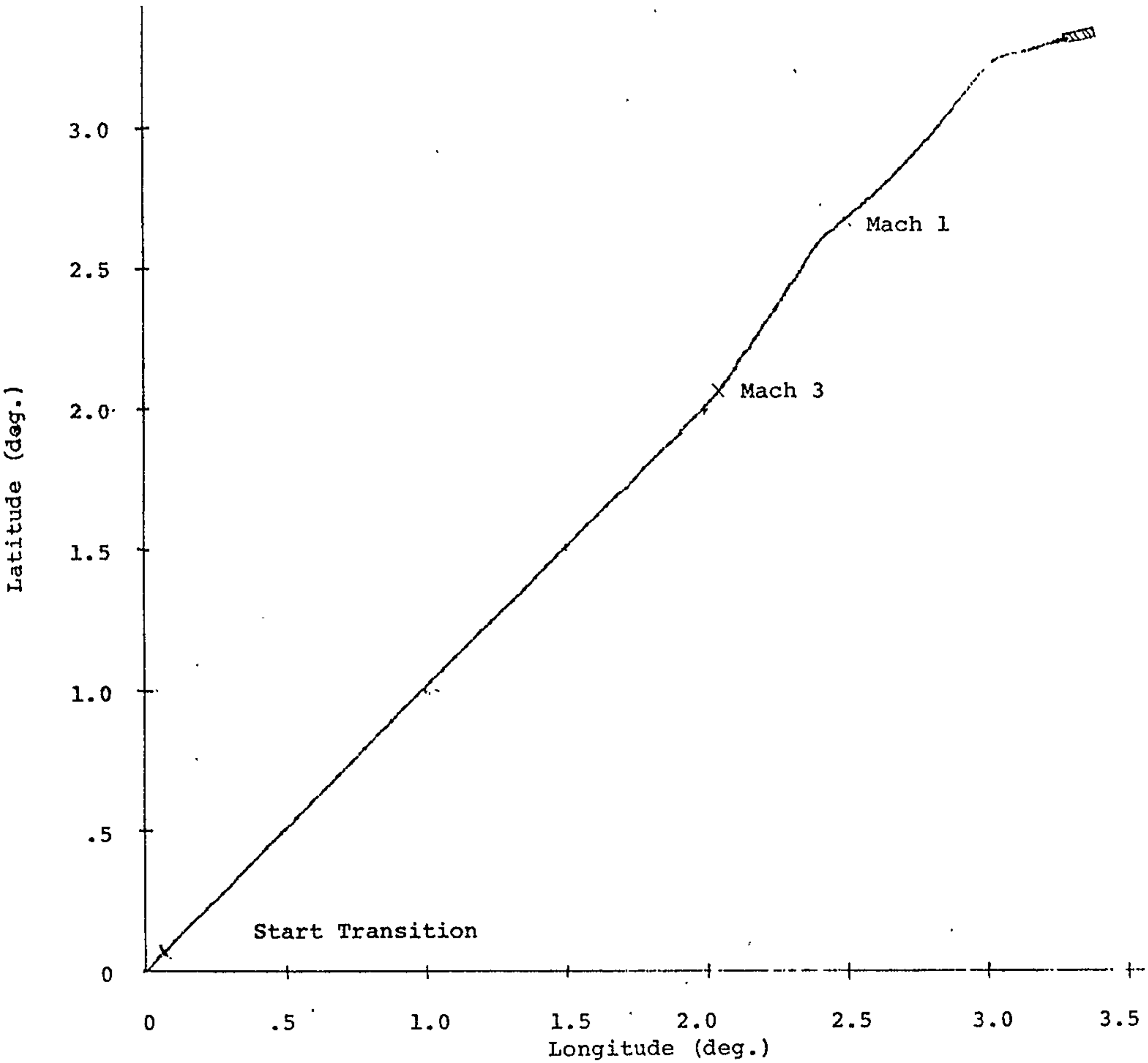

Figure 4.16 Ground Track Target at (3.3, 3.3)

11/7/72

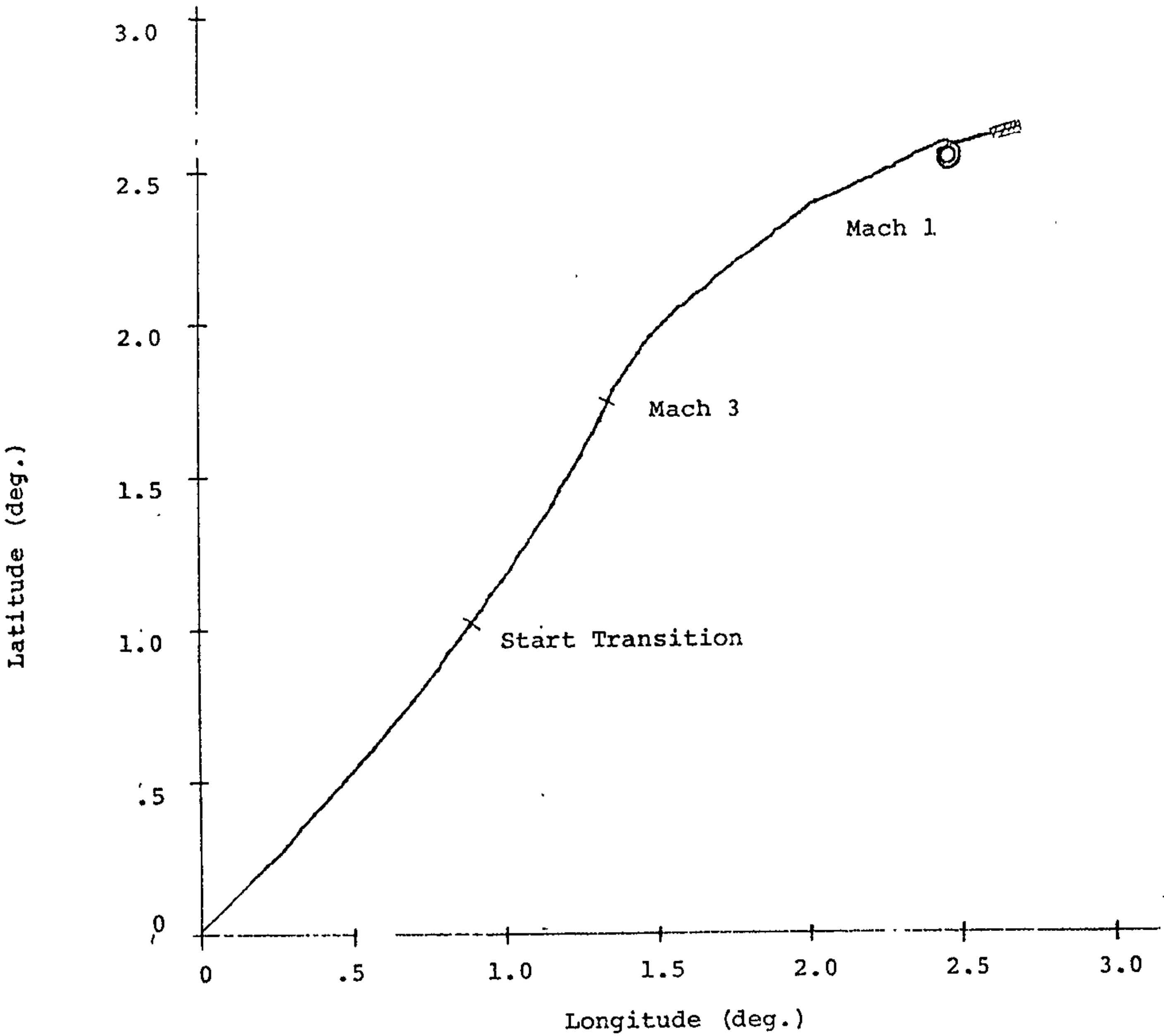

Figure 4.17: Ground Track Target at (2.6, 2.6)

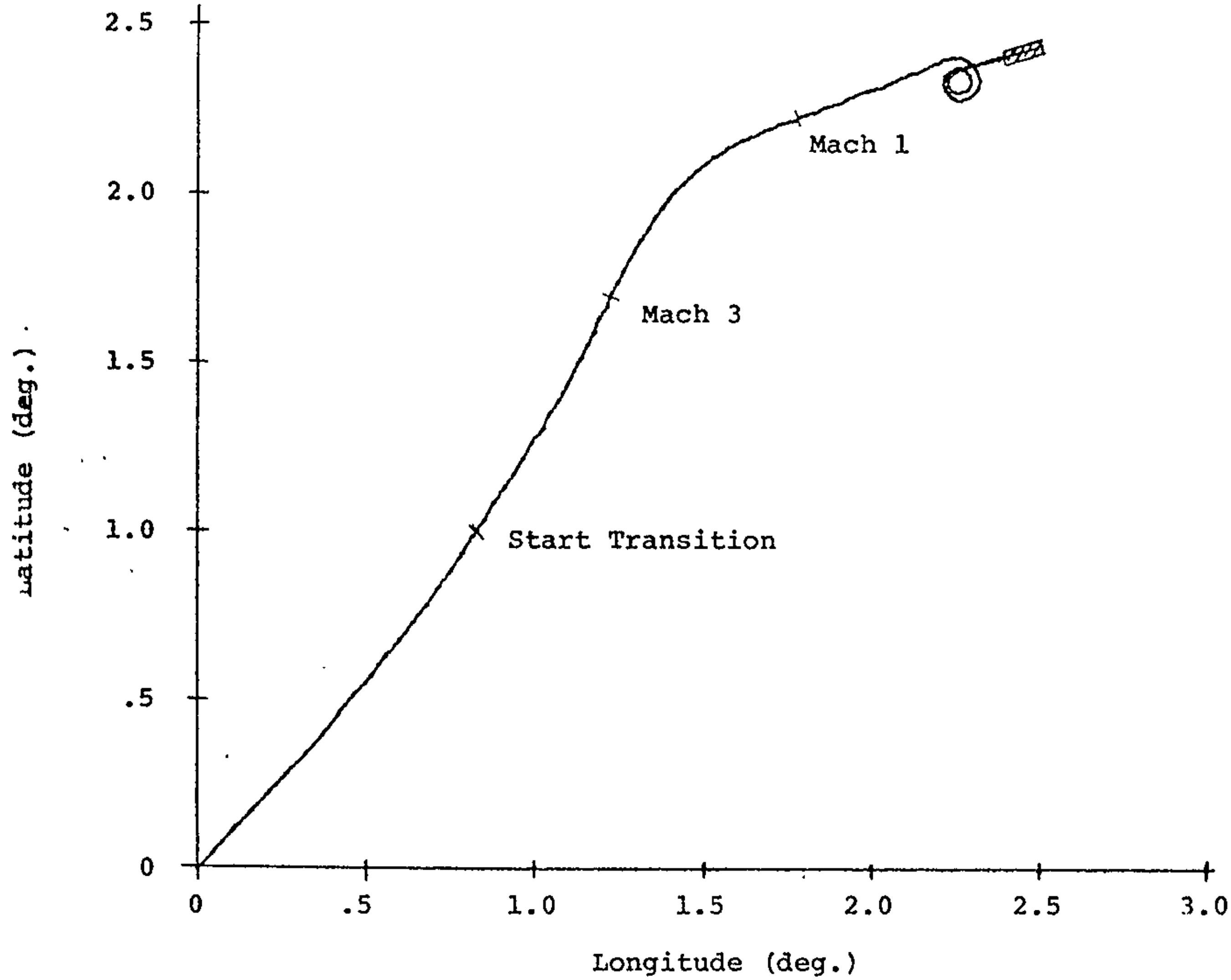

Figure 4.18: Ground Track Target at (2.4, 2.4)

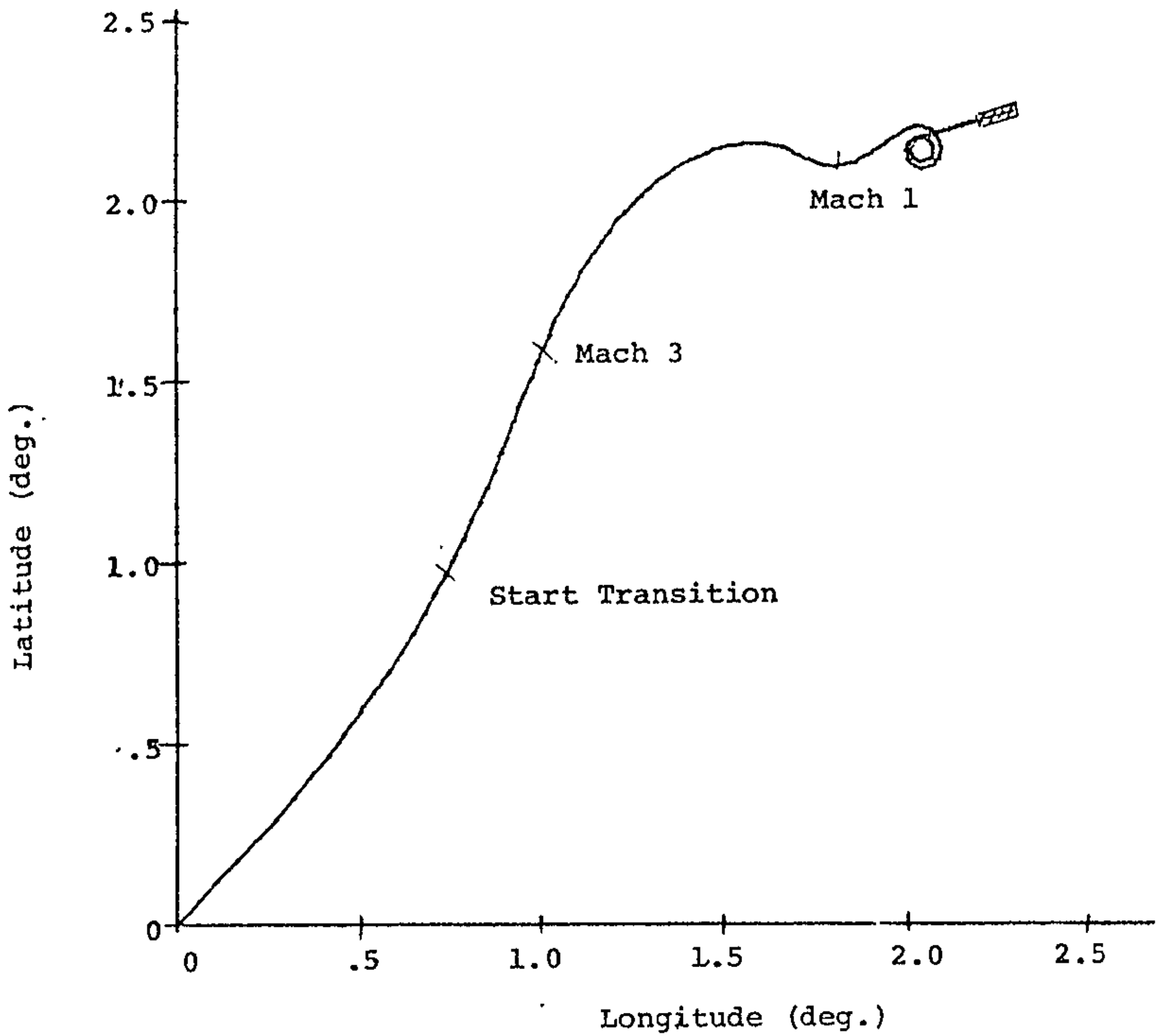

Figure 4.19: Ground Track for Target at (2.2, 2.2)

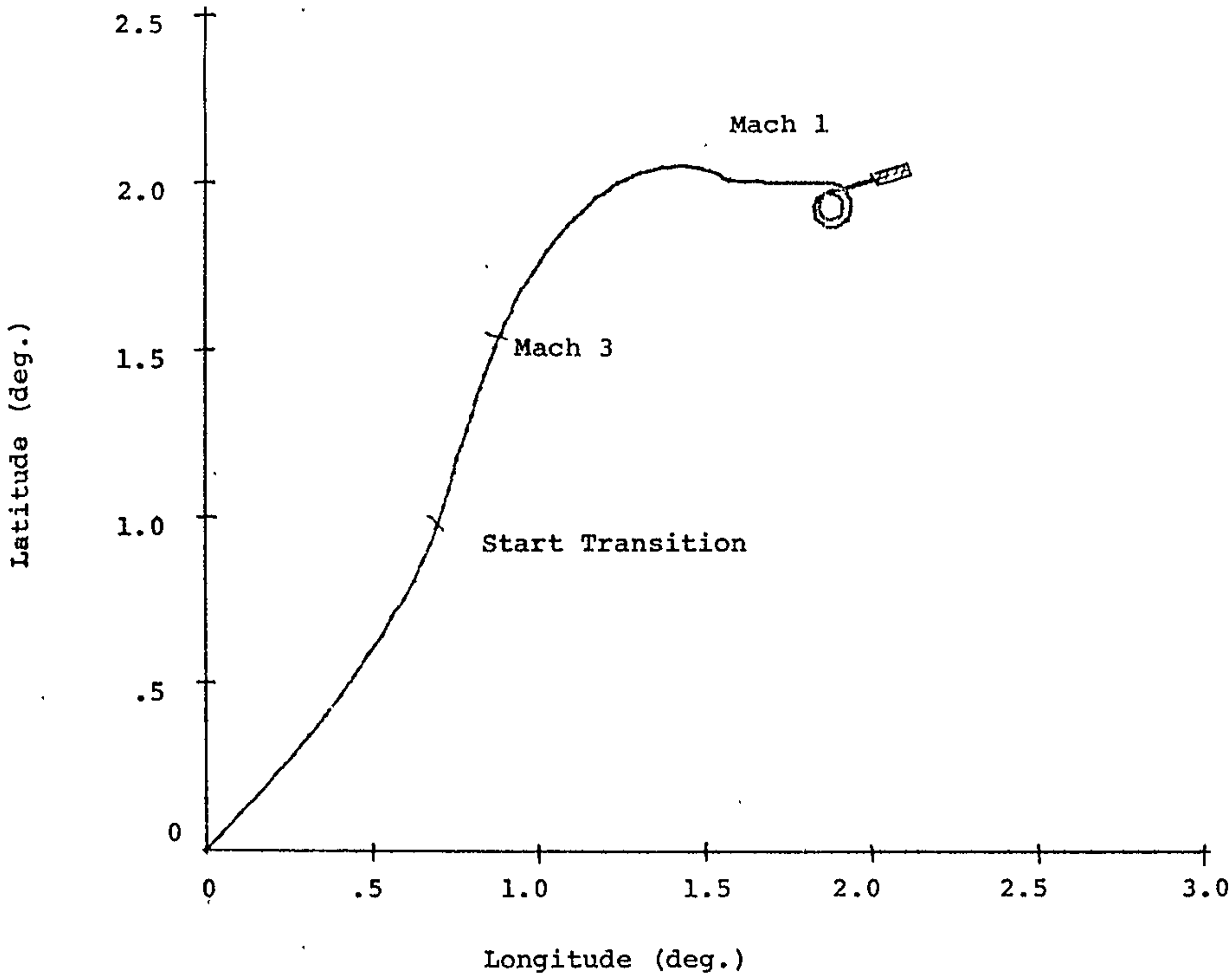

Figure 4.20: Ground Track Target at (2.0, 2.0)

11/8/72

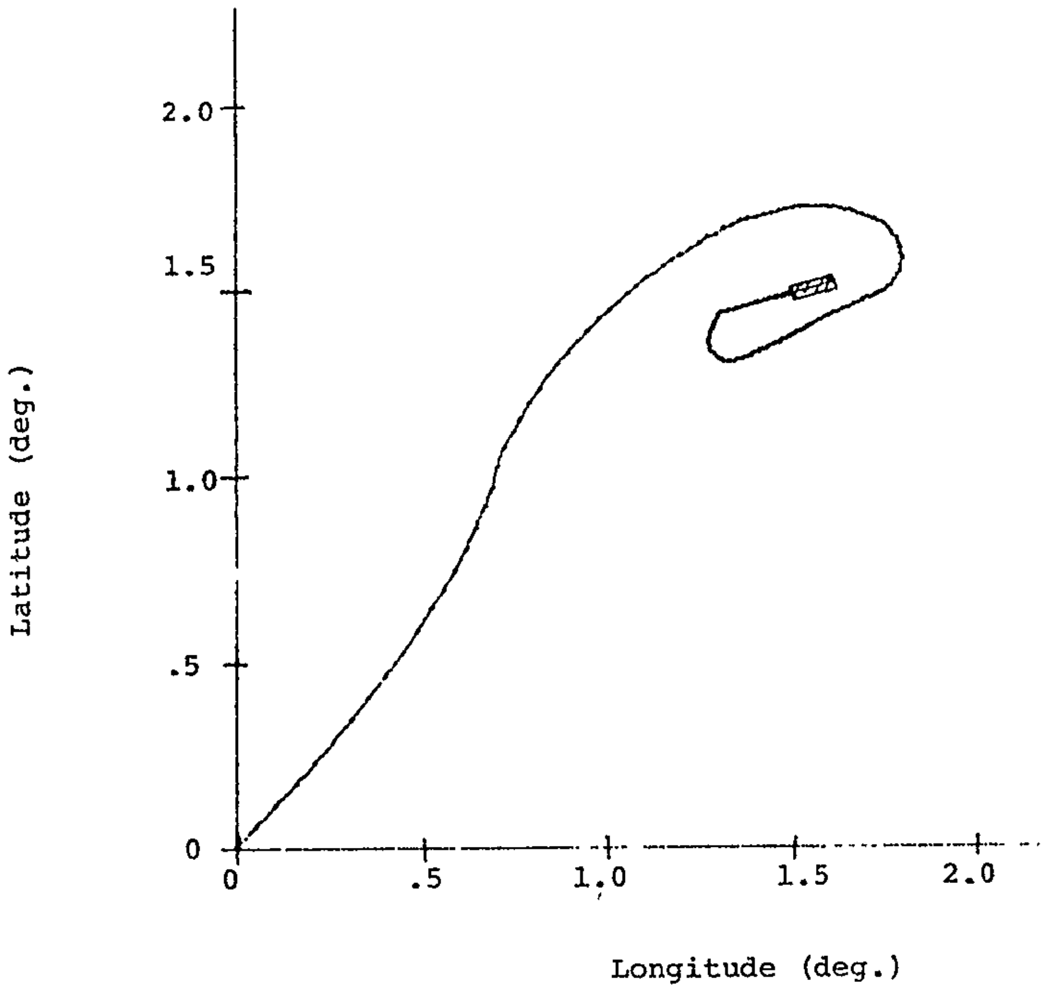

Fig.4.21: Ground Track for target at (1.5, 1.5)

10/30/72

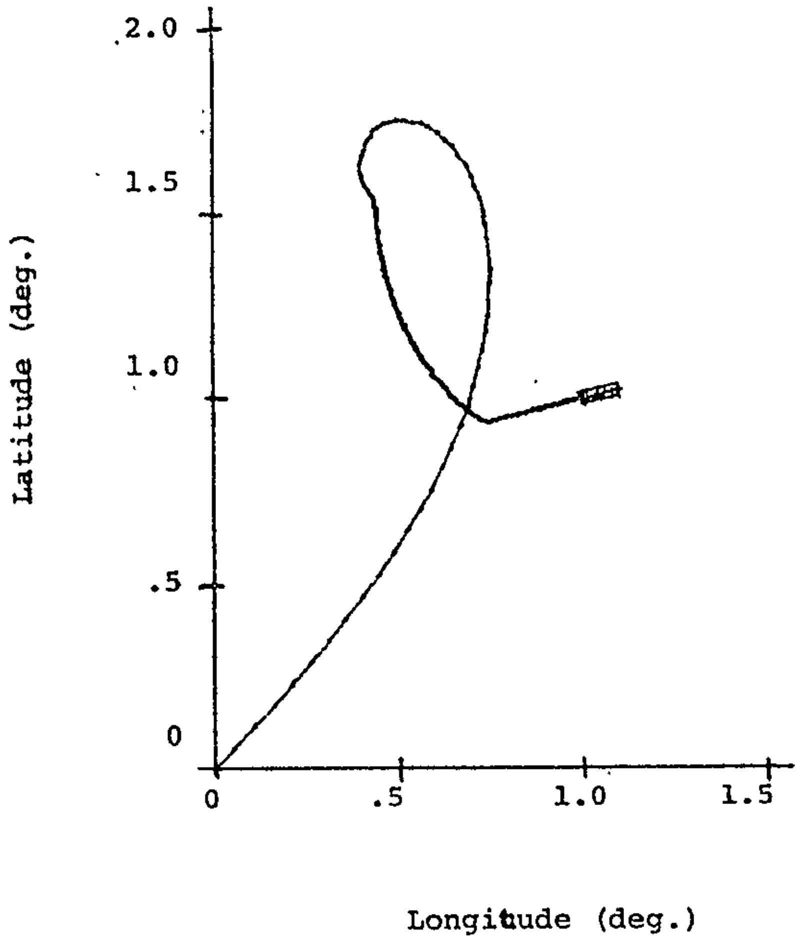

Fig. 4.22: Ground Track for Target at (1.0, 1.0)

10/30/72

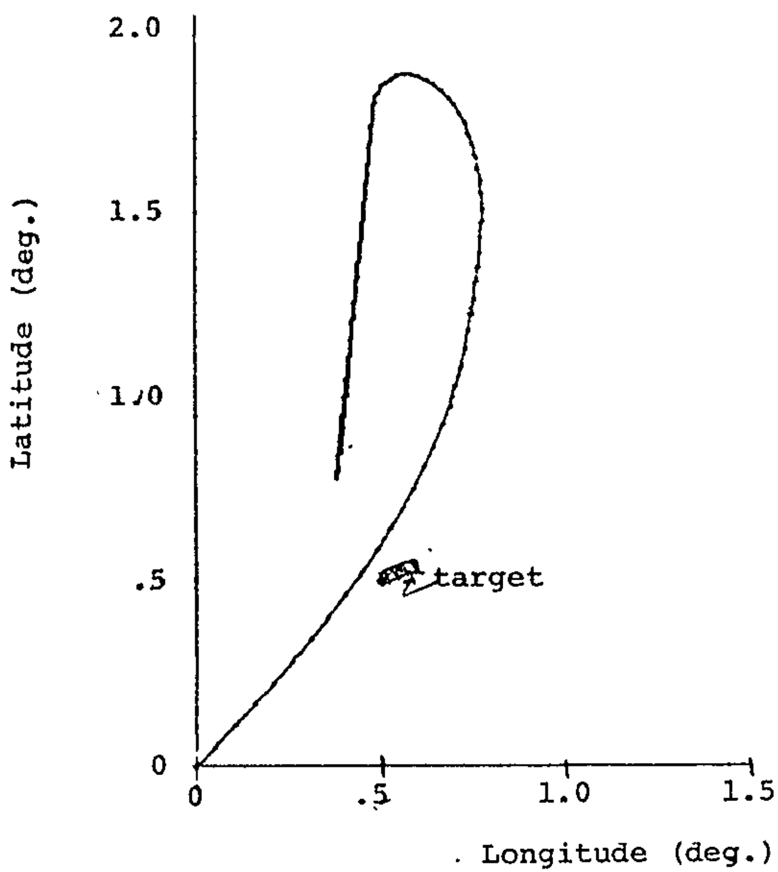

Fig. 4.23: Ground Trace for target at (.5, .5)

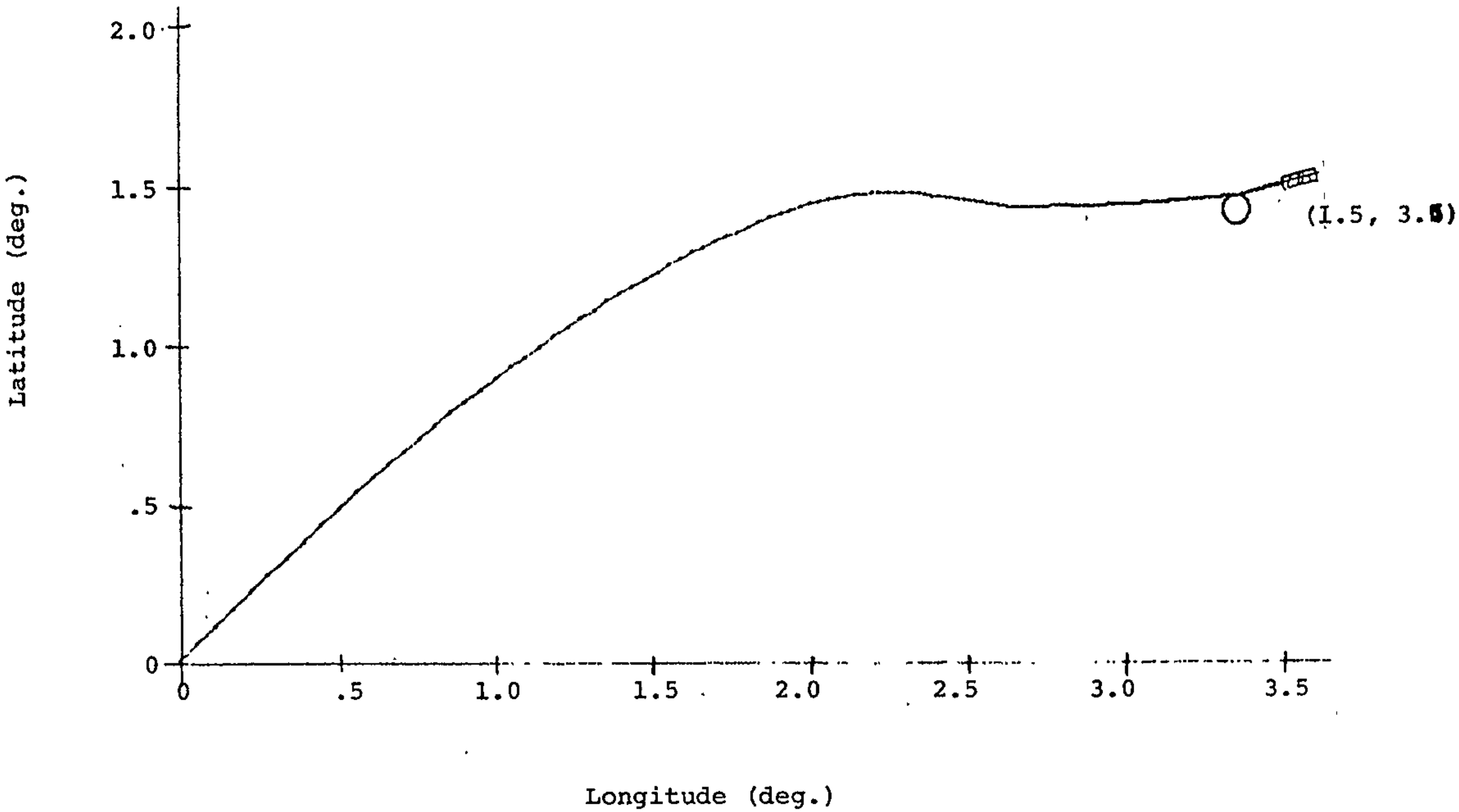

Fig. 4:24: Ground Track for target at (1.5, 3.5) 10/30/72

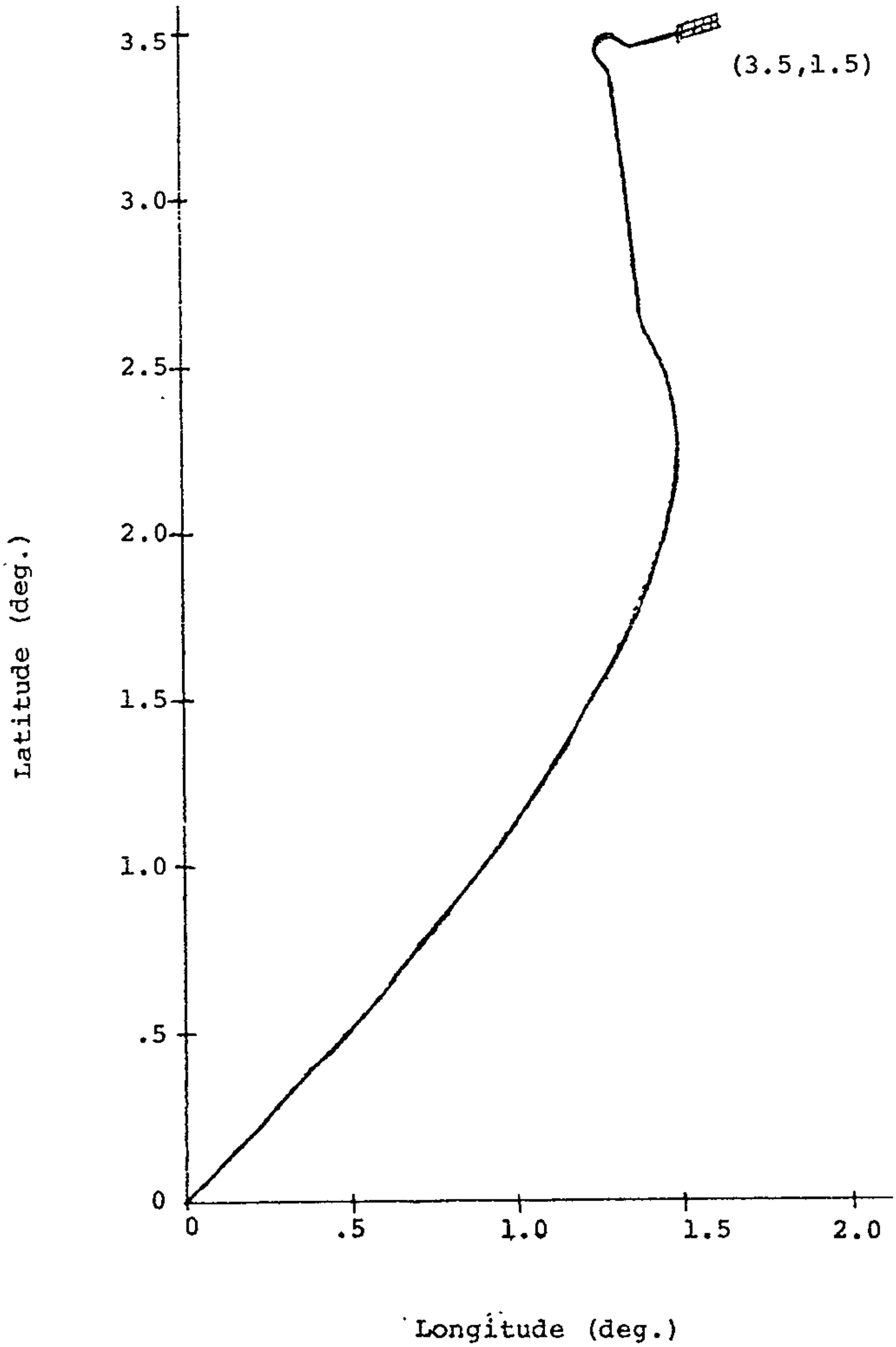

Fig. 4.25. Ground Track for Target at (3.5,1.5)

10/30/72

4.4 Wind Performance

4.4.1 Semi Steady Winds

That the design wind for Shuttle [15] is an extreme test, is shown in Fig. 4.26. Here the Shuttle attempts to land into a head wind with no compensations. The profile of this wind is also shown in Fig. 4.26.

The guidance described in Section 3 cannot compensate for this wind as shown. Successful landings with winds of 1/2 this magnitude have been made, however. The center-of-curvature control is the reason for this capability. The vehicle is blown off course and the center-of-curvature control brings it back.

Three additions to the logic will allow this capability however. They all involve knowledge of the vehicle air speed. Heretofore we steer using fround speed as inferred from the inertial measurement unit.

The first is to replace VA with VAIR, the air speed in the steering equations. Second change the bias on the landing field at the start of the offset target calculations by

$$BIAS = BIAS + KBIAST(VA-VAIR) \tag{4.1}$$

where

$$KBIAST = .03 \text{ nm/fps}$$

Note that a head wind will decrease the bias while a tail wind will increase it.

Third, modify the commanded angle-of-attack in the final phase by using this difference by an amount $D\alpha$.

$$D\alpha = KWF\ (VA-VAIR) \tag{4.2}$$

where

$$KWF = .01 \text{ deg/fps}$$

With these modifications, the trajectory for a head wind and cross wind result as shown in Figs. 4.28 and 4.35. Of most interest is the extreme action of the roll angle in Fig. 4.30 and 4.34, in compensating for the wind action. Note also that air speed not ground speed is displayed in the velocity plots.

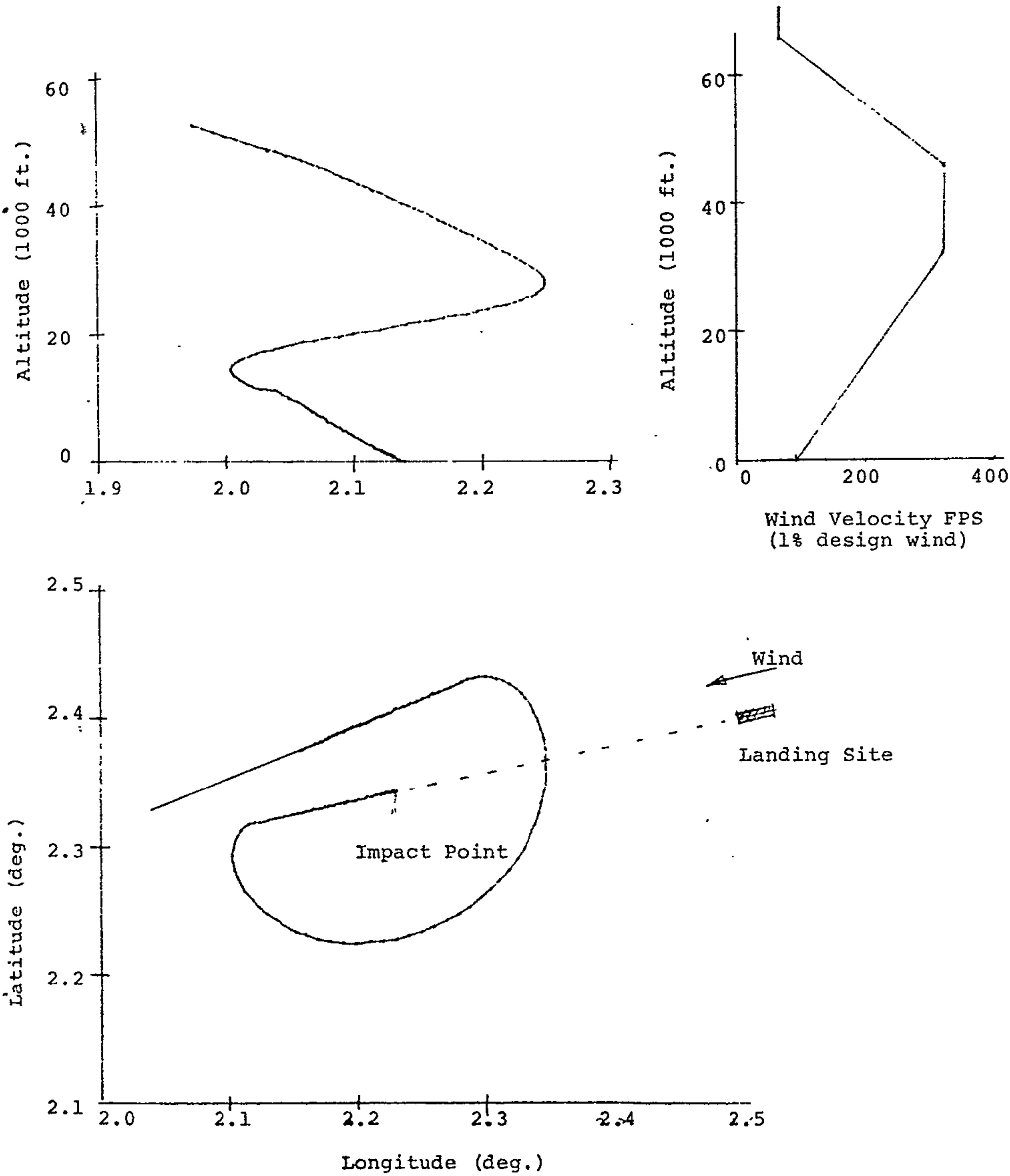

Fig 4.26: Ground Track & Elevation Views for Extreme Head Wind With No Compensation

4.4.2 Gusts

Only limited testing with gusts was made. A gust of the 1-cosine form was introduced during the final approach phase where the gust effect is most pronounced.

These tests are illustrated for a downward gust and a cross wind gust introduced at 950 secs and lasting for 30 seconds. The peak value of the gust is 40 ft/sec. The down wind gust effect on the nominal trajectory is in Fig. 4.35 and the cross wind gust is in Fig. 4.36.

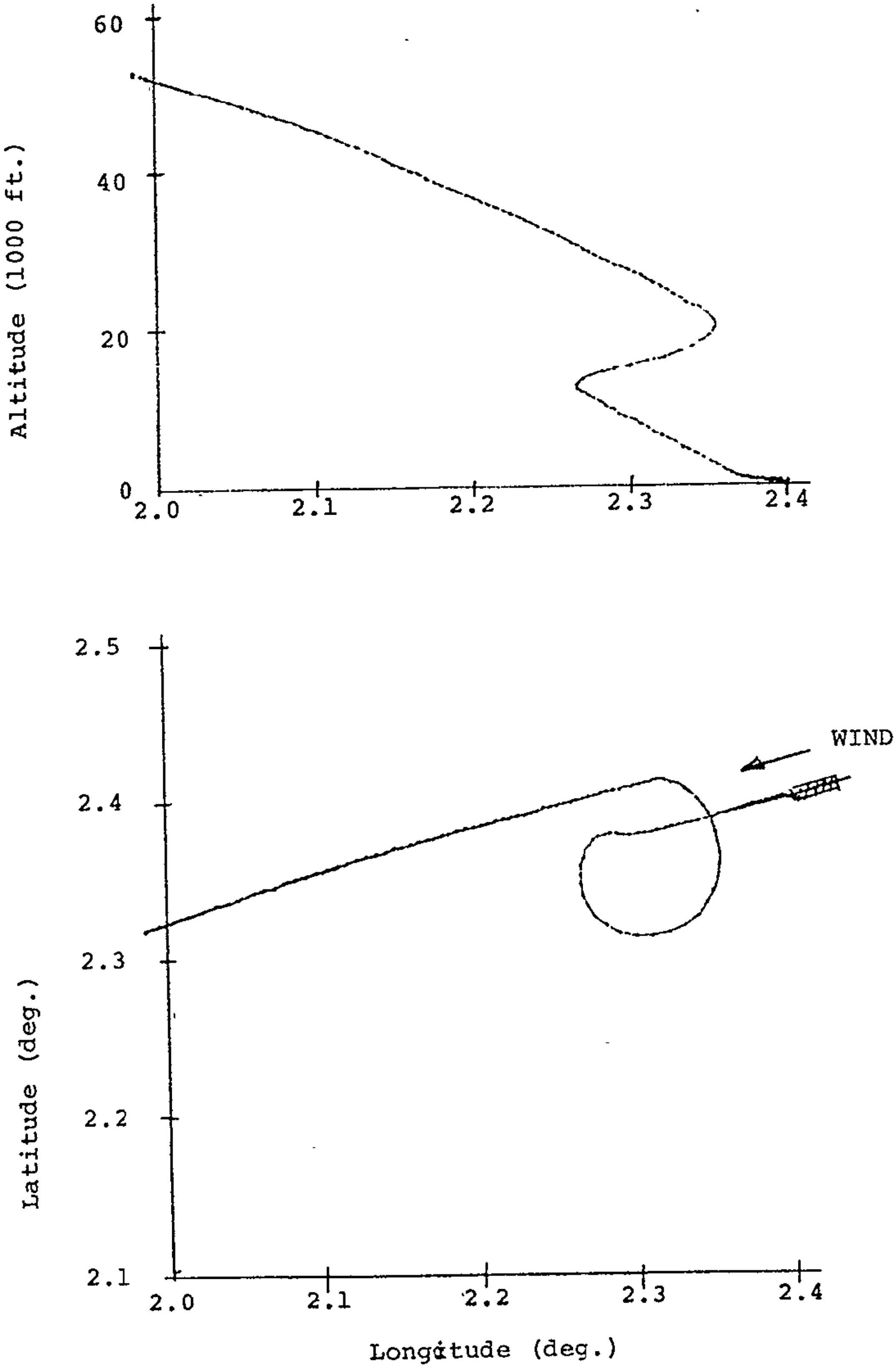

Figure 4,27:Ground Track & Elevation Views for Headwind Case

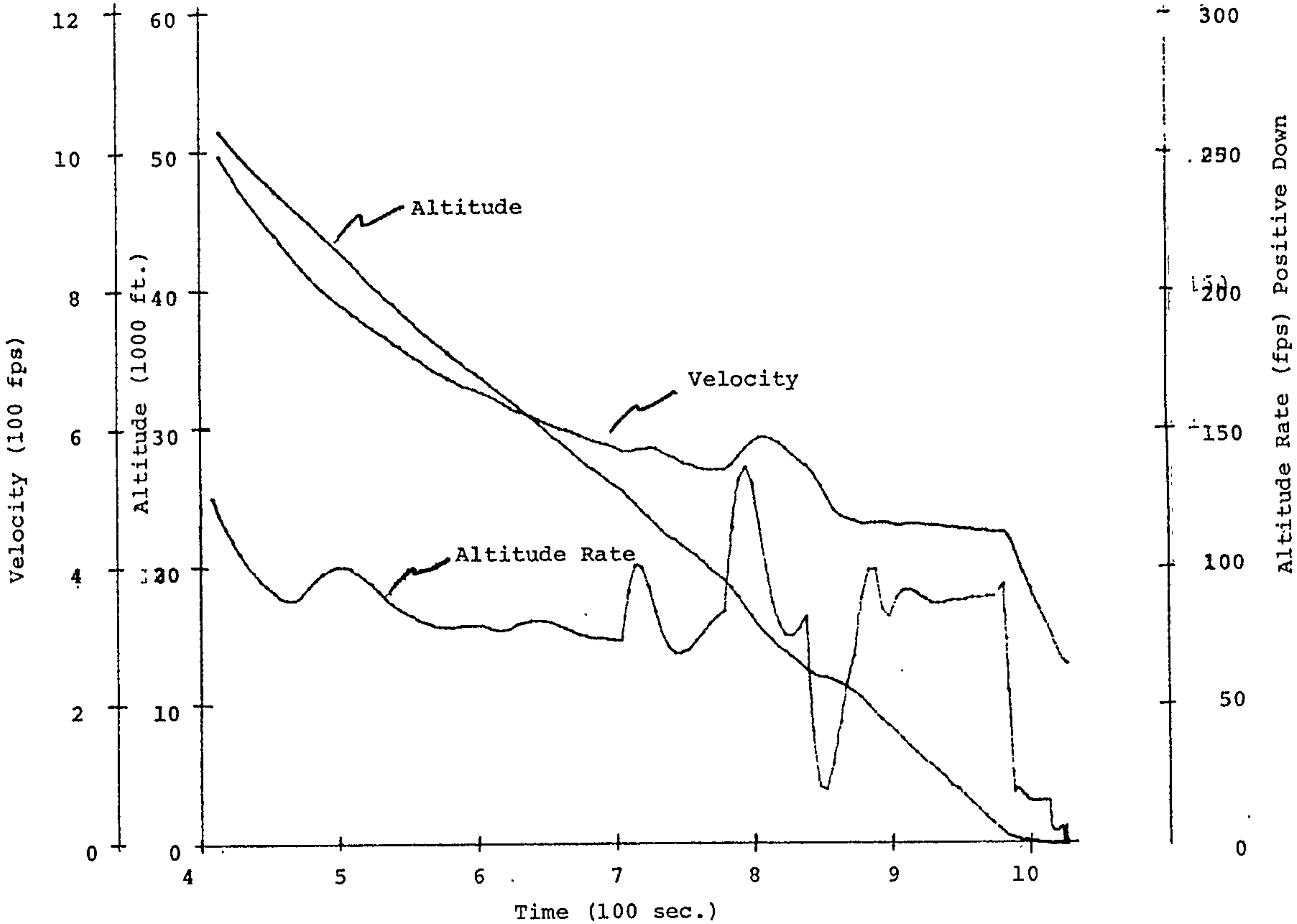

Fig. 4.28: Altitude Velocity & Altitude Rate Time Histories for Headwind Case

2/10/73

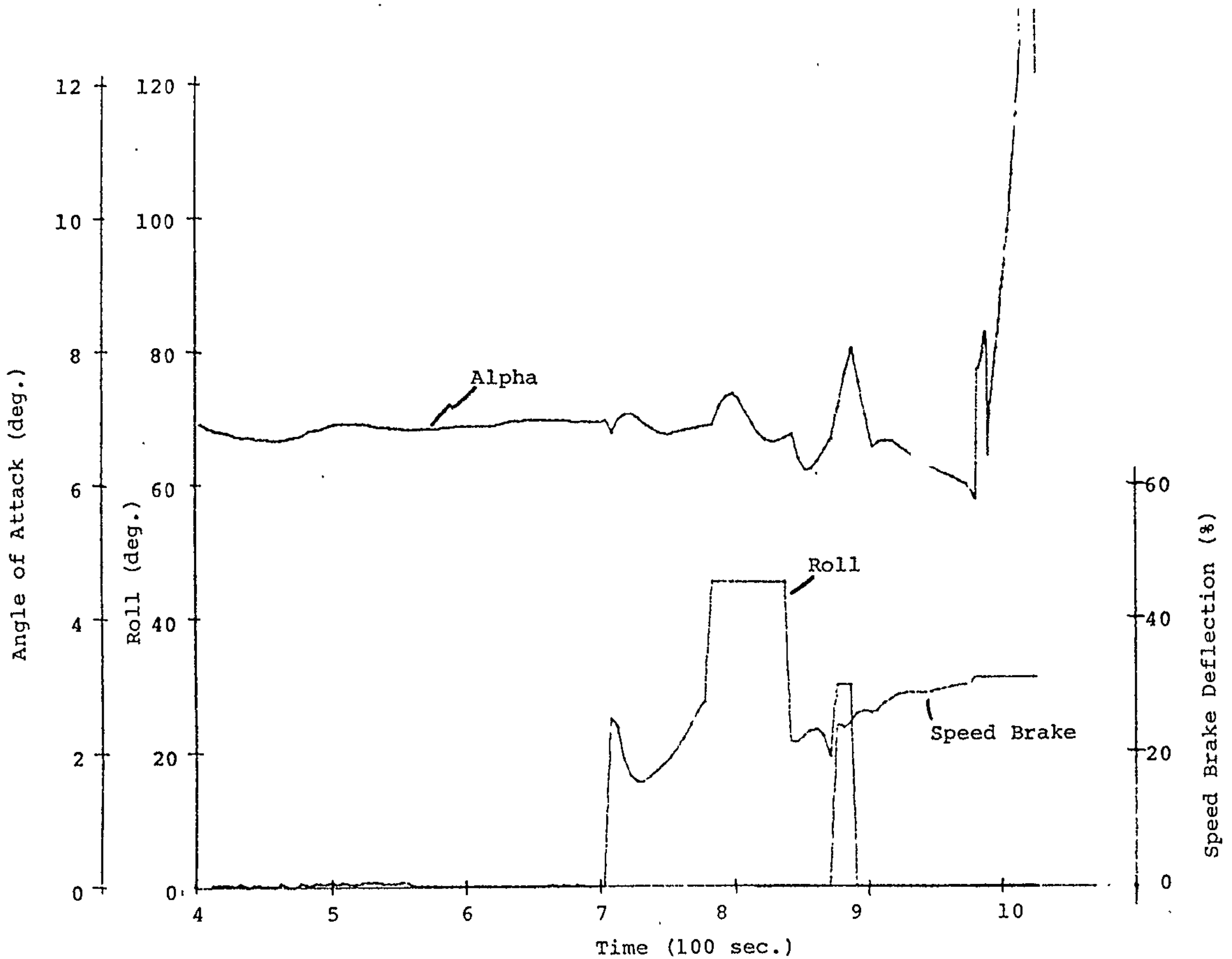

Figure 4.29:Roll, Alpha, Speed Brake Time Histories for Headwind Case

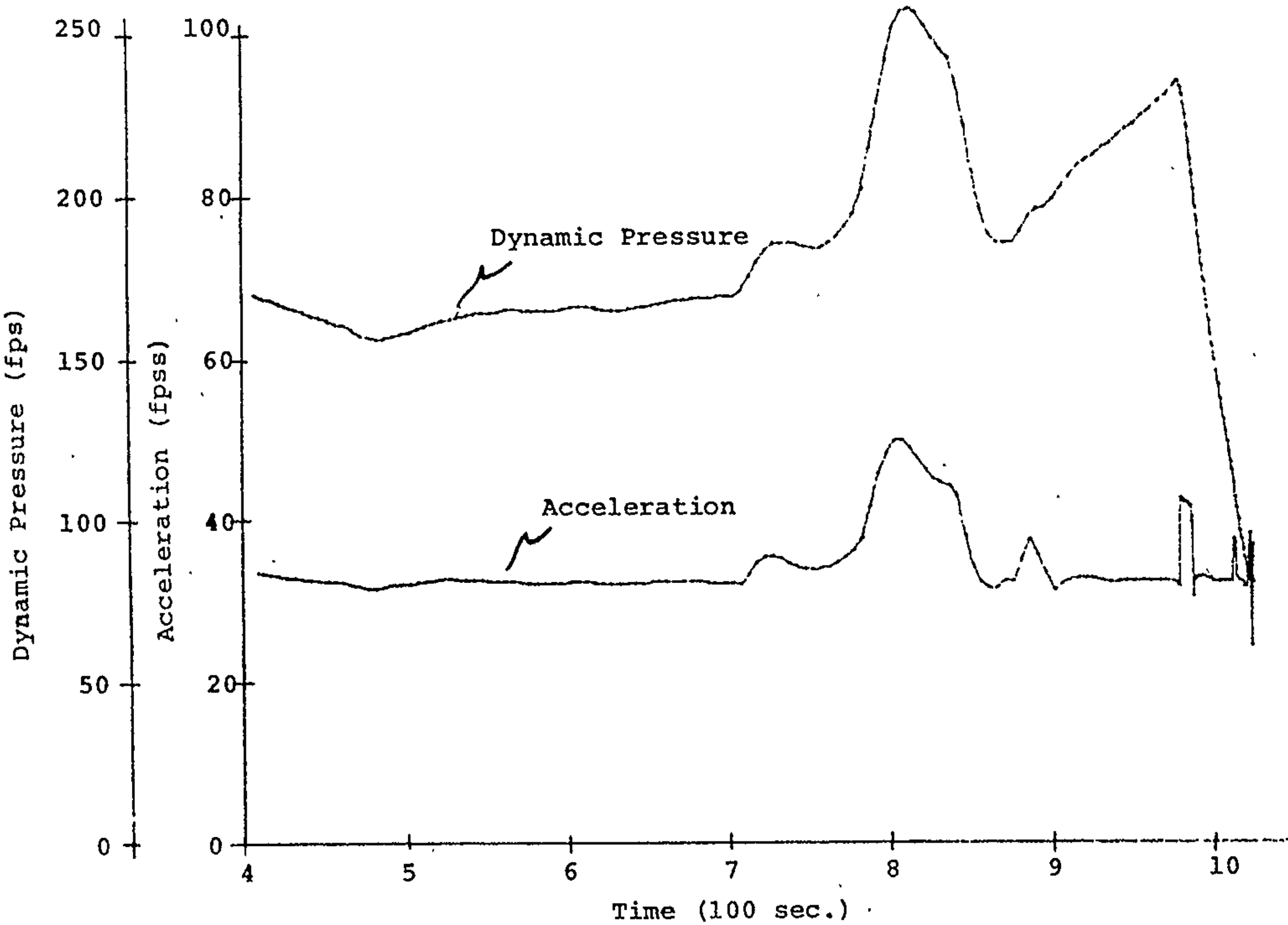

Fig. 4.30: Acceleration and Dynamic Pressure Time Histories for Headwind Case

2/14/73

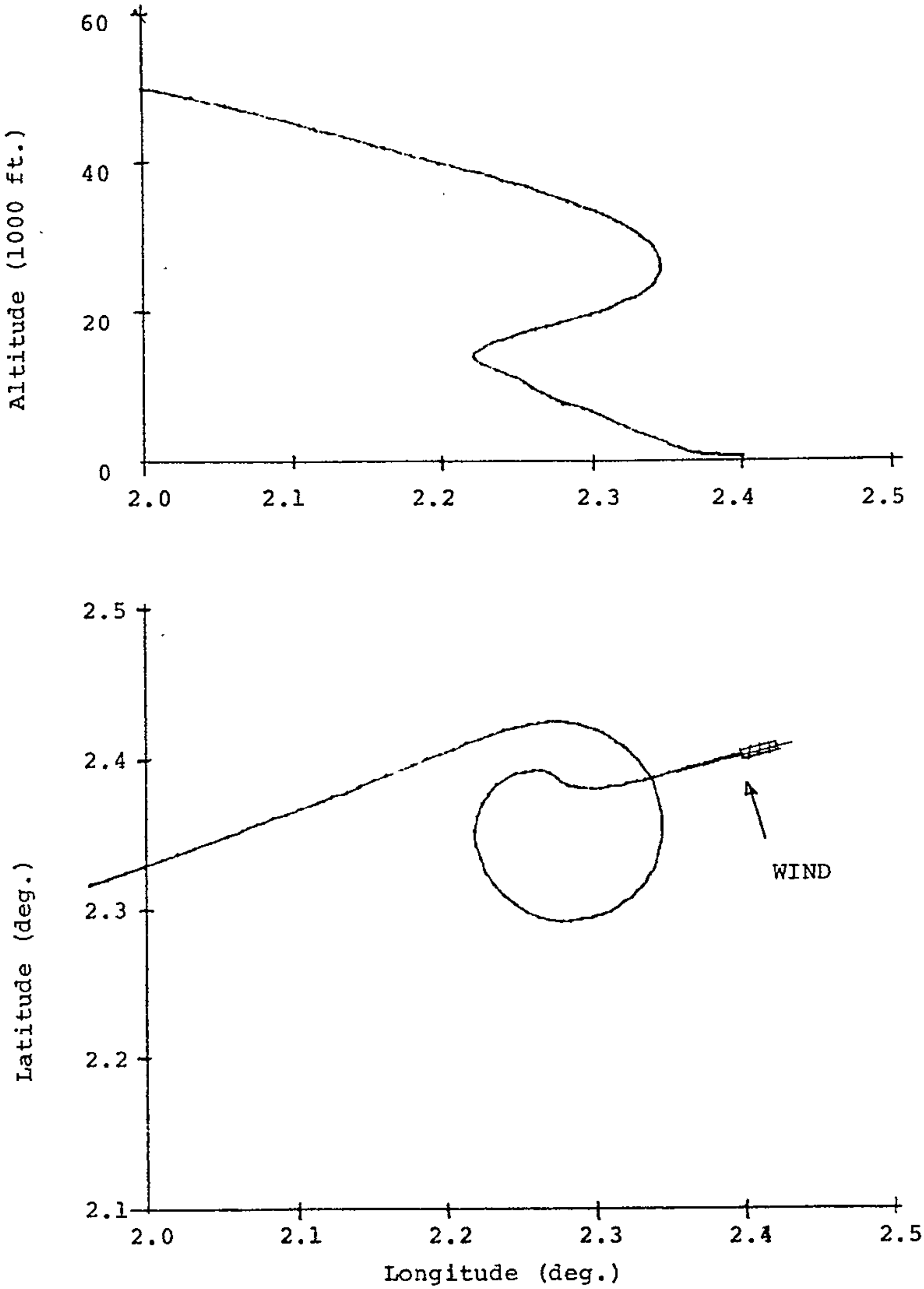

Figure 4.31: Ground Track & Elevation Views for Cross Wind Case

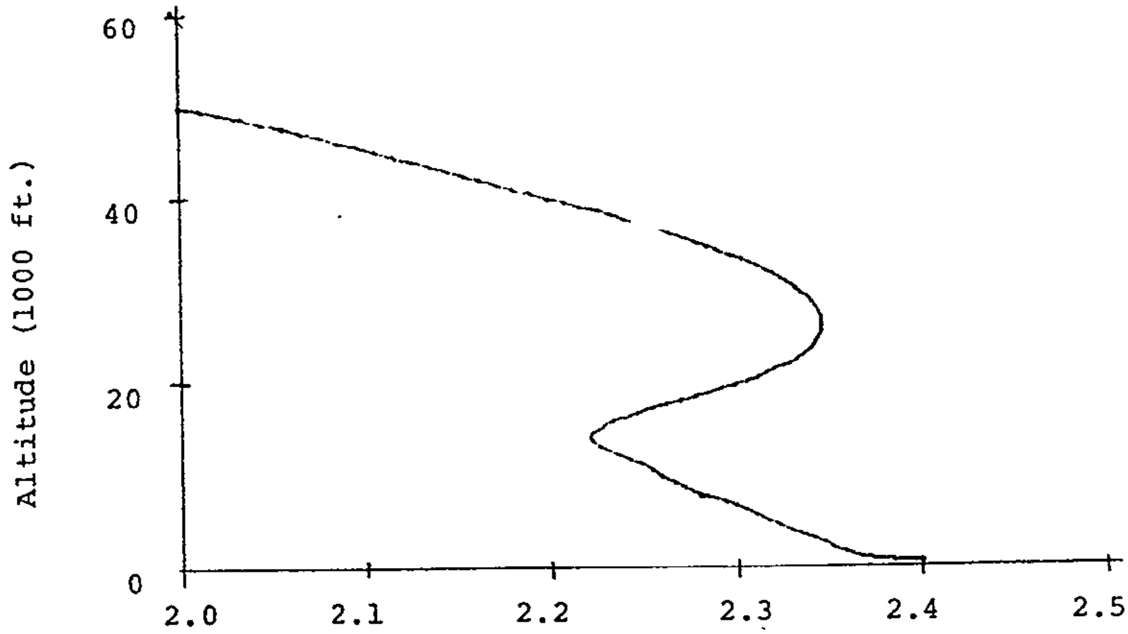

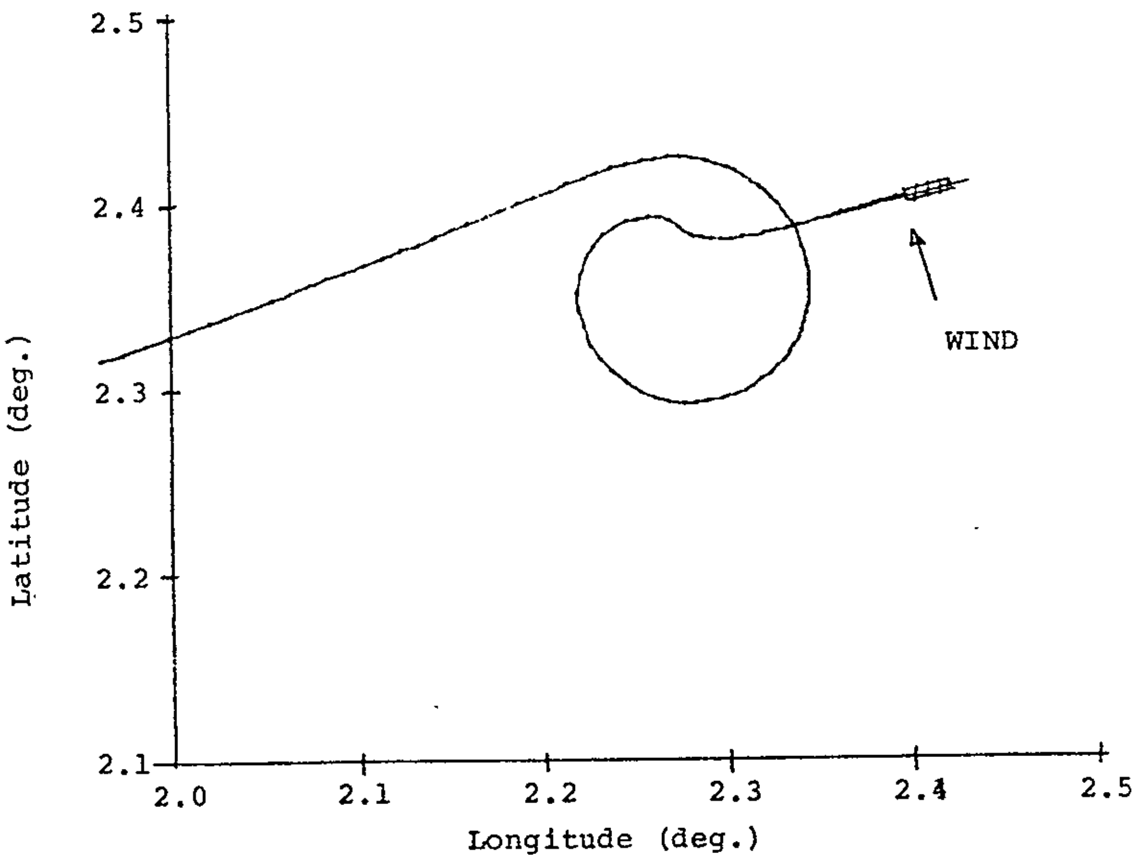

Figure 4.31: Ground Track & Elevation Views for Cross Wind Case

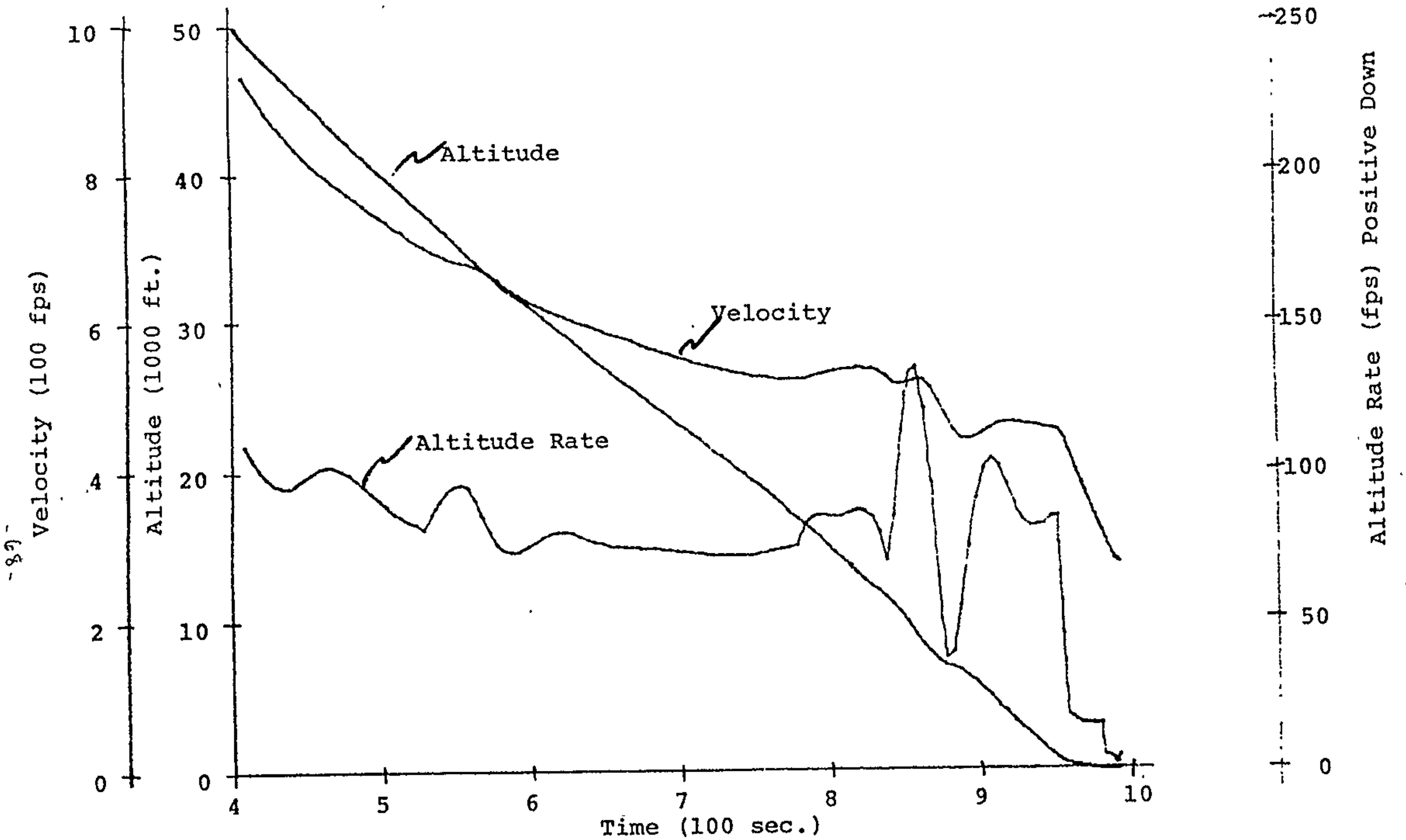

Figure 4.32: Altitude Velocity & Altitude Rate Time Histories for Cross Wind

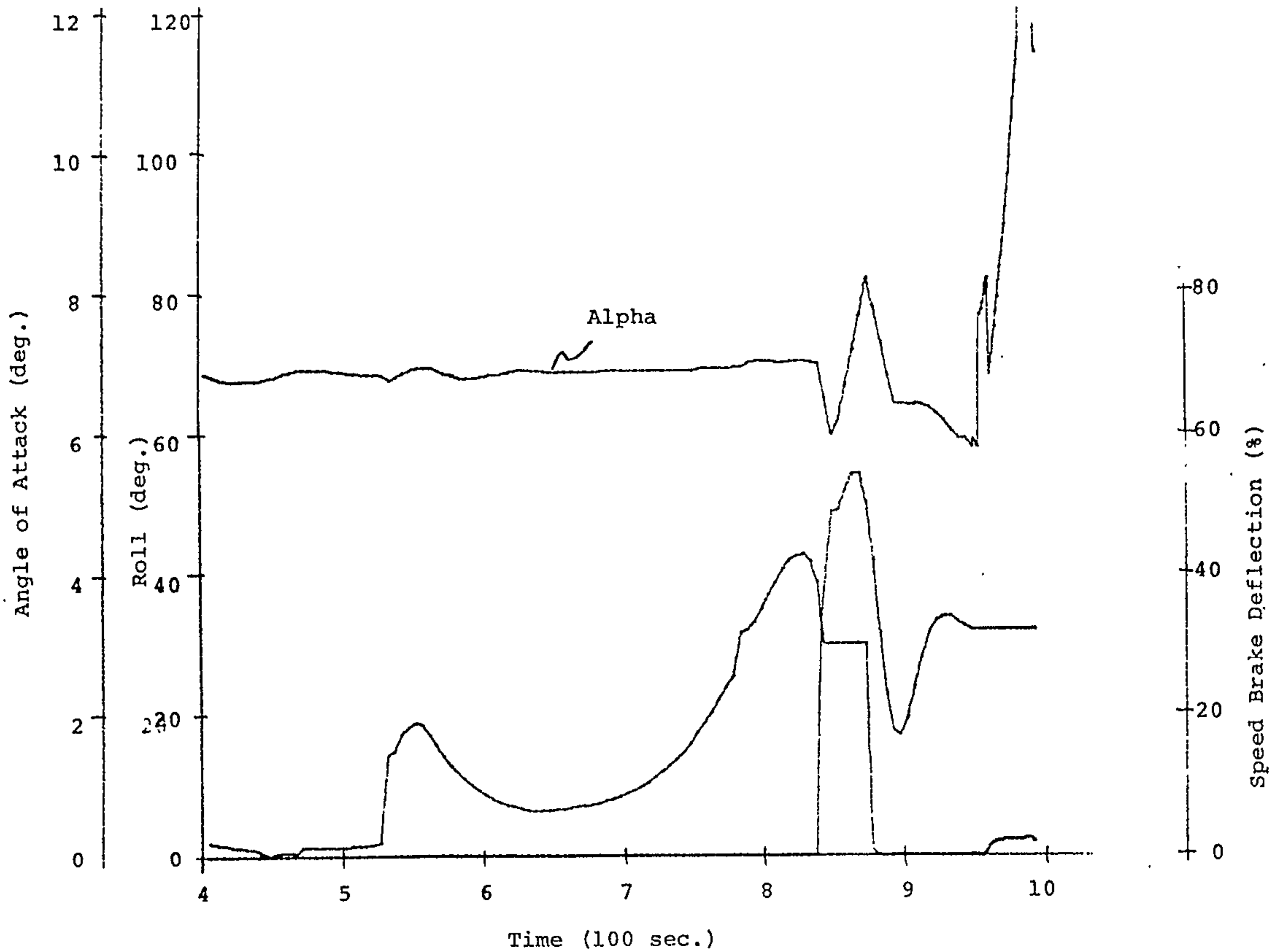

Figure 4.33: Roll, Alpha, Speed Brake Time Histories for Cross Wind Case

2/14/73

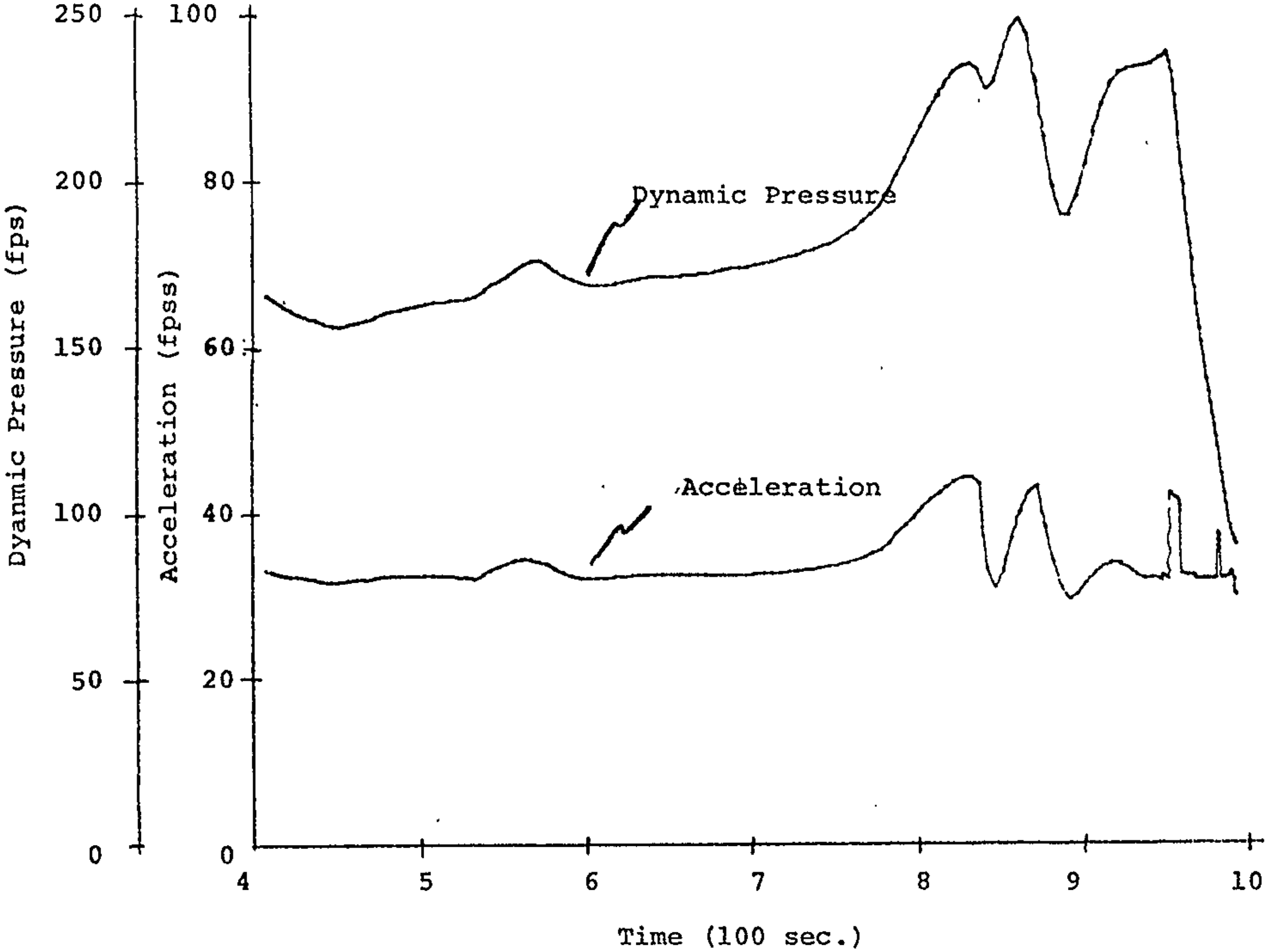

Fig. 4.34: Acceleration and Dynamic Pressure Time Histories for Cross Wind Case

2/14/73

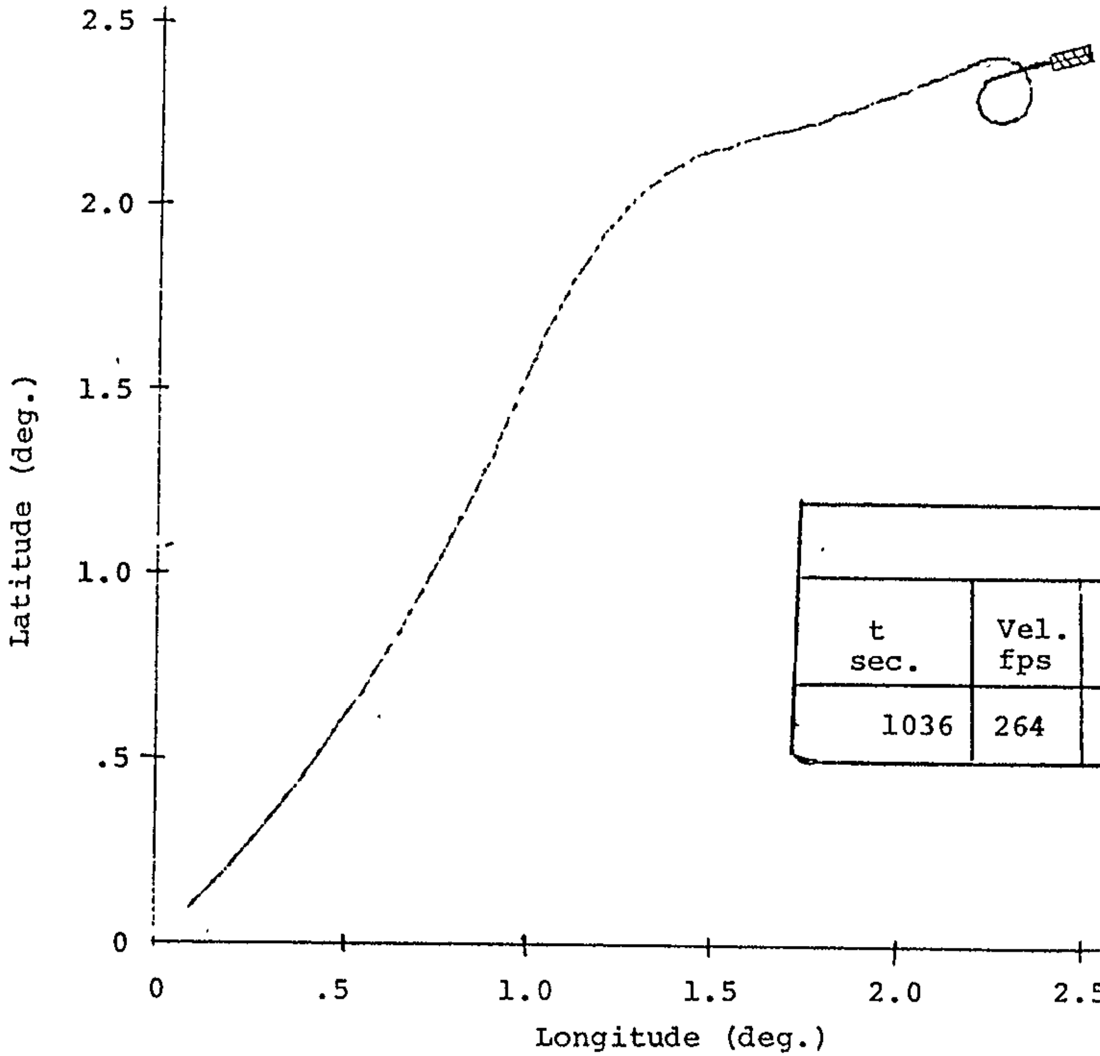

Landing Statistics				
t sec.	Vel. fps	Sink Rate fps	Azimuth	down range miss (ft.)
1036	264	-2.96	74.9	-1249

Fig. 4.35 : Ground Track for Down Gust During Final Approach

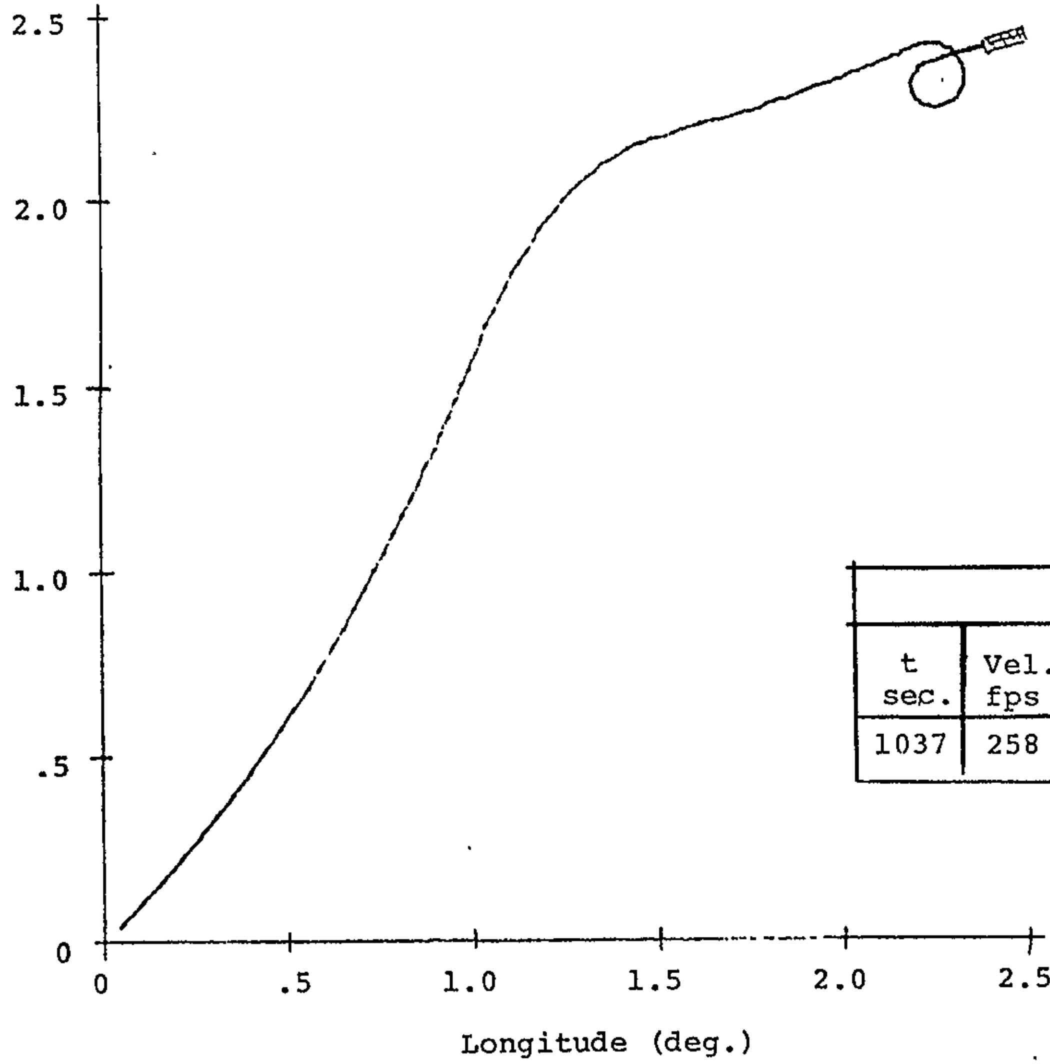

Landing Statistics				
t sec.	Vel. fps	Sink Rate fps	Azimuth	down range miss (ft.)
1037	258	-3.14	74.9	-600

Fig.4.36 : Ground Track for Cross Wind Gust During Final Approach

4.5 Vehicle Parameter Variations

In this section the vehicle mass and the vehicle L/D are each varied ± 20% for the nominal trajectory. Satisfactory performance is seen in all cases except that more information is needed in the flare logic in the low L/D case.

The heavier vehicle ground track is shown in Fig. 4.37. A higher velocity corresponding to the higher wing loading is seen. Also a tighter than nominal radius turn is made.

The lighter vehicle ground track is in Fig. 4.38. A higher than nominal turn radius is seen as is a lower than nominal landing velocity.

The high L/D vehicle ground track is shown in Fig. 4.39. A larger swing than nominal results from the transition ranging guidance responding to the higher ranging capability. Also a high landing velocity, 345 fps, shows that the flare logic could be improved with increased knowledge of L/D.

The low L/D case, Fig. 4.40 shows almost a direct path to the runway with no turn possible. The trajectory was nominal up until the flare. There the vehicle fell 7700 feet short of the runway as the range capability did not exist in the flare. Logic to allow for this possibility should be an easy addition. This logic would vary BIAS1 and HF2 as a function of the estimated maximum L/D.

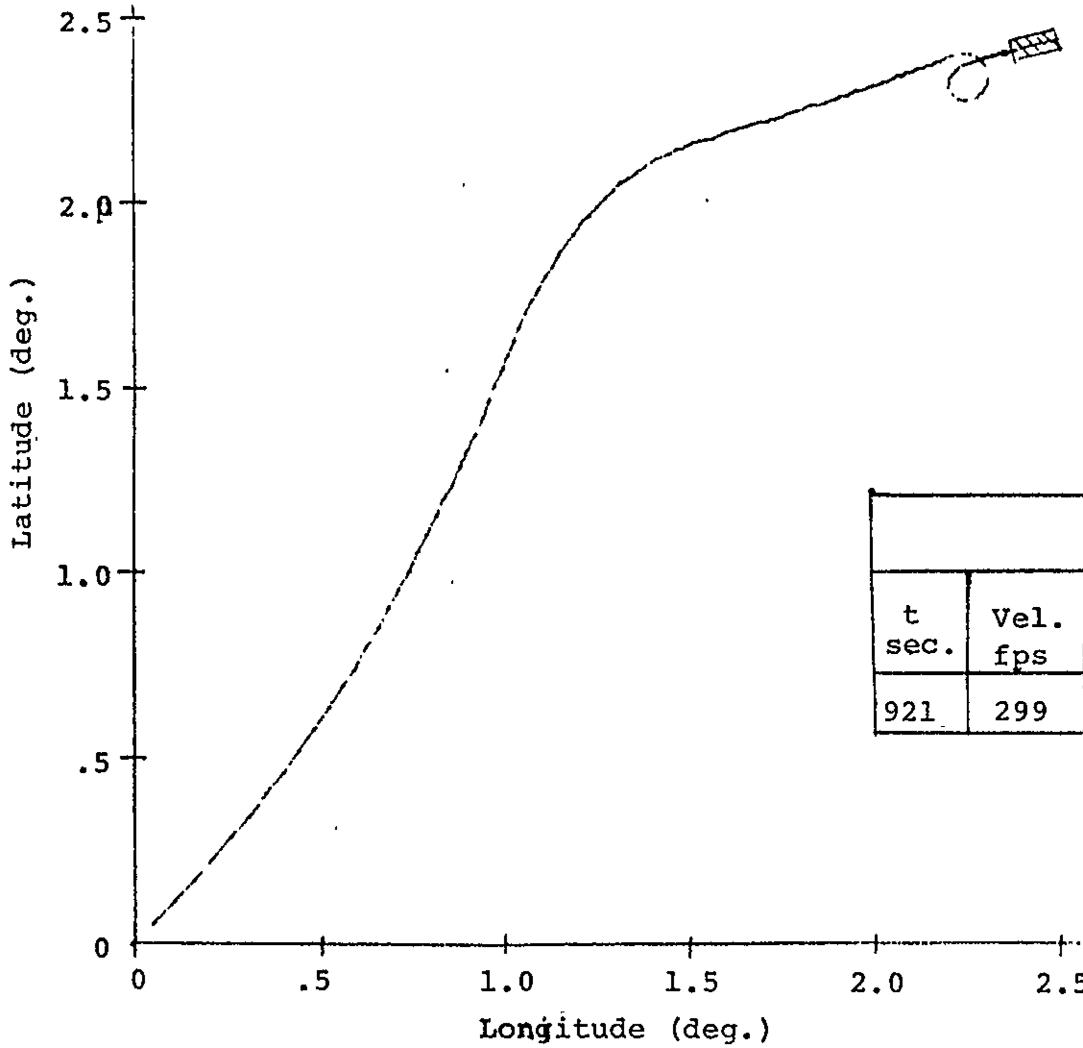

Landing Statistics				
t sec.	Vel. fps	Sink Rate fps	azimuth	down range miss (ft.)
921	299	-9.6	74.9	-2207

Fig.4.37: Ground Track for 20% Increase in Weight

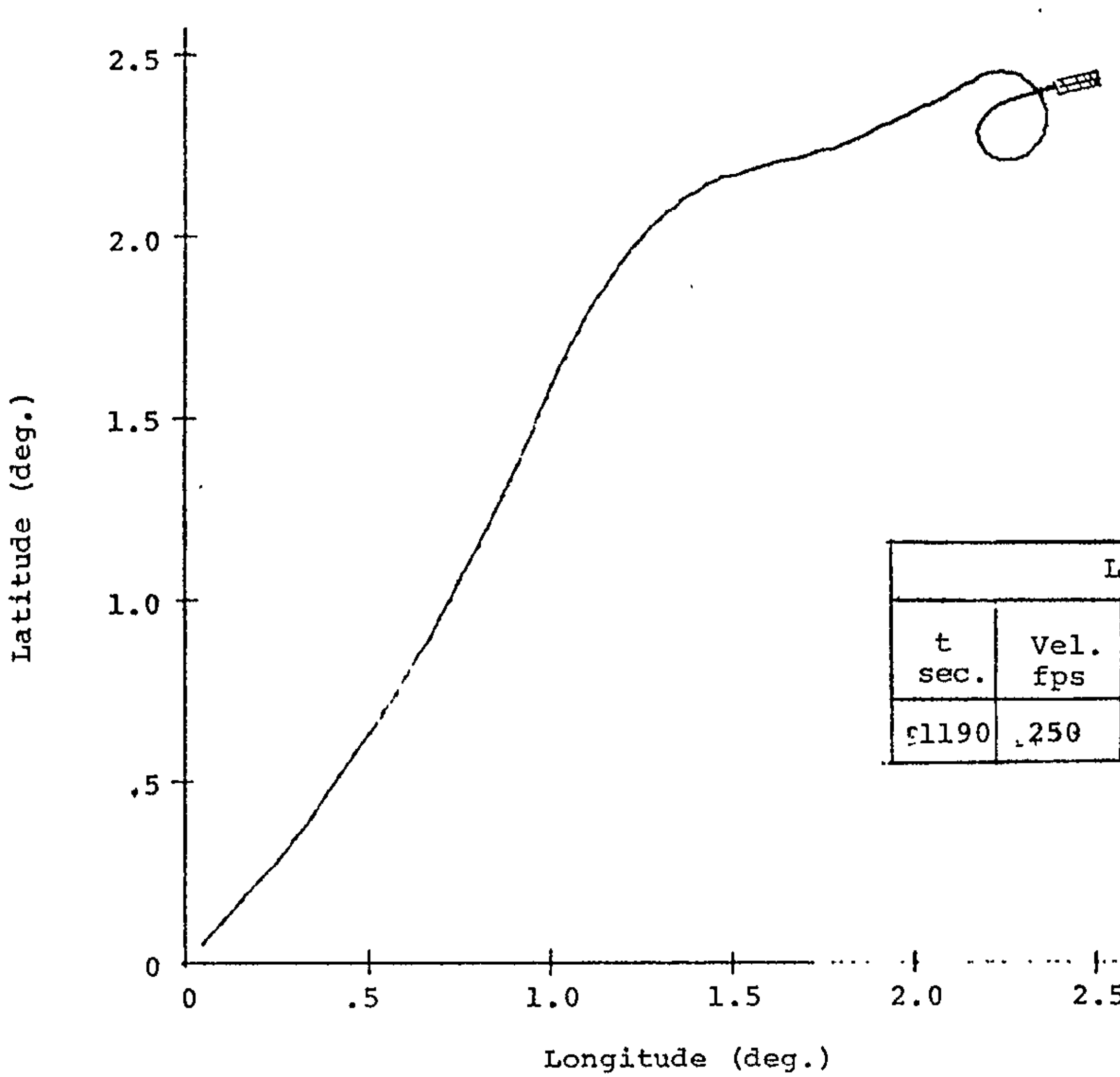

Landing Statistics				
t sec.	Vel. fps	Sink Rate fps	azimuth	down range miss (ft.)
1190	250	-4.2	74.9	-686

Fig. 4.38: Ground Track for 20% Decrease in Weight

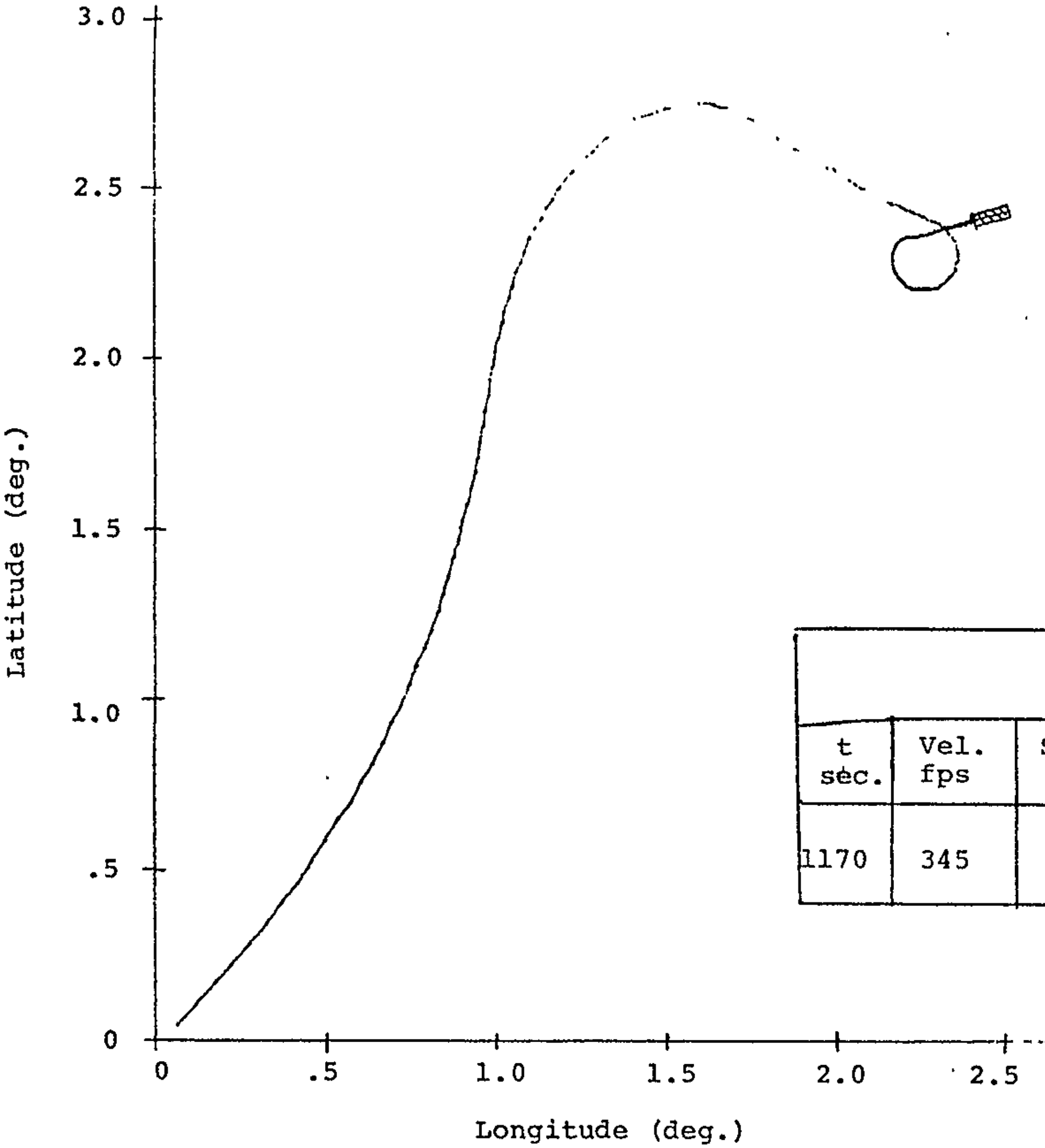

Landing Statistics

t sec.	Vel. fps	Sink Rate fps	azimuth	down range miss (ft.)
1170	345	-3.2	75.0	2109

Fig.4.39:: Ground Track for 20% Increase in L/D

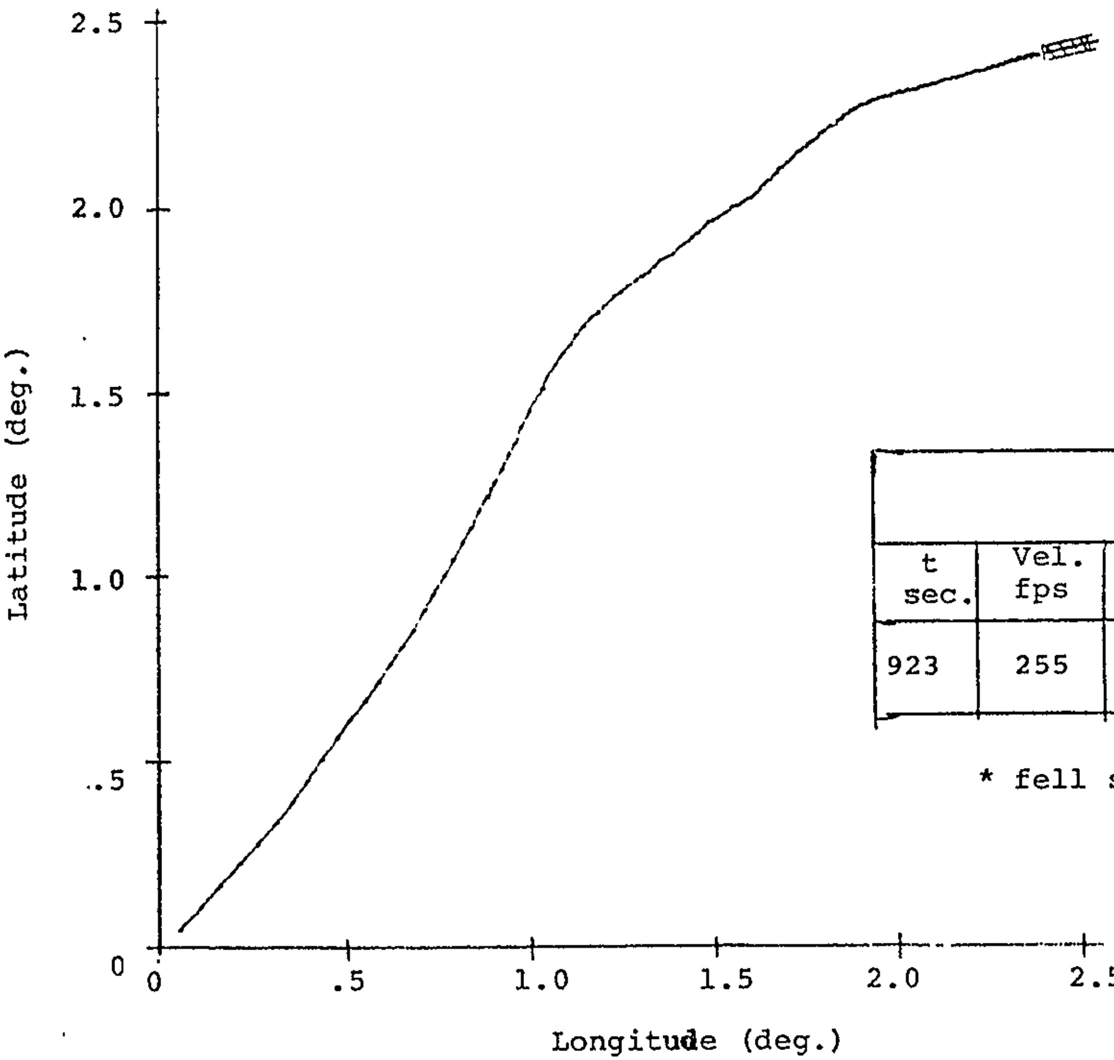

Landing Statistics

t sec.	Vel. fps	Sink Rate fps	azimuth	range down miss (ft.)
923	255	-43*	7	-7700*

* fell short of runway during flare.

Fig. 4.40 : Ground Track for 20% Decrease in L/D

4.6 Atmospheric Variations

Variations were made of ± 20% density about the nominal density as defined by the 1962 U.S. Standard Atmosphere.

The 20% decrease in density ground track is shown in Fig. 4.41. It is very similar to the low weight case, Fig. 4.37, as one might expect. Even the landing velocities of the two cases compare closely, 306 fps versus 299 fps.

The 20% increased case, Fig. 4.42 is very similar to the high mass case. Again, the landing velocities of the two cases compare very closely.

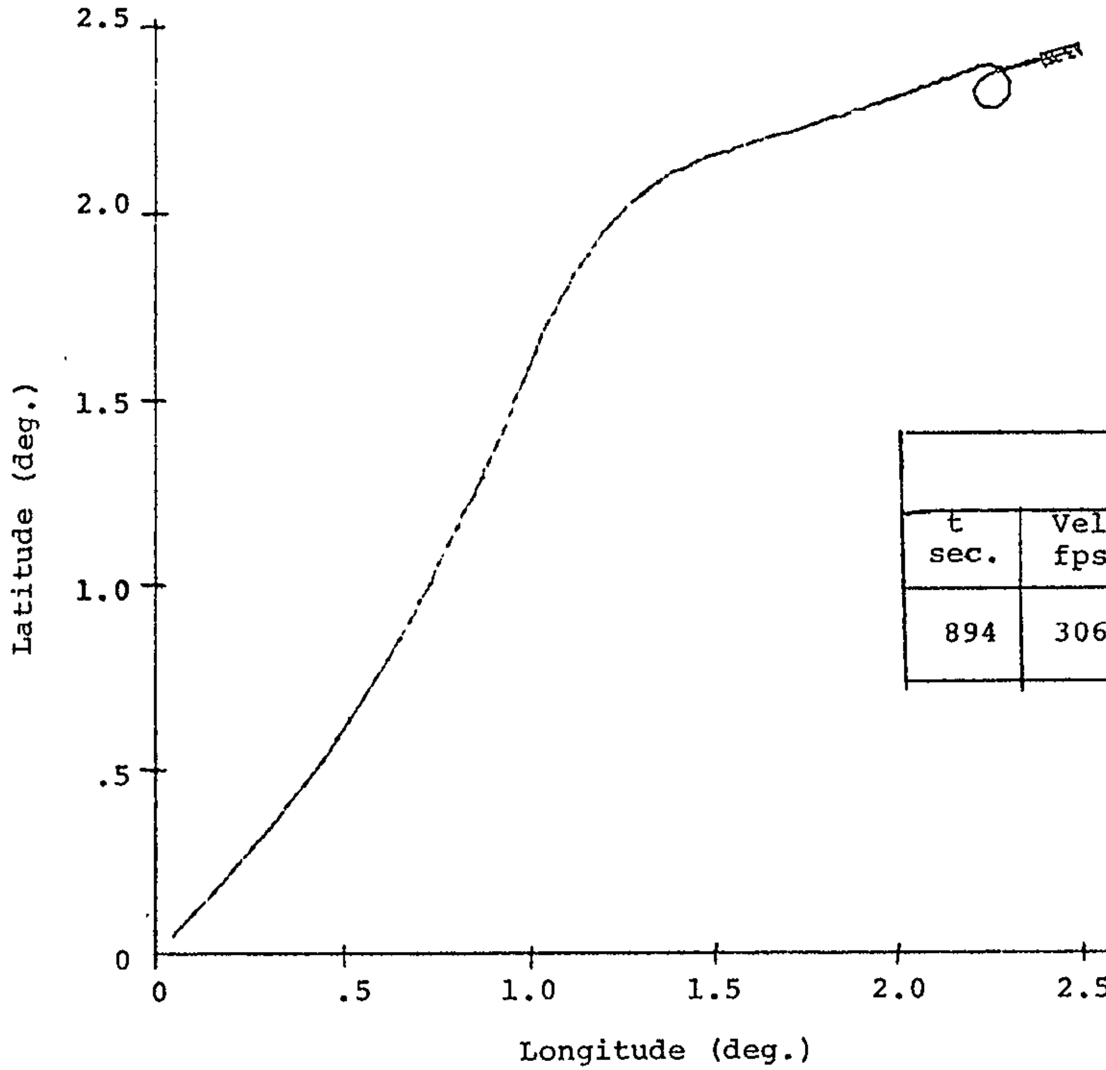

Landing Statistics				
t sec.	Vel. fps	Sink Rate fps	azimuth	down range miss (ft.)
894	306	-10.1	74.9	2093

Fig. 4.41: Ground Track for 20% Decrease in Density

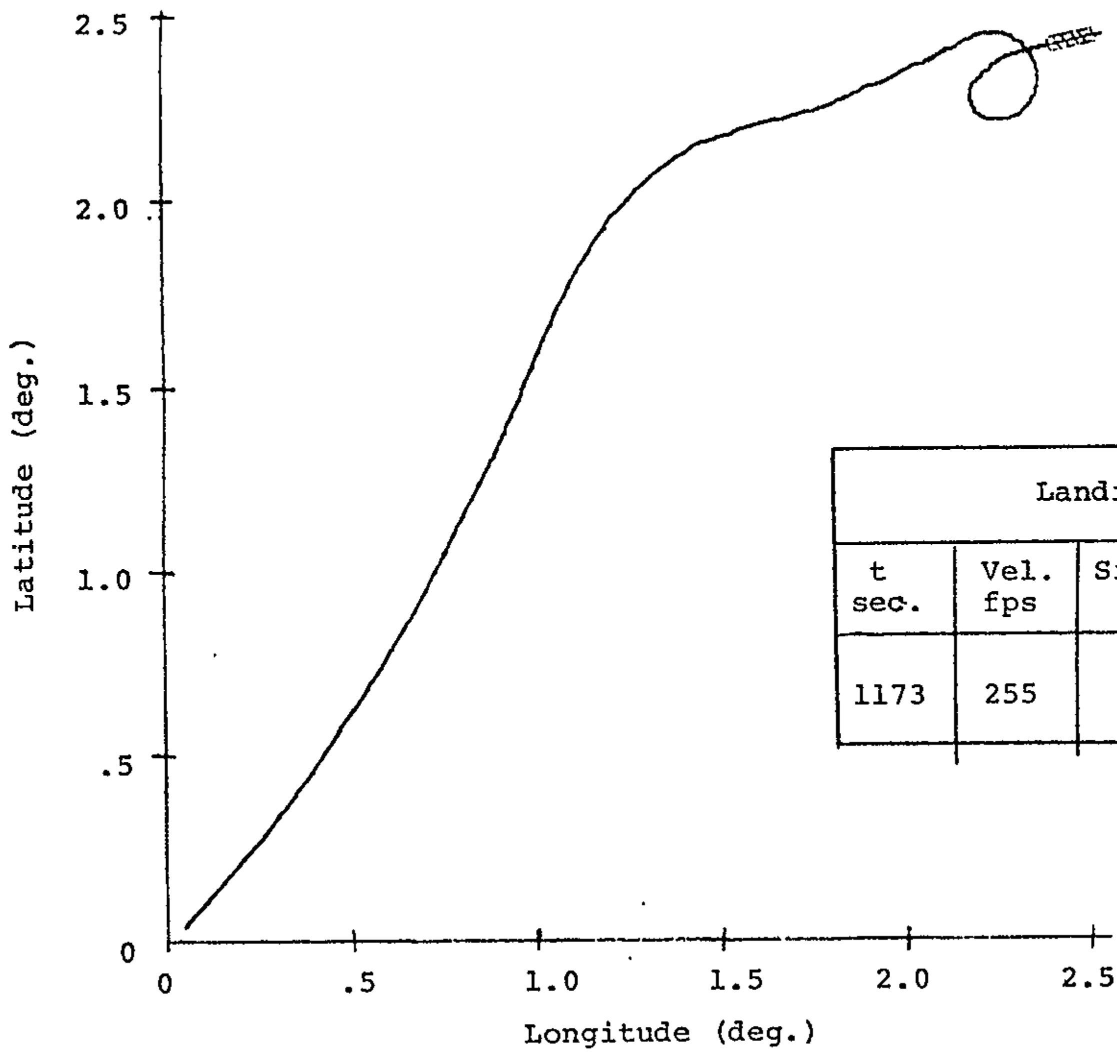

Landing Statistics				
t sec.	Vel. fps	Sink Rate fps	azimuth	down-range miss (ft.)
1173	255	-4.4	74.9	-1240

Fig.4.42:Ground Track for 20% Increase in Density

4.7 Navigation Performance

The effect of navigation errors was determined by a simulation combining the steering equations in a closed loop manner with an aided inertial navigation system. The navigation system is essentially that of ref. [12] although reasonably close agreement has been obtained with results of ref. [14].

The system details are in Appendix E.

The component parts are:

1. Kearfott KT70 Inertial Navigation Unit

2. Navigation Filter of ref. [12]

   - with 13 states (2 DME bias estimates)
   - square root formulation
   - non-linear compensation

3. Six measurements to update navigation

   1,2 DME 1 & 2
   3. Barometric altimeters
   4. Radar altimeter
   5. ILS localizer
   6. ILS glide slope

4. A second case using 3 Cubic CR100 type precision DME's was considered.

In the first case, attention was turned to the landing site at Cape Kennedy. This landing site and vehicle initial conditions are in Table 4-3.

V	= 6055 fps
H	= 143020 ft
γ	=-1.9 deg
azimuth	= 115 deg
Mach	= 5.77
α	= 29°
latitude	= 29.43
longitude	= 275.45
runway latitude	= 28.55 deg
runway longitude	= 279.39 deg
runway azimuth	= 150 deg

Table 4-3: Vehicle Initial State and Runway for Cape Kennedy Landing

The initial errors are summarized in Table 4-4. These are from Ref. [11] as typical of a once-around abort mission using Kearfott equipment. The navigation update time was 5 sec. initially, and 1 sec. on final approach. A table of significant navigation events is given in Table 4-5.

The ground track for this trajectory is shown in Fig. 4.43. The similarity to the nominal trajectory, Fig. 4. 1 , is by design. The trajectory parameters are shown in Fig. 4.44 through 4.46.

The altitude error time history is shown in Fig. 4.47. Both the actual error and computer one sigma estimate is shown. It is seen that there is little improvement in this altitude error until the barometric altimeter comes on at 215 seconds. A second improvement comes at 940 seconds under the action of the radar altimeter. See the expanded scale Fig. 4.48. There is but 40 seconds of good altitude information before touchdown. But it is enough.

The East position error time history is shown in Fig. 4.49. The initial value of 40000 meter is reduced to about 1000 meters within the first several measurements. A second improvement comes with the barometric altimeter event. And another improvement comes with the action of the ILS localizer, on at 900 sec, Fig. 4.50. Finally, the improvements effected by the radar altimeter show their effect in the East channel at about 980 sec.

The North channel errors, Fig. 4.51, are slower to converge That is because this is the largely unobservable cross track direction. But again, the barometric altimeter helps convergenc at about 200 seconds. An expanded view of this channel is in Fig. 4.52.

The only real effect of these errors is seen in the commanded roll angle, Fig. 4.44, where excursions (noise) of about 2 degrees is seen. The initial transient as the large initial errors are solved is the step from -29 to -15 degrees.

That the cross track error can be a problem is illustrated in Table 4-6. Here are one minute summaries of actual errors for the largest allowable initial cross track error ($\delta N=32000$). Larger errors cause filter divergence. This is illustrated in a failed case, Table 4-7, ($\delta N = -64000$). Here, the filter settled on a false solution displaced in track because there was no information to the contrary.

The condition was easily fixed by using the VOR portion of the DME for the first 200 seconds. Even though the VOR had a bias of 1 degree, this was enough to resolve the problem. No amount non-linear filtering will solve this problem. More information must be added. An alternate solution would be to place the two DME's further apart, thus, decreasing the geometric dilution.

4.7.1 Precision DME Navigation

Still another solution would be to use more precise DME equipment. Such is the Cubic CR100 equipment with a bias of 1 meter.

A ground track of trajectory guided with this equipment is shown in Fig. 4.53. The equipment is described in Ref. [12]. The three transponders are placed 3 Km to the side 3 Km in front and 15 Km in front of the runway. A 30 sec. update is initially made with a 5 sec. update on final approach. As can be seen from Fig. 4.54 to 4.56, a much lower level of errors results than in the preceding case. Were other considerations not overriding, such as the cost of equiping alternate runways, this equipment would certainly be preferred.

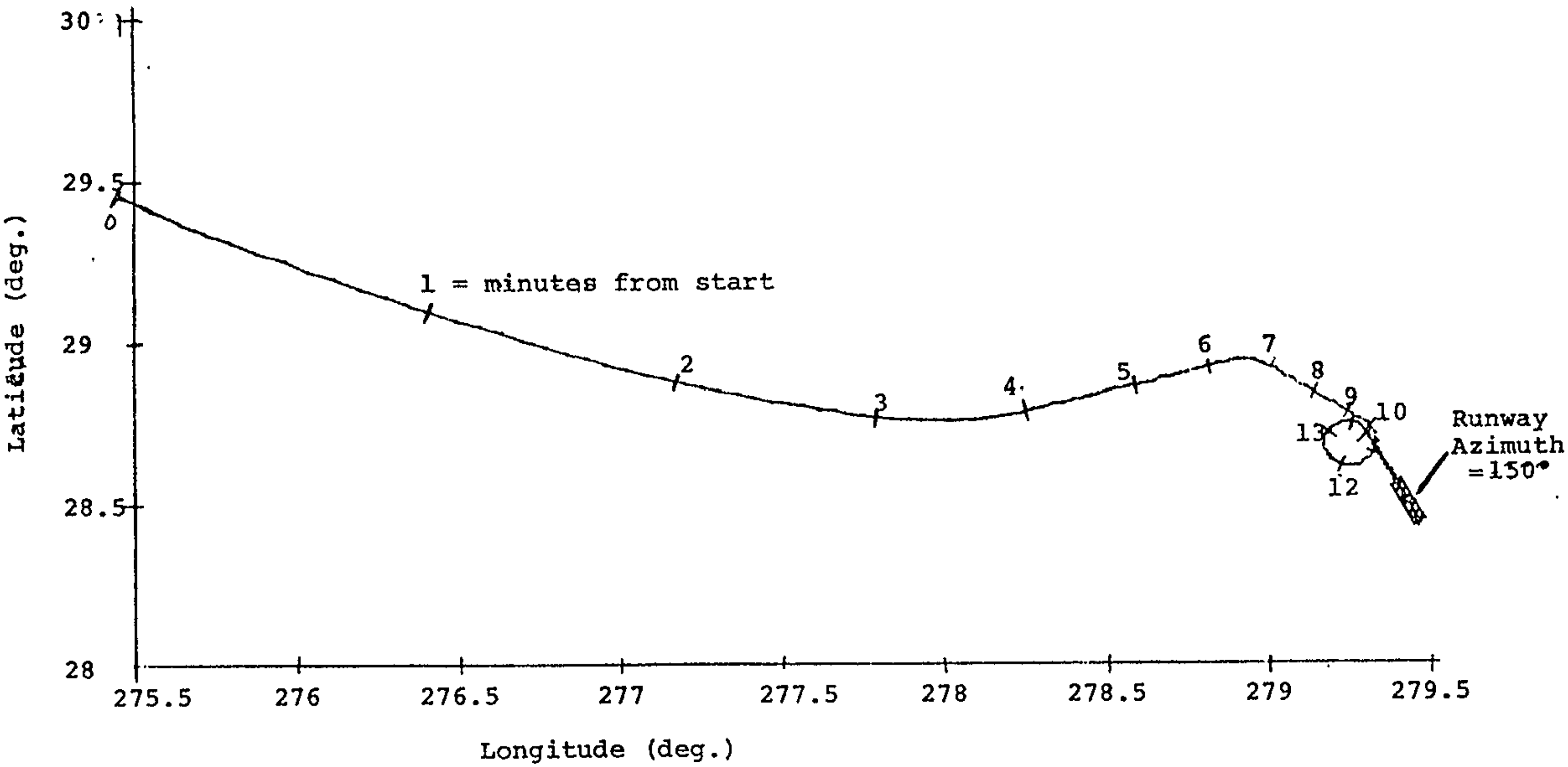

Fig. 4.43: Ground Track for Nominal Landing at Cape Kennedy

2/10/73

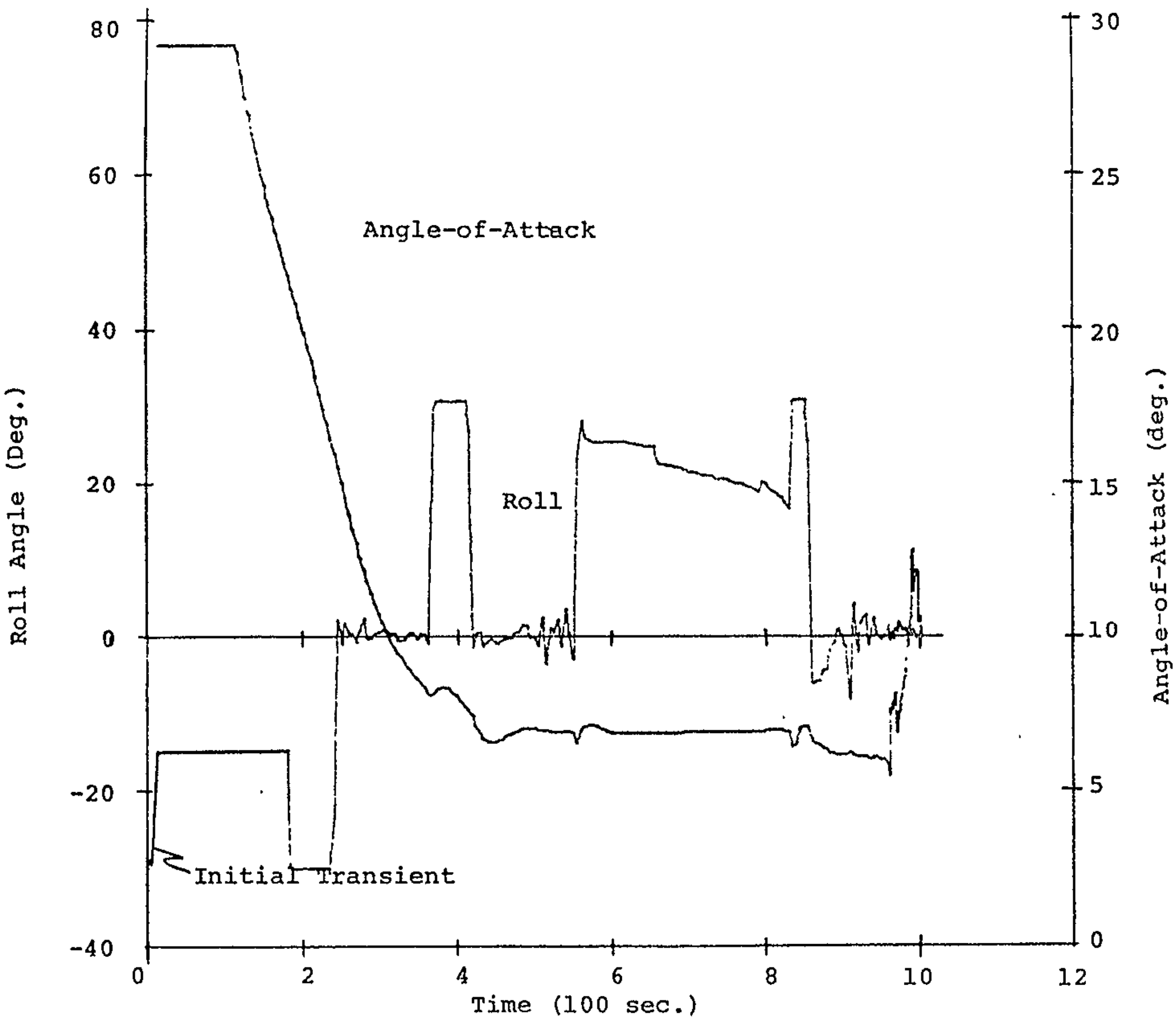

Figure 4.44: Roll and Angle-of-Attack Time Histories (With Errors)

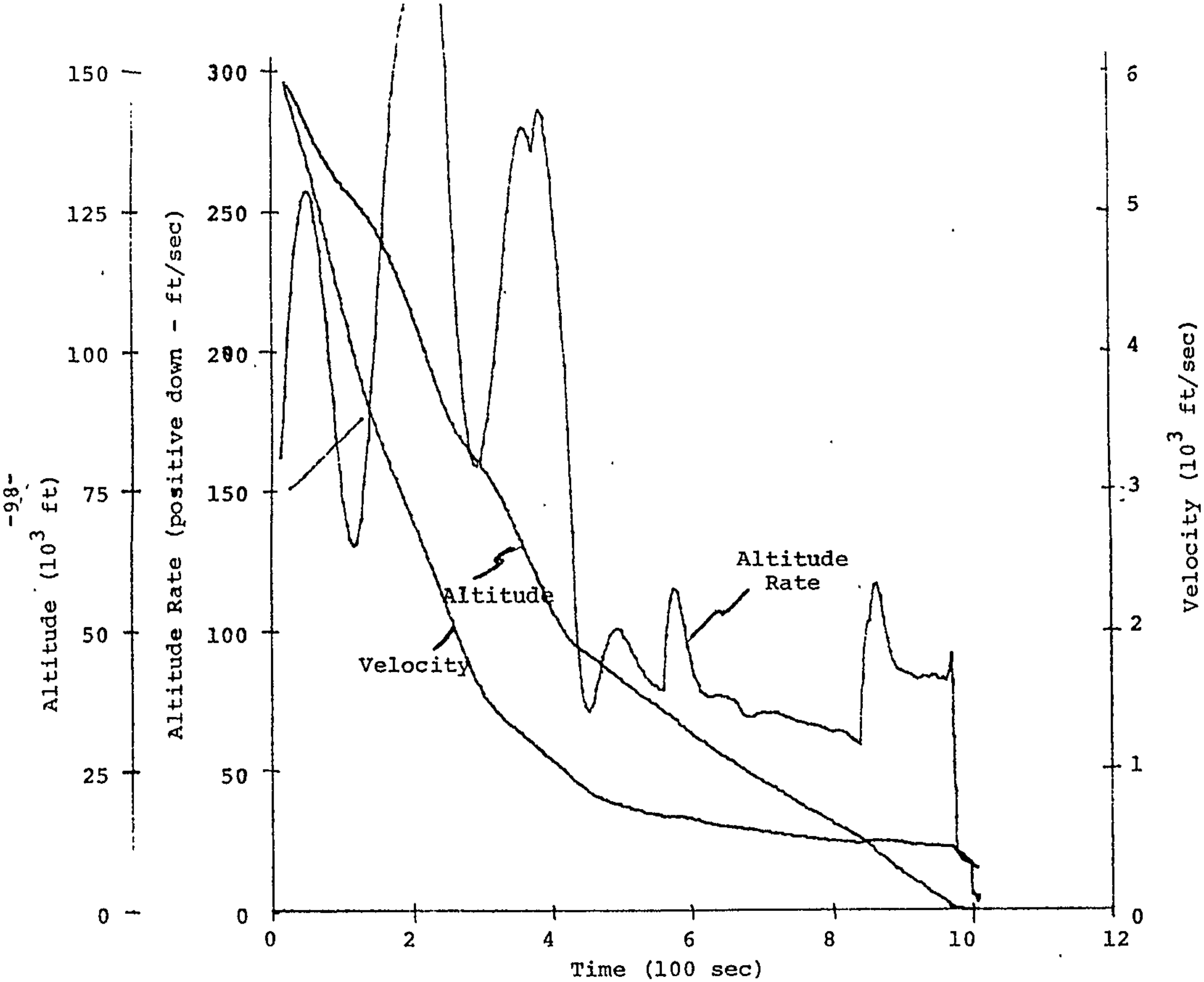

Fig. 4.45: Velocity, Altitude and Altitude Rate Time Histories (With Errors)

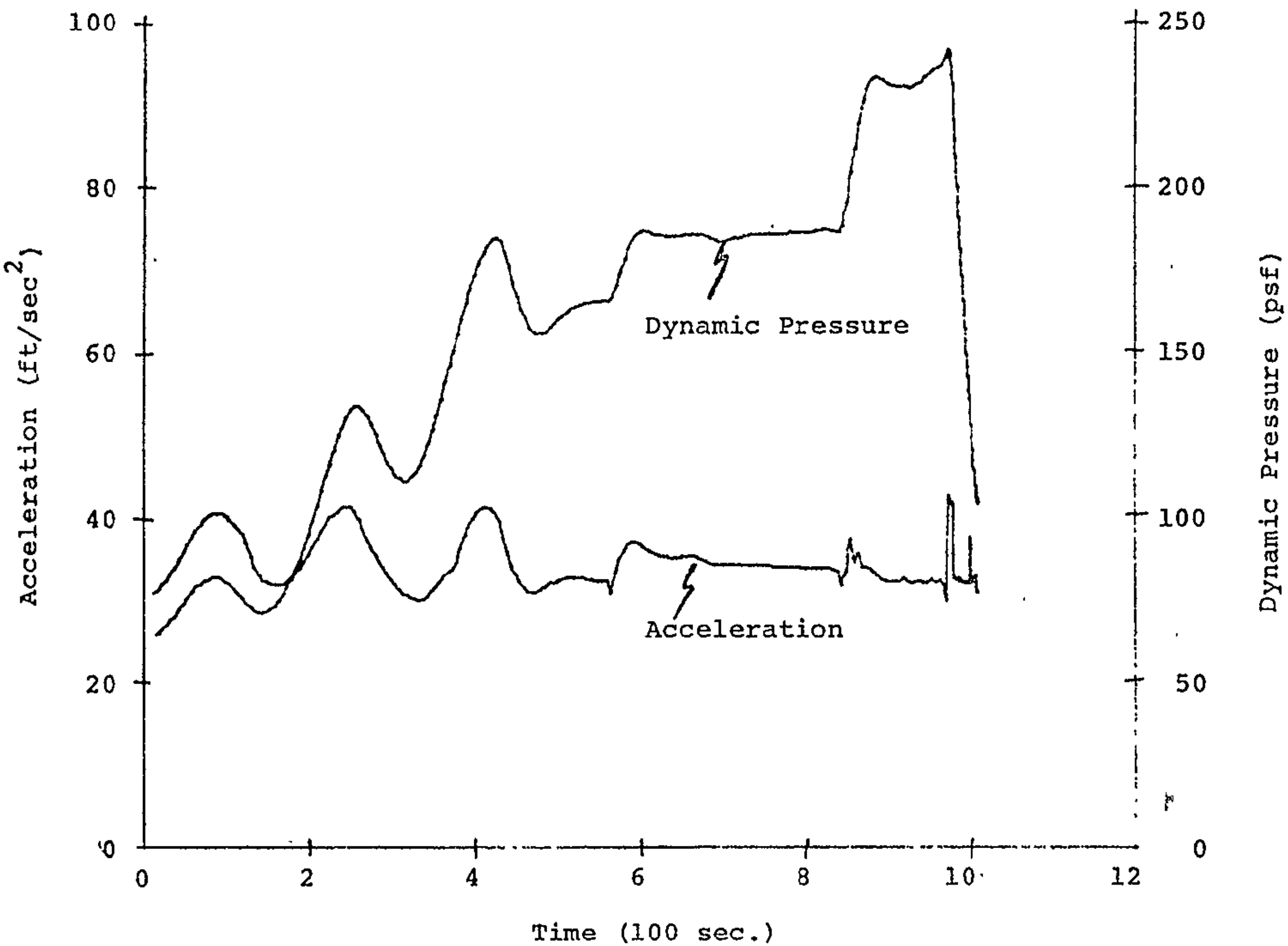

Fig.4.46: Acceleration and Dynamic Pressure - Time Histories (With Errors)

2/10/73

Direction	Position		Velocity Error	
	error (m)	Std dev (m)	error (m/sec)	Std dev (m/sec)
East	40,000	38692	.43	42.80
North	-8,000	12975	0	42.8
Up	3,000	3000	.7	13.41

Direction	Tilts	
	error (μrad)	Std dev (μrad)
about E	-690	685
about N	390	396
Azimuth	590	594

Table 4-4: Initial Errors

Time (sec)	Event
0	Start DME measurements (2)
215	Start Baro altimeter (H = 30Km)
905	Start localizer (H = 2.84m)
945	Start radar altimeter (H = 800m)
960	Start fast time update (H < 400m)
975	Closest approach to DME1 (H = 101.6m)
981	Drop DME2 (elevation less than 1°)
989	Drop DME1 (elevation less than 1°)
1001	Touch down

Table 4-5: Time History of Measurement Events

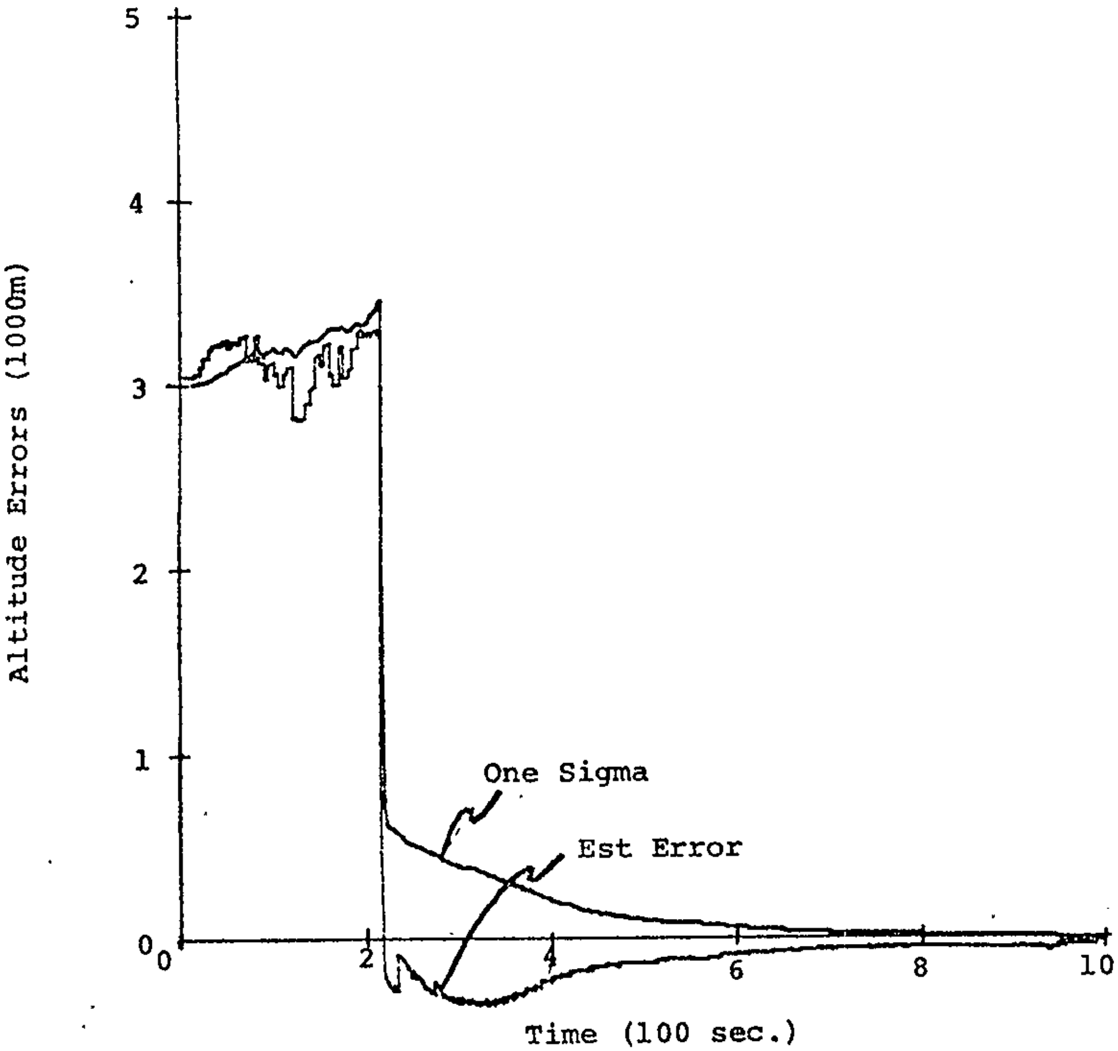

Fig. 4.47 Altitude Estimation Error & Computed One Sigma Uncertainties

2/10/73

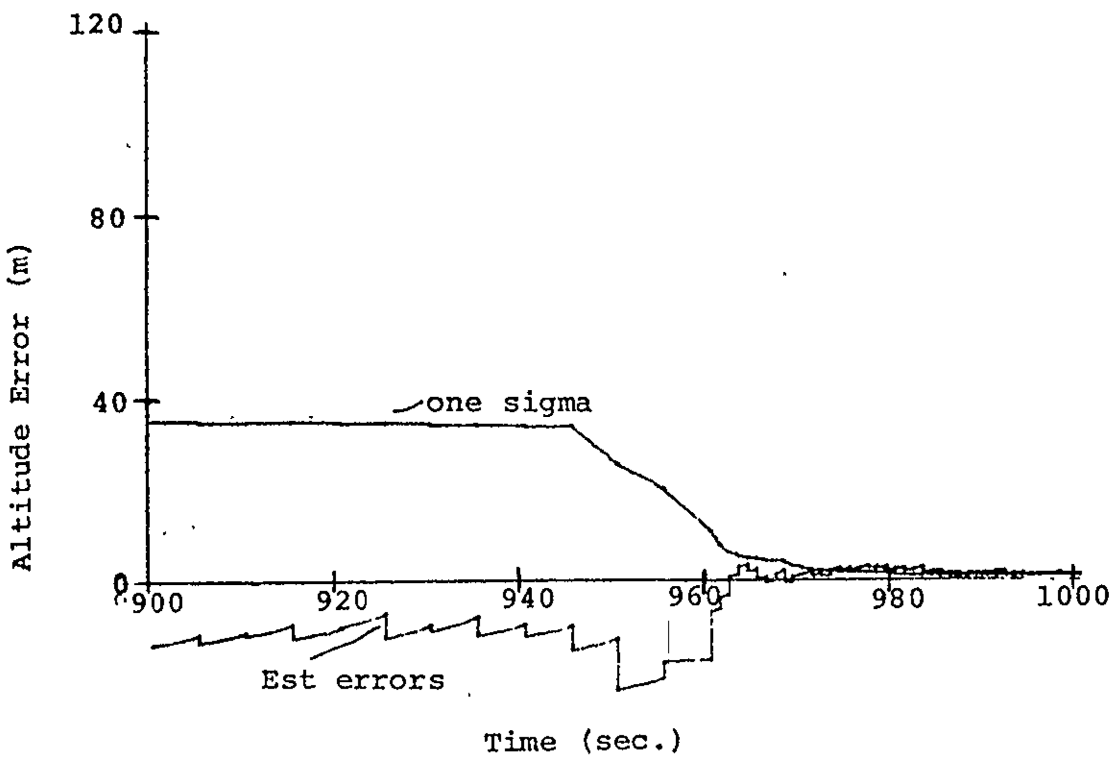

Fig.4.48:Altitude Estimation Error & Computed One Sigma Uncertainties

2/10/73

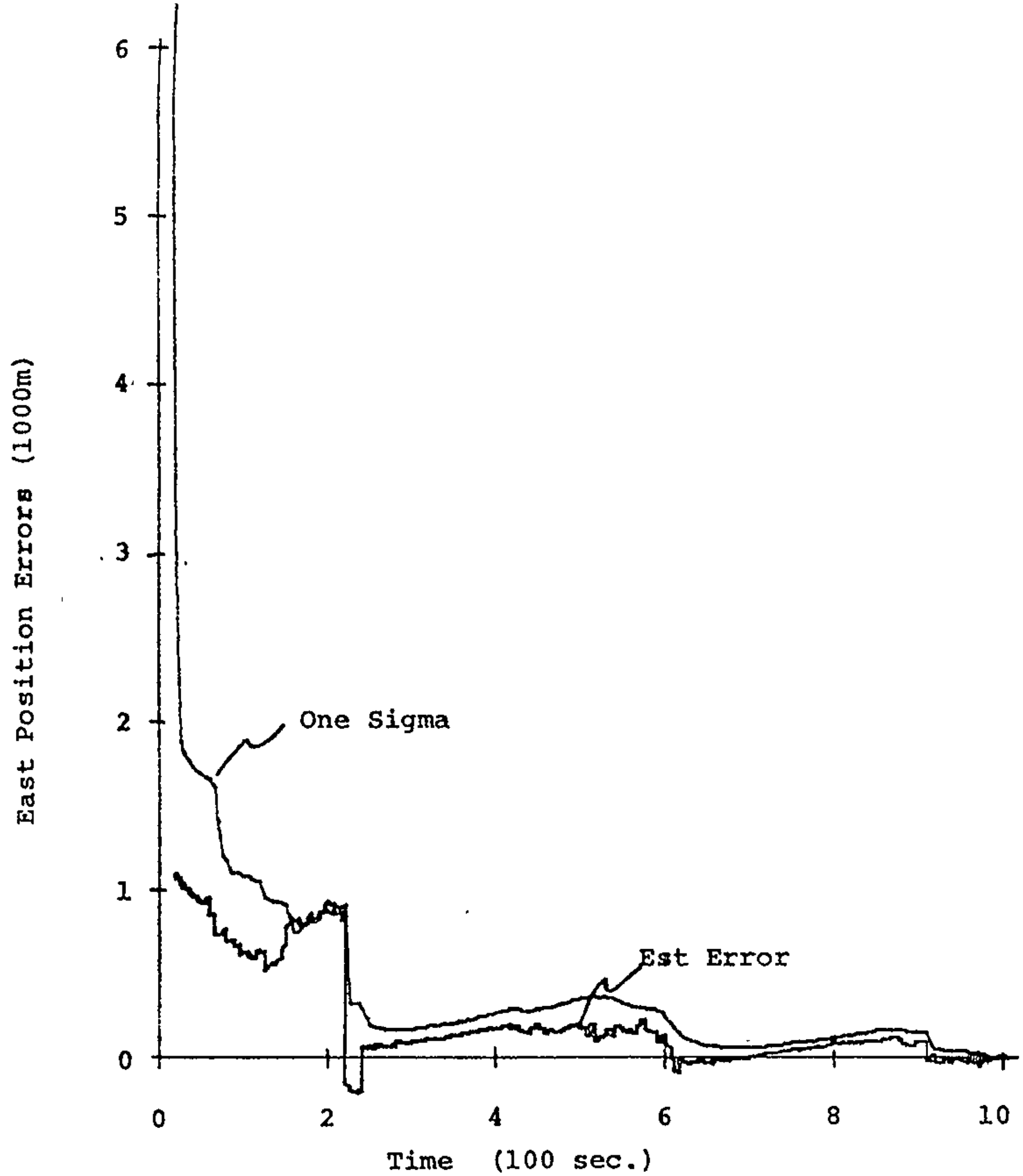

Fig. 4:49: East Position Estimation Errors & Computed One Sigma Uncertainties

2/10/73

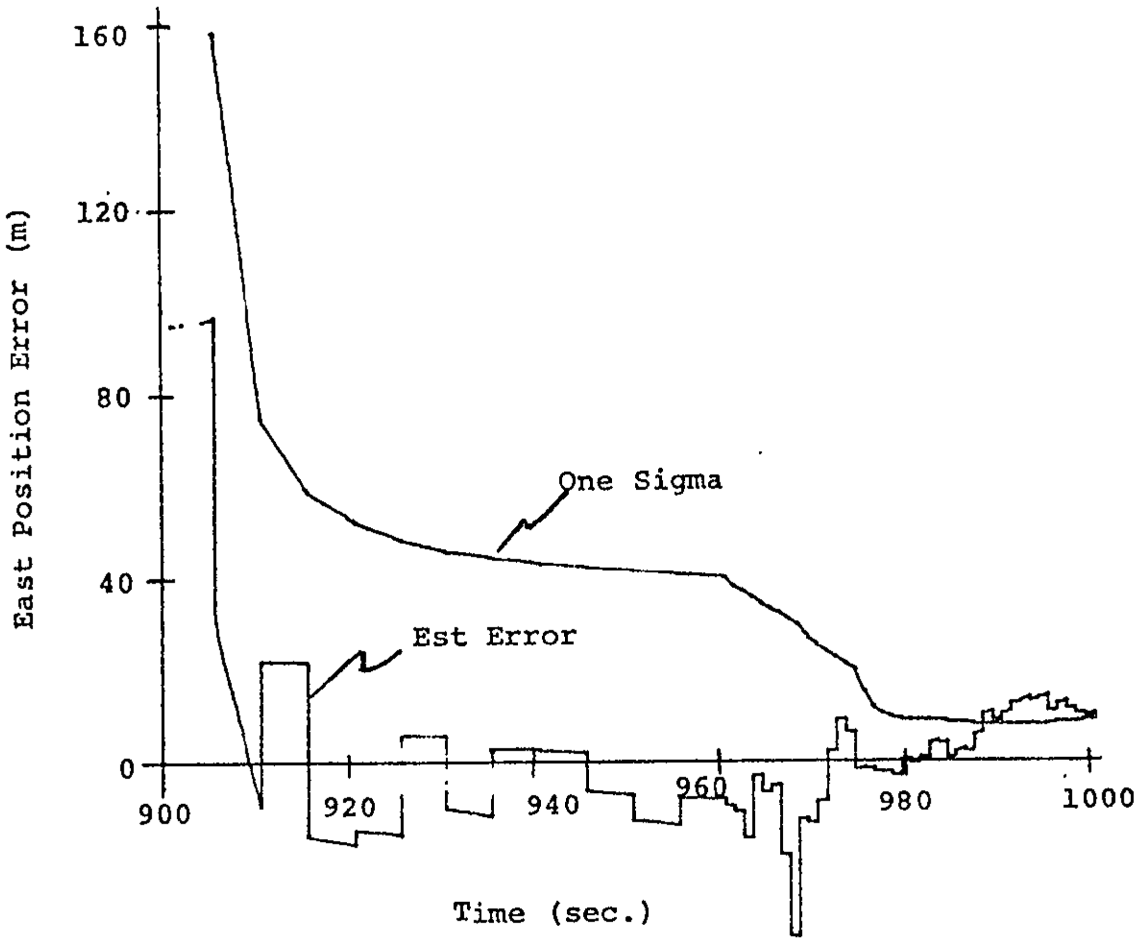

Fig. 4.50 East Position Estimation Errors & Computed One Sigma Uncertainties

2/10/73

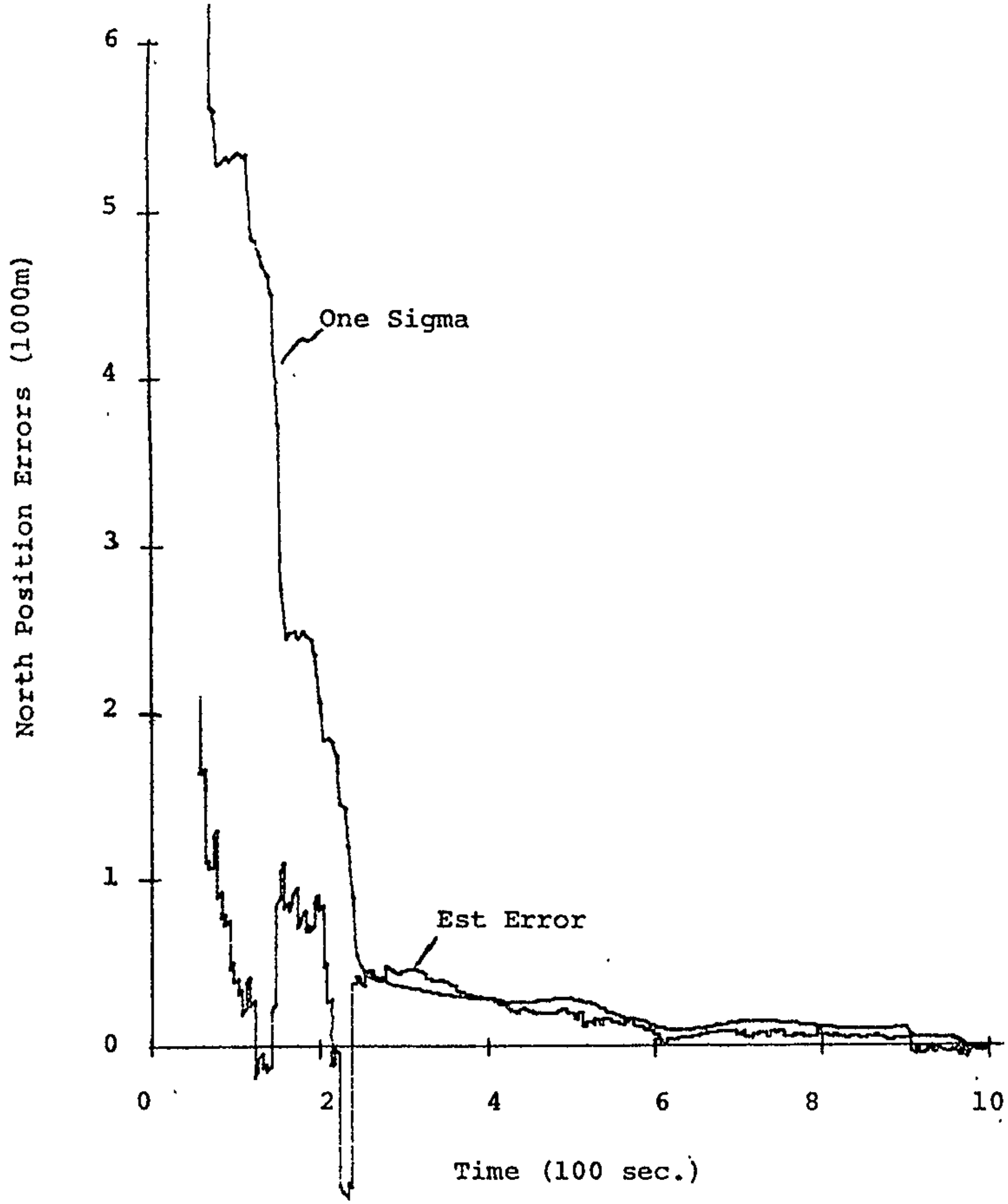

Fig.4.51: North Position Errors & Computed One Sigma Uncertainties

2/10/73

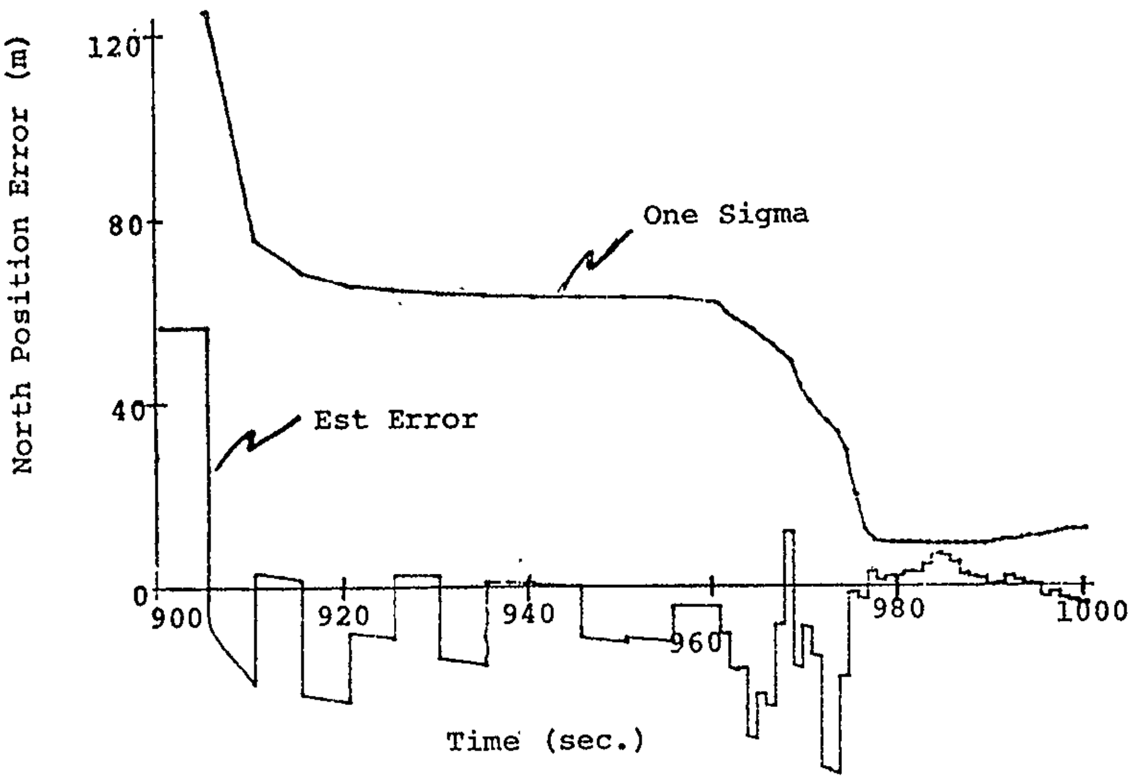

Fig.4.52:North Position Errors & Computed One Sigma Uncertainties

Time (sec)	Velocity error (m/s) V_E	V_N	V_{up}	Position error (m) δ_E	δ_N	δ_{up}
0	.43	0.0	0.7	40000	-32000	3000
60	23.87	.11	1.66	- 2655.6	-22241	3167.3
120	20.75	- 9.98	6.20	- 1096.4	-20858	4265.3
180	16.13	-38.71	2.02	- 986.91	-25689	980.50
240	7.13	18.10	44.72	- 1519.3	-11268	831.90
300	- 1.04	45.27	32.10	- 1726.8	- 6024.6	1528.6
360	-11.28	28.31	11.52	- 2810.1	- 4925.0	819.98
420	- 8.30	11.11	1.90	- 3261.0	- 3812.5	108.69
480	- 8.63	3.14	0.72	- 3434.0	- 3149.4	- 50.58
540	- .05	3.79	.83	- 2144.2	- 1338.1	- 17.09
600	5.56	- 2.78	.42	- 1186.6	- 672.51	- 25.12
660	4.26	-10.05	1.83	- 274.68	- 725.72	- 29.47
720	- 3.59	- 7.13	1.95	- 469.15	- 900.88	- 51.75
780	- .31	1.56	1.26	- 500.96	- 468.48	- 25.20
840	7.10	.81	.64	- 185.32	- 104.97	- 13.76
900	2.75	.21	.75	- 353.80	- 269.73	- 1.24
960	2.05	.98	.72	33.98	8.60	- 4.97
1014	- 1.25	- .23	.04	- 9.05	- 1.72	.69

Table 4-6: Time History of Position and Velocity Errors with Large Initial Latitude Error

2/6/73

Time (sec)	Velocity Error (m/s) V_E	V_N	V_{up}	Position error (m) δ_E	δ_N	δ_{up}
0	0.43	0.0	0.7	40000	-64000	3000
60	105.16	4.99	1.48	- 3476	-76296	2809
120	106.09	2.83	5.85	2949	-76522	3122.8
180	96.59	- 22.40	2.84	7418	-75163	- 550.27
240	93.51	- 88.94	- 93.95	14687	-88546	-10745
300	19.82	-202.97	206.95	4240.9	-80166	10284
360	17.58	-573.22	19.21	13699	-132520	10417
420	113.37	-472.61	19.77	20136	-161300	4435.9
480	371.52	7.22	57.60	37796	-163290	2186.9
540	417.00	199.29	- 34.83	78504	-161940	1288.7
600	773.33	120.09	32.85	136140	-156420	534.57
660	638.78	503.49	23.07	162840	-134580	904.24
720	426.31	528.02	- 6.11	181350	-102590	258.17
780	284.50	693.54	36.43	190770	-76417	816.73
840	7.92	626.86	- 13.03	186200	-41012	587.43
900	-189.56	656.10	32.77	177700	-13577	884.22
960	-340.35	521.03	- 19.25	159880	10274	- 40.25

Table 4-7: Aided Inertial Navigation with Large Initial Latitude Error

2/7/73

Time (sec)	Velocity error (m/s) V_E	V_N	V_{up}	Position error (m) δ_E	δ_N	δ_{up}
0	.43	0.0	0.7	40000	-64000.0	3000
60	3.01	-7.12	1.93	56.45	- 2533.1	2994.3
120	1.35	-7.63	-0.93	47.09	- 2245.5	1889.2
180	3.14	-1.88	3.72	443.97	- 1922.9	2884.3
240	.34	1.81	-1.09	33.43	- 244.72	301.10
300	- .61	2.15	-4.03	- 10.44	63.91	- 122.18
360	- .83	.87	-3.03	- 51.15	46.94	- 228.06
420	- .94	- .08	-1.50	- 83.55	- 23.85	- 148.73
480	- .88	- .39	- .68	- 97.34	- 30.65	- 134.40
540	- .26	- .20	- .08	- 1.83	45.08	- 105.66
600	- .15	- .12	.17	11.55	50.99	- 73.59
660	- .06	- .005	.44	- 17.28	37.67	- 48.31
720	.48	.006	.67	19.02	33.20	- 30.83
780	.60	- .05	.64	47.64	44.50	- 24.31
840	.70	.000	.52	90.06	54.45	- 19.12
900	- .33	- .40	.50	- 45.55	- 43.42	- 13.79
960	.48	.27	.61	12.28	- 3.60	15.84
1007	- .01	.38	.02	.41	11.59	- .17

Table 4-8:Time History of Position and Velocity Errors with Large Initial Latitude Error Using VOR/DME.

2/8/73

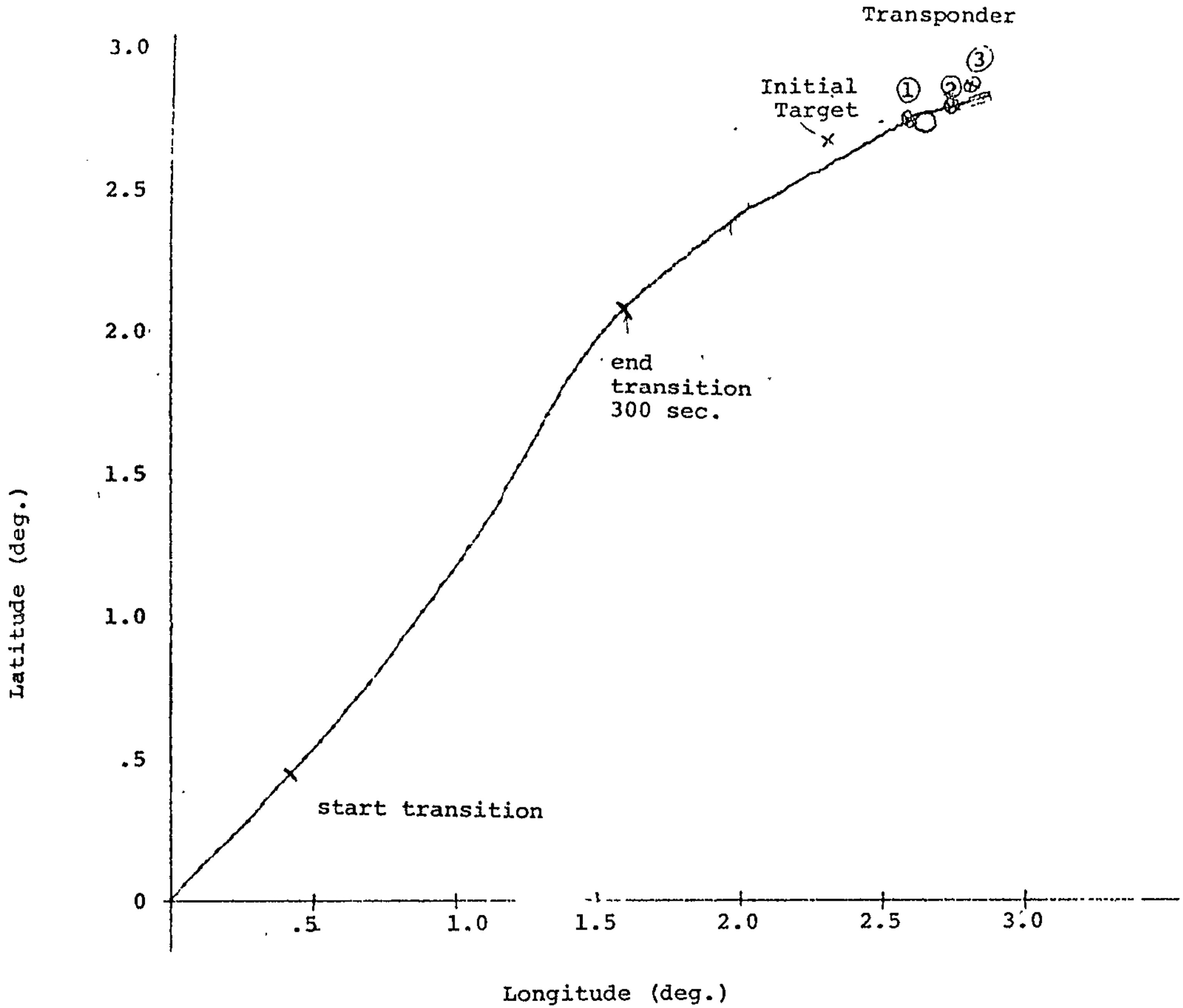

Fig.4.53: Ground Track for Precision DME

10/20/72

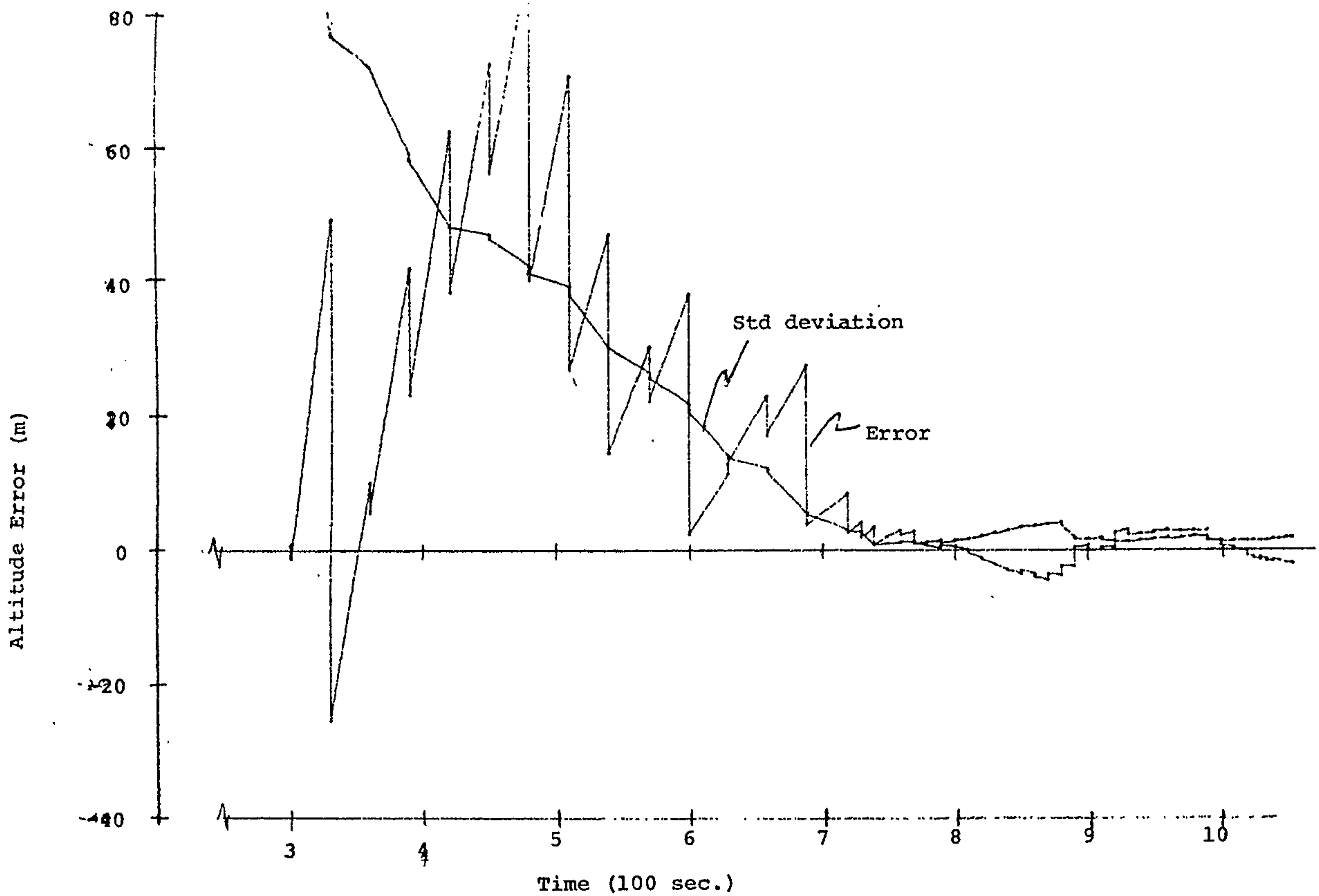

Fig.4.54: ALtitude Error for Precision DME

10/30/72

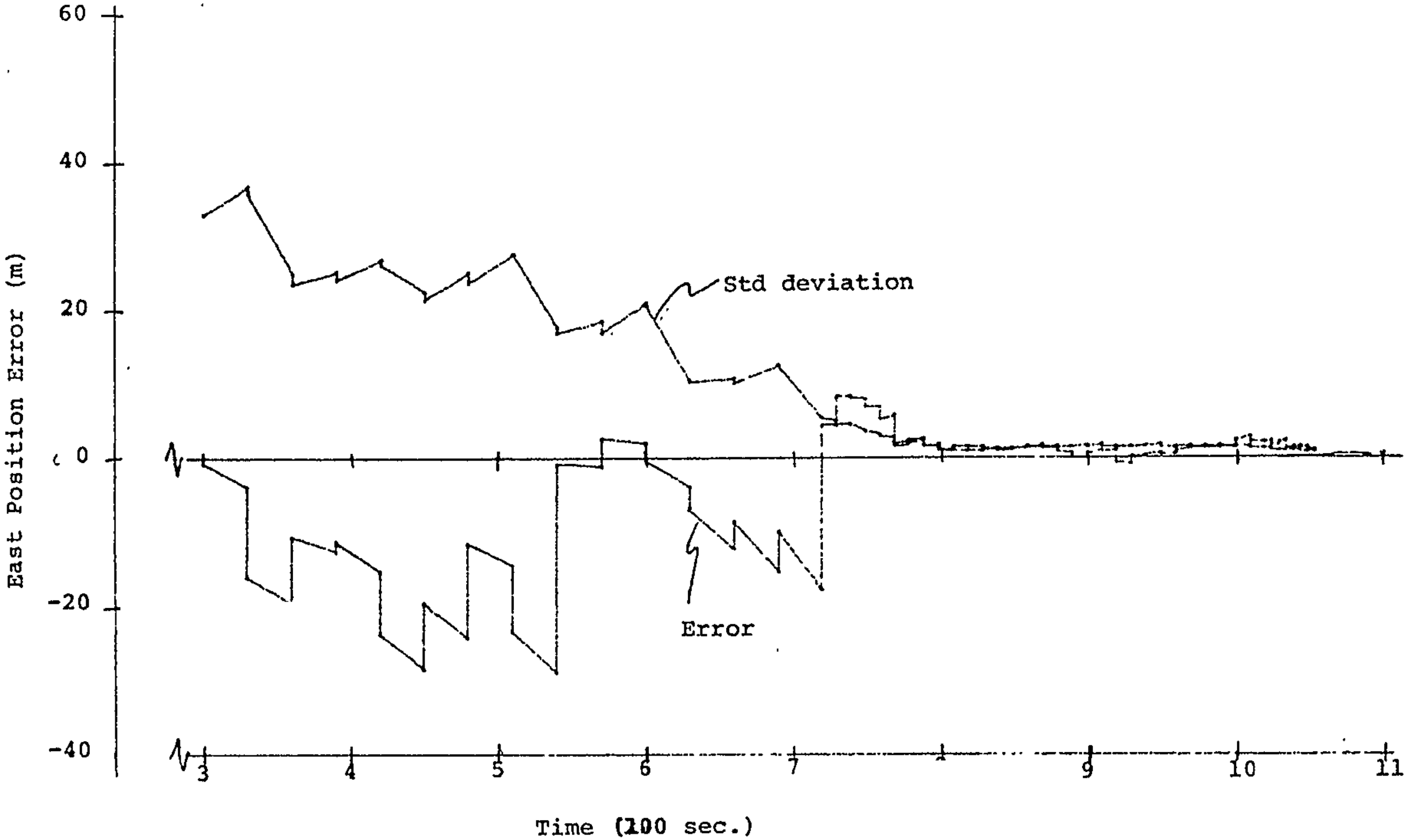

Fig. 4.55: East Position Error for Precision DME

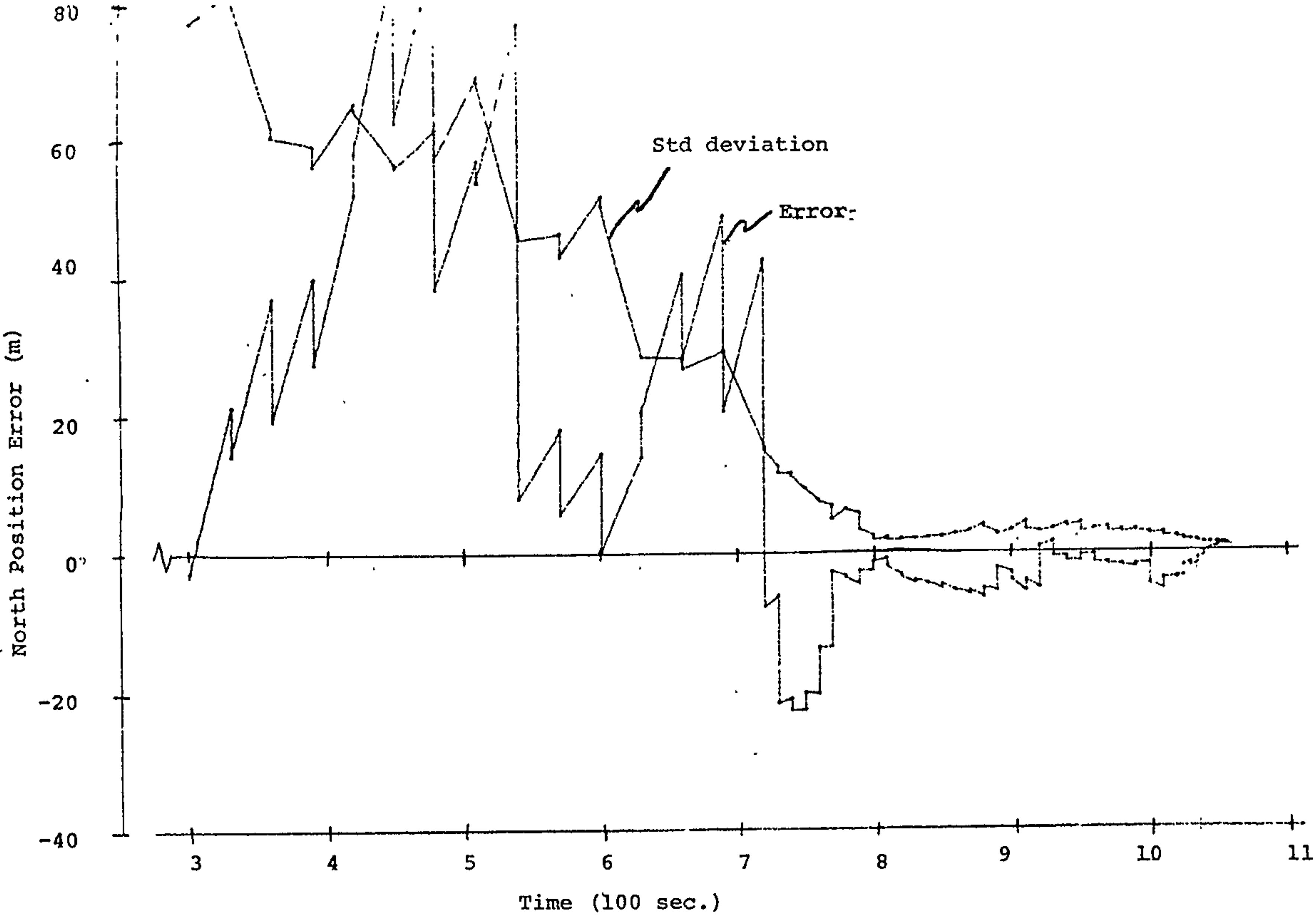

Fig. 4.56:North Position Errors for Precision DME

10/30/72

CHAPTER 5

CONCLUSIONS

Satisfactory performance has been demonstrated for this steering over a large spectrum of conditions. This leads to the main conclusion of this report that analytic techniques can lead to an effective and flexible Shuttle guidance system. The spiral mode may not be most desirable. But the spiral approach does put one in the vicinity of the airport at maximum altitude, a desirable feature. And the circling descent keeps the vehicle in close contact with landing strip, also desirable. The near constant bank angle mode provides a relatively smoother ride than other guidance modes. Wind compensation through center-of-curvature control has shown dramatic performance. But all these features are away from the main point, which is whatever scheme is selected, it should be analytic in nature. Each of the flight segments of any of the methods studied can be represented by simple formulae. By representing the vehicle capabilities with simple formulae and then closing guidance loops around these representations, a smooth natural type trajectory is almost certain to evolve. And new mission constraints will not be precluded as they might in some rigid type approach.

A combined guidance and navigation study has been accomplished. These studies showed that satisfactory performance is possible with conventional landing aids. The convergence of the large initial errors to low values is within several time steps and the noise in the navigation is seen as small one or two degree roll angle excursions.

But there is a real danger in the use of the navigation aids proposed as the standard for this study. Navigation divergence can result from large initial errors which push the navigation filter into the non-linear and unobservable regions.

In particular, large cross-track errors can cause filter divergence. The fixes are obvious, but the trend has appeared. Namely, the proposed navigation equipment seems to be tending to a bare minimum type system. If this is true, careful attention must be given to extreme cases such as the non-linear problem that arose in this study.

A much happier solution to the navigation problems is the precision ranging equipment. It is too bad that this type system has lost favor because of such things as cost and availability at alternate landing sites.

CHAPTER 6

SUGGESTIONS FOR FURTHER WORK

Some areas of the guidance system were not exhaustively studies. The navigation ranging is one. The flare logic in the presence of large vehicle variations is another. The pilot-guidance system interface is another. These as well as all the phases can benefit from more work. But in all these cases, only minor improvements will possibly result.

Some larger areas that need work are:

1. Develop criteria by which to judge the many candidate systems.

2. Use the closed loop guidance system in a failure analysis to determine what critical parts need be protected and what others to be self corrected by the navigation system. For example, where would an undetected accelerometer failure cause navigation errors that the Kalman filter could not correct?

3. Add the inner loop rotational freedoms. The commanded rates are not large but this should be checked out. The supersonic and transonic lateral stability is always a problem for these delta wing gliders.

4. Perform man-in-the-loop simulations to further determine pilot capabilities and desires.

It appears that this solution to the Shuttle approach and landing problem is fundamentally a good one. It has been my experience that the early stages of a program show large variations in vehicle parameters, mostly in the adverse direction. The latest baseline Shuttle vehicle has considerably less flying ability than the 040a. Another large area of work would therefore be to:

1. Adapt the design to these changes or verify that these changes are within the guidance capability.

2. Define performance limits below which the Shuttle vehicle may not go.

Preceding page blank

APPENDIX A

DERIVATION OF TURN ANGLE AS A FUNCTION OF INITIAL AND FINAL VELOCITY

This derivation is essentially the same as that of ref. [1]. An additional term has been added as suggested in ref. [9] to allow for a non negligible $\frac{dV}{dt}$ in the equilibrium altitude rate term. Ref. [9] assumed constant dynamic pressure and the dynamic pressure appears explicitly. Here, constant dynamic pressure is implied with assumed constant C_L & C_D and assumed equilibrium.

If we assume equilibrium flight, the centrifugal acceleration is g tan ϕ so that the rate of turn is

$$\frac{d\theta}{dt} = \frac{g \tan \phi}{V} \tag{A.1}$$

We can differentiate the equation for lift to solve for the rate of change of velocity

$$\frac{dL}{dt} = \frac{1}{2} SC_L (V^2 \frac{d\rho}{dt} + 2\rho V \frac{dV}{dt}) \tag{A.2}$$

Since in equilibrium the lift is constant, this derivative is equal to zero so we can solve for rate of change of velocity

$$\frac{dV}{dt} = - \frac{V}{2\rho} \frac{d\rho}{dt} \tag{A.3}$$

In an exponential atmosphere, $\rho = \rho_o e^{-\beta H}$, so we have

$$\frac{d\rho}{dt} = - \beta\rho \frac{dH}{dt} \tag{A.4}$$

and

$$\frac{dV}{dt} = \frac{V\beta}{2} \frac{dH}{dt} \tag{A.5}$$

The particle equations are

$$\frac{dV}{dt} = - g \sin \gamma - \frac{D}{m} \qquad (A.6)$$

$$V\dot{\gamma} = \frac{L}{m} \cos \phi - g \cos \gamma \qquad (A.7)$$

In equilibrium, $V\dot{\gamma}$ in eq. (A.7) is negligibly small, so we can write

$$0 = \frac{L}{m} \cos \phi - g \cos \gamma$$

or

$$\frac{L}{m} \cos \phi = g \qquad (A.8)$$

since $\cos \gamma = 1$.

We can solve for $\tan \gamma$ using Eq. (A.6) & (A.8)

$$\tan \gamma = - \frac{1 + \frac{dV}{dt}/\frac{D}{m}}{(\frac{L}{D}) \cos \phi} \qquad (A.9)$$

We assume $\tan \gamma = \sin \gamma$ so we can write

$$\frac{dH}{dt} = V \sin \gamma = V \tan \gamma$$

$$= - \frac{V\left(1 + (\frac{dV}{dt})/\frac{D}{m}\right)}{(\frac{L}{D}) \cos \phi} \qquad (A.10)$$

Using Eq. (A.8) we can write for D/m

$$D/m = \frac{L}{m}/(\frac{L}{D}) = \frac{g}{(\frac{L}{D}) \cos \phi} \qquad (A.11)$$

Substitute Eq. (A.10) & (A.11) into Eq. (A.5)

$$\frac{dV}{dt} = - \frac{V^2 \beta}{2 (\frac{L}{D}) \cos \phi} \left(1 + \frac{(\frac{L}{D}) \cos \phi}{g} \frac{dV}{dt}\right) \qquad (A.12)$$

Solve for $\frac{dV}{dt}$

$$\frac{dV}{dt} = - \frac{V^2 \beta}{2 (\frac{L}{D}) \cos \phi} \quad \frac{1}{(1 + \frac{V^2 \beta}{2g})} \qquad (A.13)$$

Use Eq. (A.13) to eliminate time from Eq. (A.1)

$$\frac{d\theta}{dV} = -2g \frac{L}{D} \frac{\sin\phi}{\beta V^3} (1 + \frac{V^2\beta}{2g})$$

$$= -2g (\frac{L}{D}) \frac{\sin\phi}{\beta V^3} - (\frac{L}{D}) \frac{\sin\phi}{V} \qquad (A.14)$$

Integrate Eq. (A.14)

$$\theta_2 - \theta_1 = g(\frac{L}{D})\frac{\sin\phi}{\beta} (\frac{1}{V_2^{\,2}} - \frac{1}{V_1^{\,2}})$$

$$+ (\frac{L}{D})\sin\phi \ln(\frac{V_1}{V_2}) \qquad (A.15)$$

Note that constant dynamic pressure is implied so that

$$\frac{1}{2} \rho_1 V_1^{\,2} = \frac{1}{2} \rho_2 V_2^{\,2}$$

and

$$\ln(\frac{V_1}{V_2}) = \frac{1}{2} \ln \frac{\rho_2}{\rho_1} = \frac{1}{2} \beta(h_1 - h_2) \qquad (A.16)$$

by using the exponential atmosphere property. Finally we can rewrite Eq. (A.15) by substituting Eq. (A.16) into Eq. (A.15)

$$\theta_2 - \theta_1 = g(\frac{L}{D}) \frac{\sin\phi}{\beta} (\frac{1}{V_2^{\,2}} - \frac{1}{V_1^{\,2}})$$

$$+ \frac{1}{2} \beta (\frac{L}{D}) \sin\phi (h_1 - h_2) \qquad (A.17)$$

The first term in Eq. (A.17) was the form used in ref. [1]. The second term is the correction due to non negligible $\frac{dV}{dt}$ and can account for 15% of the turn angle as described in ref. [9].

APPENDIX B

DETAILED FLOW GRAPHS

The succeeding pages show the detailed flow graphs for the steering logic. This is for the steering program, LNDSTR3 shown in Appendix D. The nomenclature and list of computer constraints for this program are in Appendix C.

INPUTS TO STEERING PROGRAM

$\bar{R}$, $\bar{V}$, $\bar{U}$EO, VAX, VIX, H, AMAG, DT

OUTPUTS FROM STEERING PROGRAM

ROLL, ALPH, LG, SB (CONTROL VARIABLES)

LATT, LONGT, AZIM, SB3, RTOGO, HFL (DISPLAY VARIABLES)

INITIALIZE

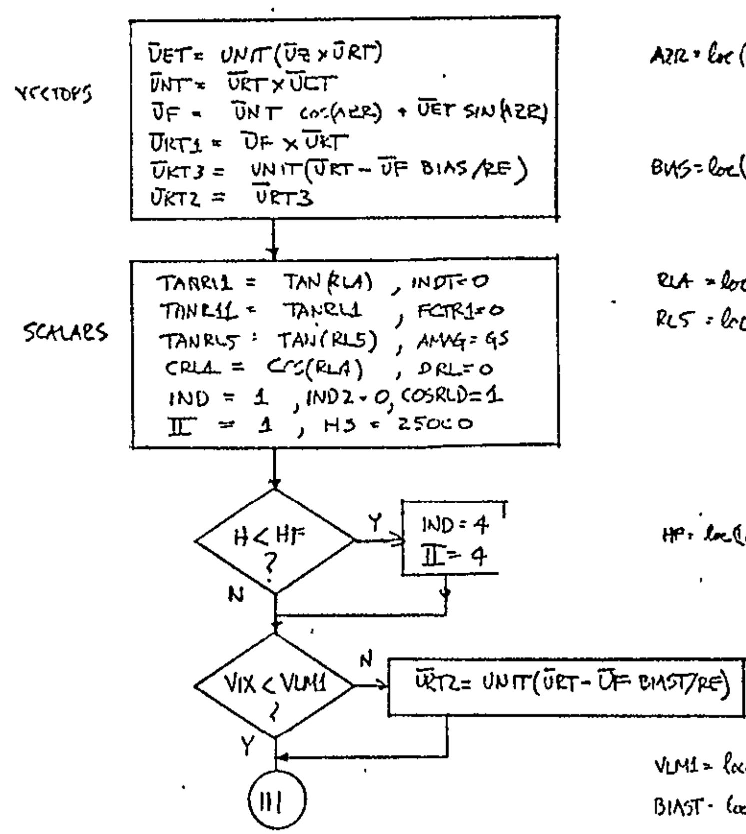

AZR = loc(161)

BIAS = loc(50) = 10

RLA = loc(CB) = 30

RLS = loc(AE) = 30

HF = loc(65) = 10 000

VLM1 = loc(123) = 1200

BIAST = loc(E9) = 30

START AFTER INITIALIZE

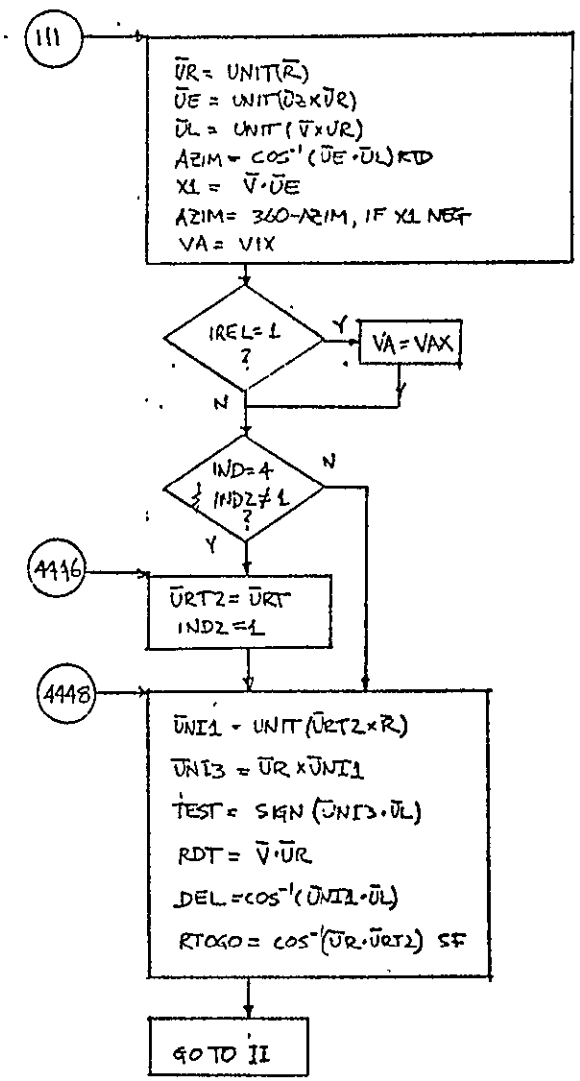

IREL = loc(84) = 0

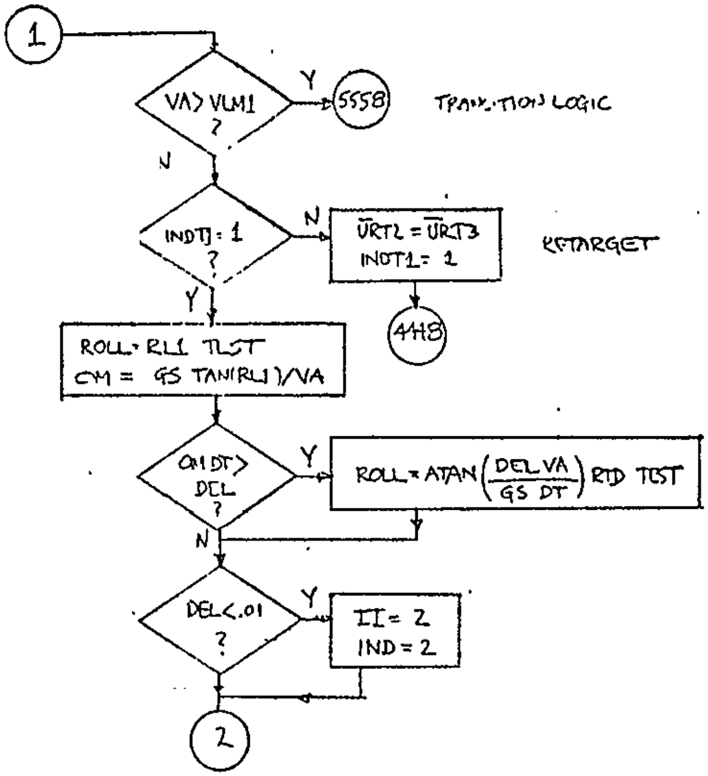

1
VA > VLM1 ?
Y
N
5558
TRANSITION LOGIC
INDT1 = 1 ?
N
Y
URT2 = URT3
INDT1 = 1
RETARGET
4418
ROLL = RL1 TEST
CM = GS TAN(RL1)/VA
CM DT > DEL ?
Y
N
ROLL = ATAN (DEL VA / GS DT) RTD TEST
DEL < .01 ?
Y
II = 2
IND = 2
2

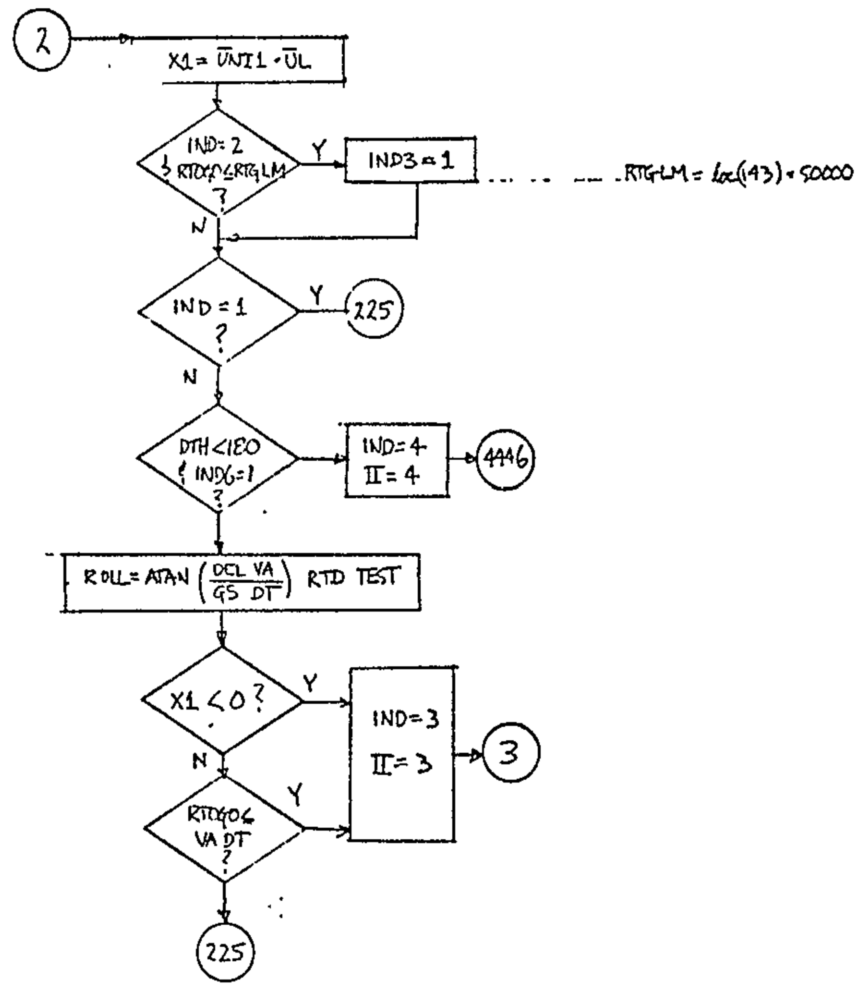

2
X1 = UNT1 · UL
IND = 2
Y
N
IND3 = 1
RTGLM = loc(143) * 50000
IND = 1 ?
Y
N
225
DTH < 180 & IND6 = 1 ?
IND = 4
II = 4
4446
ROLL = ATAN (DEL VA / GS DT) RTD TEST
X1 < 0 ?
Y
N
IND = 3
II = 3
3
VA DT ?
Y
225

TRANSITION LOGIC

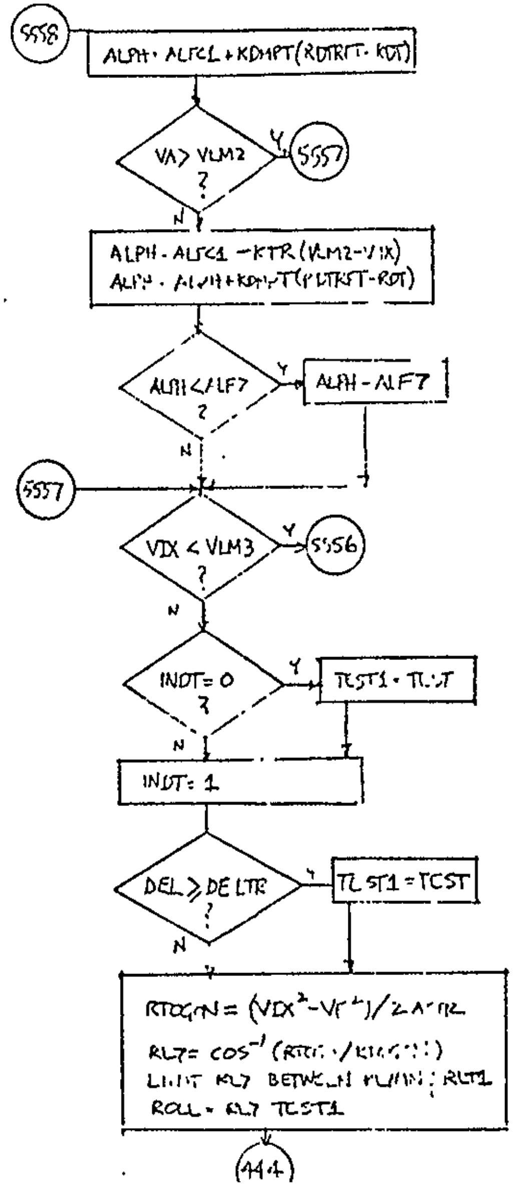

VLM2 = loc(122) = [illegible]

KTR = loc(121) = .0075
KDMPT = loc(??) = .02
KDTRT = loc(79) = -250

ALF7 = loc(120) = 7

VLM3 = loc(96) = 3000

DELTR = loc(97) = .5

VF = loc(??) = 1000
ACTR = loc(??) = 15.
RL7MIN = loc(92) = 15
RLT1 = loc(??) = 45

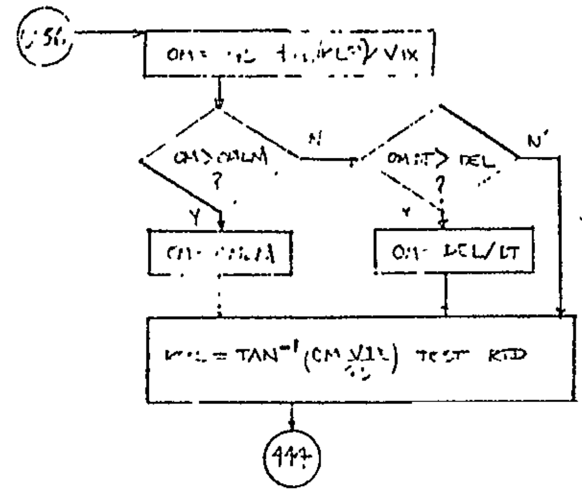

R = loc(91) = 30

OMLM = loc(??) = .01

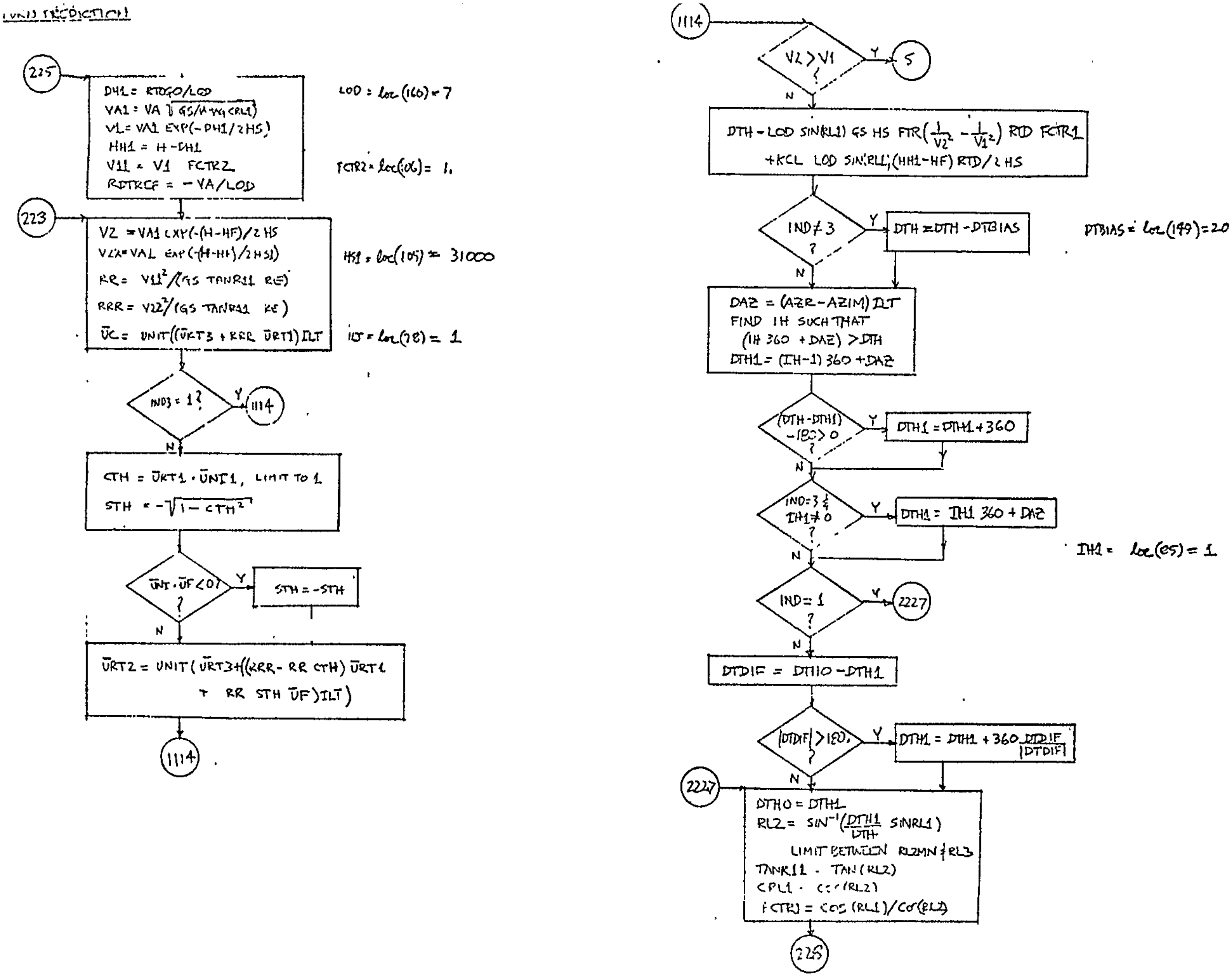
225
DH1 = RTOGO/LOD
VA1 = VA √(GS/(HS WI CRL1))
VL = VA1 EXP(-DH1/2HS)
HH1 = H - DH1
V11 = V1 FCTR2
RDTRCF = -VA/LOD
LOD = loc(160) = 7
FCTR2 = loc(106) = 1.
223
V2 = VA1 EXP(-(H-HF)/2 HS
V22 = VAL EXP(-(H-HF)/2HS1)
RR = V11²/(GS TANRL1 RE)
RRR = V22²/(GS TANRL1 RE)
UC = UNIT((URT3 + RRR URT1) ILT
HS1 = loc(105) = 31000
ILT = loc(78) = 1
IND3 = 1?
Y
N
1114
CTH = URT1 · UNI1, LIMIT TO 1
STH = -√(1 - CTH²)
UNI · UF < 0?
STH = -STH
URT2 = UNIT(URT3 + ((RRR - RR CTH) URT1 + RR STH UF) ILT)
1114
V2 > V1?
5
DTH = LOD SIN(RL1) GS HS FTR(1/V2² - 1/V1²) RTD FCTR1 + KCL LOD SIN(RL1)(HH1 - HF) RTD/2 HS
IND ≠ 3?
DTH = DTH - DTBIAS
DTBIAS = loc(149) = 20
DAZ = (AZR - AZIM) ILT
FIND IH SUCH THAT
(IH 360 + DAZ) > DTH
DTH1 = (IH-1) 360 + DAZ
(DTH - DTH1) - 180 > 0?
DTH1 = DTH1 + 360
IND = 3 & IH1 ≠ 0?
DTH1 = IH1 360 + DAZ
IH1 = loc(85) = 1
IND = 1?
2227
DTDIF = DTH0 - DTH1
|DTDIF| > 180?
DTH1 = DTH1 + 360 DTDIF/|DTDIF|
2227
DTH0 = DTH1
RL2 = SIN⁻¹(DTH1/DTH SINRL1)
LIMIT BETWEEN RL2MN & RL3
TANRL1 = TAN(RL2)
CRL1 = COS(RL2)
FCTR1 = COS(RL1)/COS(RL2)
225

TURN CONTROL

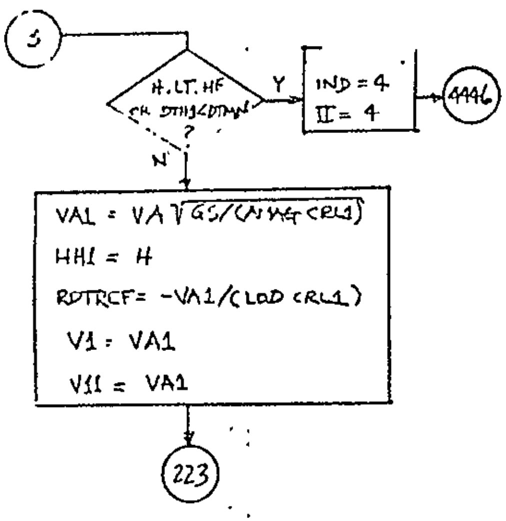

HF = loc (165) = 10000
DTMN = loc (135) = 45

CENTER CONTROL

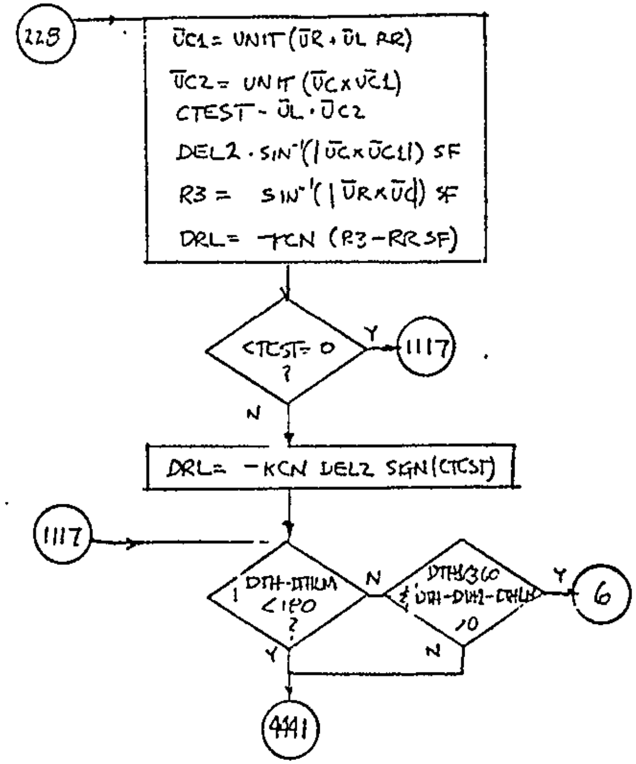

DTHLM = loc(154) = 3600

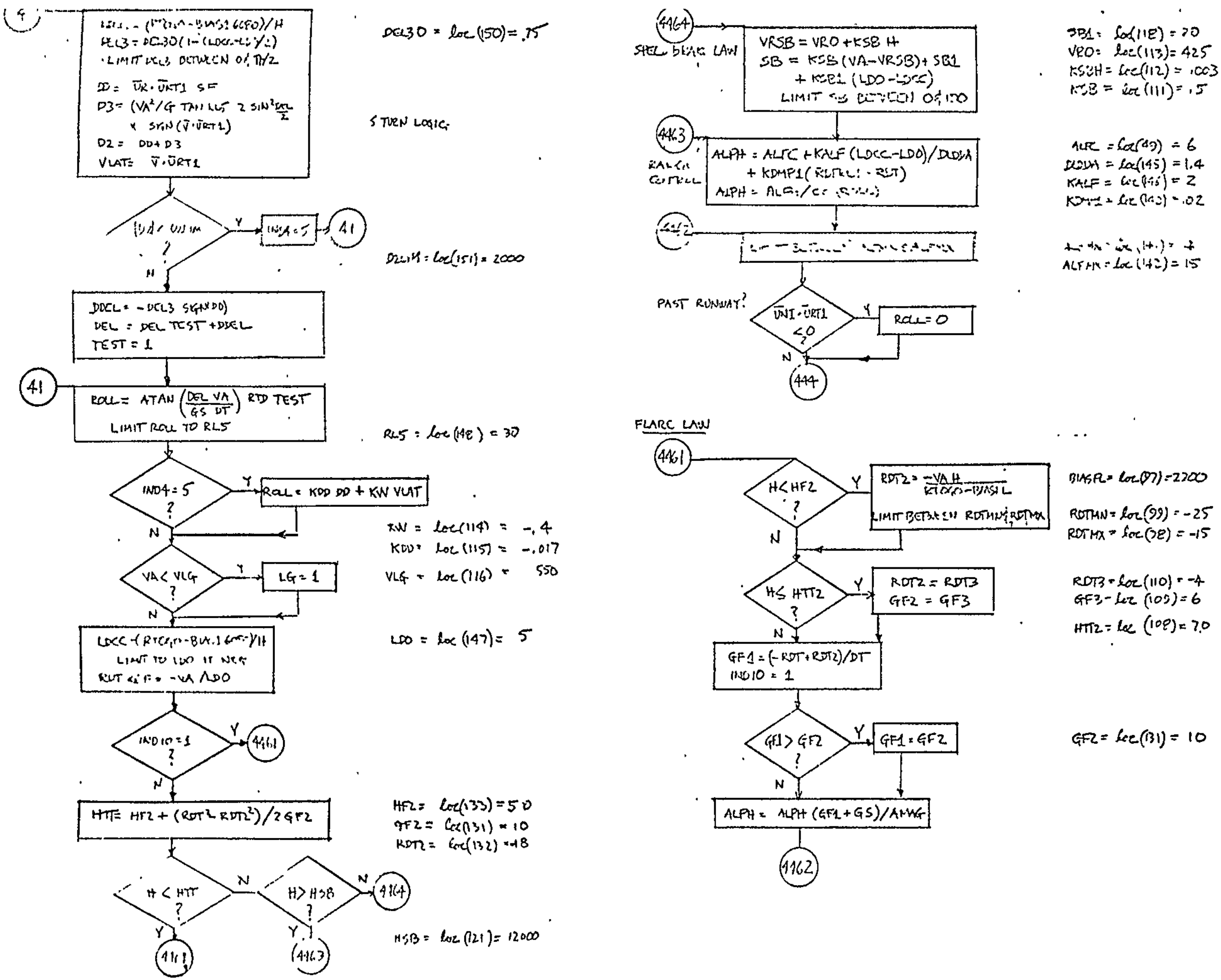
DEL30 = loc(150) = .75
DEL3 = DEL30 (1 − (LOCC−LC)/2)
LIMIT DEL3 BETWEEN 0, π/2
DD = UR · URT1
D3 = (VA²/G TAN LLS 2 SIN² DEL/2
× SIGN (V · URT1)
D2 = DD + D3
VLAT = V · URT1
S TURN LOGIC
41
DLIM = loc(151) = 2000
DDEL = − DEL3 SIGN(DD)
DEL = DEL TEST + DDEL
TEST = 1
ROLL = ATAN (DEL VA / GS DT) RTD TEST
LIMIT ROLL TO RLS
RLS = loc(148) = 30
IND4 = 5 ?
ROLL = KDD DD + KV VLAT
KV = loc(114) = −.4
KDD = loc(115) = −.017
VA < VLG ?
LG = 1
VLG = loc(116) = 550
LIMIT TO LDO IF NEG
LDO = loc(147) = 5
IND10 = 1 ?
4461
HTT = HF2 + (RDT² RDT2²)/2 GF2
HF2 = loc(133) = 50
GF2 = loc(131) = 10
RDT2 = loc(132) = −18
H < HTT ?
H > HSB ?
4464
4463
HSB = loc(121) = 12000
Y
N
4464
SPEED BRAKE LAW
VRSB = VRO + KSB H
SB = KSB (VA−VRSB) + SB1
+ KSB1 (LDO − LOCC)
SB1 = loc(118) = 70
VRO = loc(113) = 425
KSBH = loc(112) = .003
KSB = loc(111) = .5
4463
ALPH = ALFC + KALF (LOCC−LDO)/DLDA
+ KDMP1 (
ALFC = loc(49) = 6
DLDA = loc(145) = 1.4
KALF = loc(146) = 2
ALFMX = loc(142) = 15
PAST RUNWAY?
UNI · URT1 < 0 ?
ROLL = 0
444
FLARE LAW
H < HF2 ?
LIMIT BETWEEN RDTMN, RDTMX
BIASFL = loc(97) = 2200
RDTMN = loc(99) = −25
RDTMX = loc(98) = −15
H ≤ HTT2 ?
RDT2 = RDT3
GF2 = GF3
RDT3 = loc(110) = −4
GF3 = loc(109) = 6
HTT2 = loc(108) = 70
GF1 = (−RDT + RDT2)/DT
IND10 = 1
GF1 > GF2 ?
GF1 = GF2
GF2 = loc(131) = 10
ALPH = ALPH (GF1 + GS)/AMAG
4462

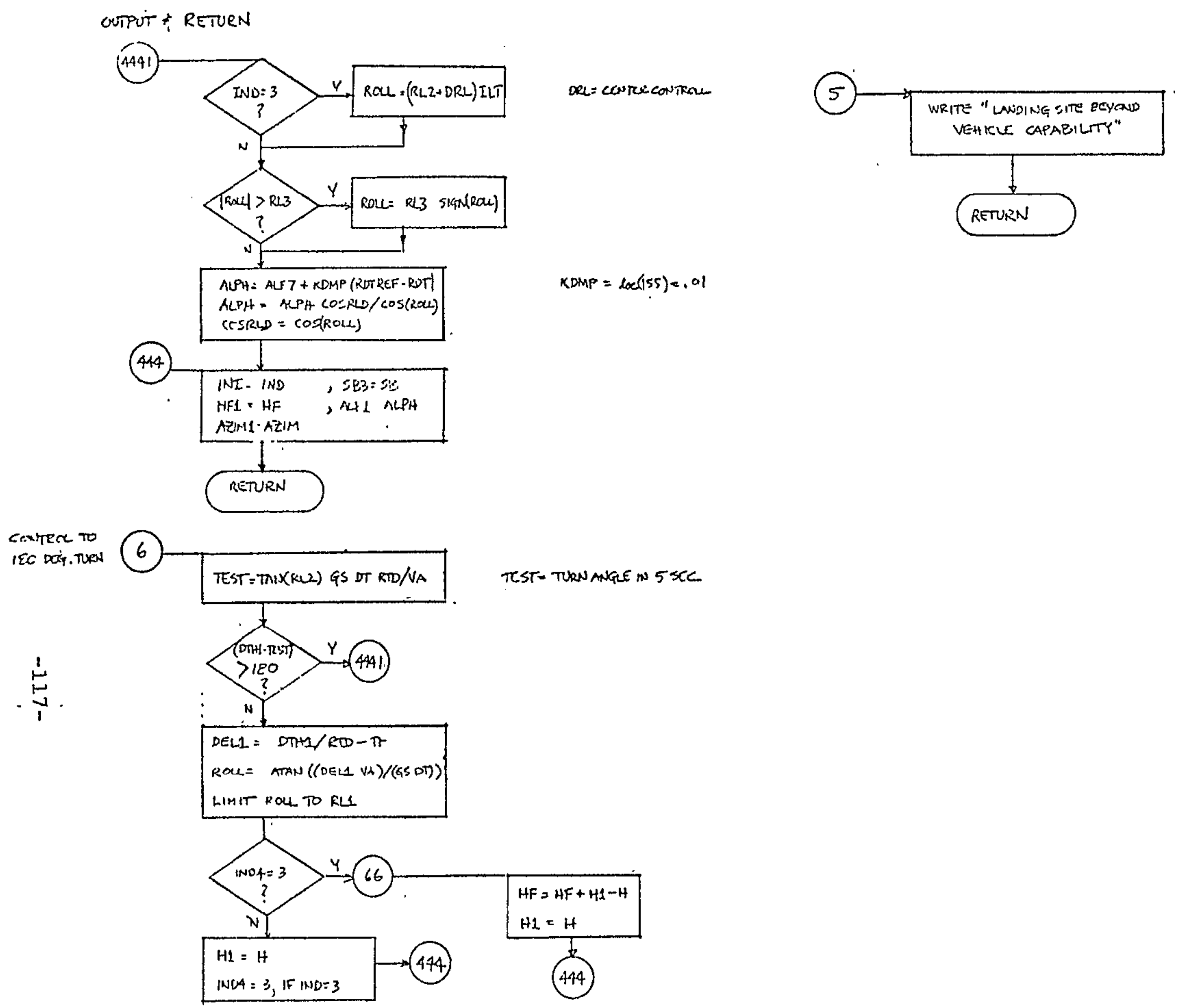
OUTPUT & RETURN
4441
IND=3 ?
Y
N
ROLL = (RL2+DRL) ILT
DRL = CONTROL CONTROL
|ROLL| > RL3 ?
ROLL = RL3 SIGN(ROLL)
ALPH = ALF7 + KDMP (RDTREF - RDT)
ALPH = ALPH COSRLD/COS(ROLL)
COSRLD = COS(ROLL)
KDMP = loc(155) * .01
444
IN1 = IND , SB3 = SB
HF1 = HF , AL1 = ALPH
AZIM1 = AZIM
RETURN
CONTROL TO 180 DEG. TURN
6
TEST = TMIX(RL2) GS DT RTD/VA
TEST = TURN ANGLE IN 5 SEC.
(DTH1-TEST) > 180 ?
DEL1 = DTH1/RTD - PI
ROLL = ATAN ((DEL1 VA)/(GS DT))
LIMIT ROLL TO RL1
IND4 = 3 ?
66
HF = HF + H1 - H
H1 = H
H1 = H
IND4 = 3, IF IND=3
5
WRITE "LANDING SITE BEYOND VEHICLE CAPABILITY"
RETURN

Appendix C: Nomenclature for Computer Listings

VARIABLES FOR STEERING PROGRAM

NAME	UNITS	DESCRIPTION
AMAG	FPS	TOTAL ACCELERATION
ALPH	DEG	COMMANDED ANGLE OF ATTACK
ALFOLD	DEG	OLD COMMANDED ANGLE OF ATTACK
AZIM	DEG	AZIMUTH
CAZR	N.D.	COS OF RUNWAY AZIMUTH
SAZR	N.D.	SIN OF RUNWAY AZIMUTH
CTH	N.D.	COS TURN ANGLE
STH	N.D.	SIN OF TURN ANGLE
CRL1	N.D.	COS OF RL2
CTEST	N.D.	INDICATOR OF CENTER CONTROL
DALF	DEG	CHANGE IN ALPHA
DAZ	DEG	AZIMUTH ERROR
D	FT	LATERAL DISPLACEMENT
D EL	FT	CALCULATED LEAD ANGLE IN S-TURN
DRL	DEG	ROL ANGLE INCREMENT
DEL1	RAD	TURN ERROR FOR 180 DEG CASE
DEL2	FT	DISTANCE BETWEEN DESIRED AND TRUE CENTER
DEL3	RAD	LEAD ANGLE IN S-TURN
DH1	FT	CALCULATED ALTITUDE LOSS IN TURN
DRL	DEG	ROL ANGLE INCREMENT
DT	SEC	TIME INCREMENT
DT TF	DEG	TURN ANGLE (DTH0-DTH1)
DTH	DEG	PREDICTED TURN ANGLE
DTH1	DEG	DESIRED TURN ANGLE
DTH0	DEG	PREVIOUS VALUE OF DTH1
D2	FT	LATERAL DISPLACEMENT FROM RUNWAY
D3	FT	LATERAL DISP WITH NOMINAL ROL.
FCTR1	ND	FACTOR IN TURN ANGLE CALC
GS	FPS	CONVERSION FROM G'S TO FPS
H	FT	ALTITUDE
H 1	FT	ALTITUDE IN TURN ANGLE CALC
HT	FT	ALTITUDE TO START FIRST FLARE
HS	FT	SCALE HEIGHT
H1	FT	ALTITUDE IN 180 DEG TURN CALC
IND	N.D.	INDICATOR FOR MODE
IND2	N.D.	INDICATOR TO RETARGET FINAL PHASE
IND3	N.D.	INDICATOR TO START S TURN
IND4	N.D.	INDICATOR FOR S TURN
IND10	N.D.	INDICATOR FOR FLARE
INDT	N.D.	INDICATOR FOR ROLL REVERSAL IN TRANSITION
INDT1	N.D.	INDICATOR FOR RETARGET AFTER TRANSITION
I	N.D.	SELECTED MODE
DEL	RAD	AZIMUTH ERROR
I4	N.D.	INDEX IN DTH1 CALC
LG	N.D.	LANDING GEAR INDICATOR
LAT	DEG	TARGET LATITUDE
LNGT	DEG	TARGET LONGITUDE
LDC	N.D.	COMMANDED L/D
OM	RAD/SEC	TURN RATE

RTOGO	FT	RANGE-TO-GO
RTOGON	FT	NOMINAL RANGE TO GO
RDTREF	FPS	REFERENCE ALTITUDE RATE
RDT	FPS	ALTITUDE RATE
RTD	DEG	CONVERT RADIANS TO DEGREES
RE	FT	EARTH RADIUS
ROL	DEG	COMMANDED ROL
R	FT	FINAL TURN RADIUS
R	FT	INITIAL TURN RADIUS
RL7	DEG	COMMANDED ROL IN TRANSITION
RL2	DEG	COMMANDED ROL (UNSIGNED)
R3	FT	DISTANCE BETWEEN DESIRED AND ACTUAL CENTERS
SF	FT/RAD	CONVERT RAD TO FT
SB3	%	SPEED BRAKE TERM
SB	%	COMMANDED SPEED BRAKE
TANRL1	N.D.	TAN(RL1)
TANR1	N.D.	TAN(RL2)
TANRL5	N.D.	TAN(RL5)
TEST	N.D.	DESIRED SIGN OF ROL
TEST1	N.D.	DESIRED SIGN OF ROL
VA	FPS	VELOCITY MAGNITUDE
VAX	FPS	RELATIVE VELOCITY MAGNITUDE
V1	FPS	VELOCITY AT TURN START
VA1	FPS	EQUILIBRIUM VELOCITY AT RL2
VIX	FPS	INERTIAL VELOCITY MAGNITUDE
V1	FPS	V1 IN R CALC (
VLAT	FPS	LATERAL VELOCITY
V2	FPS	VELOCITY AT END OF TURN
V2	FPS	V2 IN R CALC
VRSB	FPS	VELOCITY IN SB CALC
X1	-	DUMMY VARIABLE
X2	-	DUMMY VARIABLE

VECTOR VARIABLES

R	FT	POSITION VECTOR
V	FPS	VELOCITY VECTOR
URT2	N.D.	PROJECTED TARGET UNIT VECTOR
UC1	N.D.	UNIT VECTOR AT DESIRED CENTER
UNI1	N.D.	UNIT NORMAL TO PLANE OF VEHICLE AND TARGET
UR	N.D.	UNIT POSITION VECTOR
UC2	N.D.	UNIT NORMAL TO PLANE OF UC AND UC1
UE	N.D.	UNIT VECTOR EAST
UE0	N.D.	INITIAL UNIT VECTOR EAST
UET	N.D.	UNIT VECTOR EAST AT TARGET
UNI3	N.D.	UR X UNI1 (CROSS PRODUCT)
URT3	N.D.	INITIAL BIASED UNIT TARGET VECTOR
UL	N.D.	UNIT NORMAL TO PLANE OF R AND V
UNT	N.D.	UNIT VECTOR NORTH AT TARGET
URT1	N.D.	UF X URT (CROSS PRODUCT)
UF	N.D.	UNIT VECTOR ALONG FIELD
UC	N.D.	UNIT VECTOR AT INSTANTANEOUS CENTER
UZ	N.D.	UNIT VECTOR NORTH

END OF DATA

INDEX FOR CONTROL VARIABLES FOR LNDST3 - 1/31/73

	VAR	UNITS	VALUE	DESCRIPTION
49	ALFC	DEG	6	NOM ALPH - FINAL PHASE
50	BIAS	N.M.	10	BIAS ON TARGET - BEFORE FINAL PHASE
78	ILT	N.D.	1.	INDICATOR FOR LEFT TURN LOGIC
79	RDTREF	FPS	-250	REF RDOT DURING TRANSITION
80	KOMPT	N.D.	.0 2	DAMPING GAIN DURING TRANSITION
81	IND22	N.D.	1.	IND. FOR COMPENSATING ROLL TRANSIENT WITH ALPH
82	KBIAST	N.D.	0.	GAIN TO BIAS FINAL PHASE ALPHA FOR WIND
83	KBIASW	N.D.	0.	GAIN TO BIAS TARGET COMPENSATI G FOR WINDS
84	IREL	N.D.	0.	INDICATOR FOR USING RELATIVE VELOCITY
85	TH1	N.D.	0.	TURN COUNTER
86	IND13	N.D.	1.	INDICATOR FOR CENTER OF CURVATURE CONTROL
87	DALF 4	DEG	.5	LIMIT ALPHA RATE (SIMULATING AUTOPILOT)
88	RCT1	DEG	45	LIMIT ROLL IN TRANSITION
89	BIAST	N.M.	30	BIAS ON TARGET BEFORE FINAL PHASE
90	OML	RAD/S	.01	MAX AZIMUTH RATE SUPERSONICALLY
91	RL8	DEG	30	MAX ROLL IN TRANSITION
92	RL7MN	DEG	15	MIN ROLL IN TRANSITION
93	ACTR	FPS	15	NOM ACCEL DURING TRANSITION
94	VF	FPS	10	FINAL VEL FOR TRANSITION RANGE PREDICTION
95	DELTR	RAD	.5	LIMIT HEADING ERROR IN TRANSITION
96	VLM3	FPS	30	VELOCITY TO START AZIMUTH RATE LIMIT
97	BIASFL	FT	120	BIAS ON TARGET DURING FIRST FLARE
98	RDTMX	FPS	-15	MAX ALT RATE IN FLARE
99	RDTMN	FPS	-25	MIN ALT RATE IN FLARE
100	KSB1	N.D.	0	NOT USED
101	HSB	FT	1200	MAX ALT FOR SPEED BRAKE
102	RL2MN	DEG	15	MIN VALUE OF RL2
103	KCN	N.D.	.0003	GAIN FOR CURVATURE CONTROL
104	KBLND	N.D.	0	BLENDING GAIN FOR ALPHA
105	HS1	FT	310	SCALE HEIGHT IN TURN CALC
106	FCTR2	N.D.	1.	FACTOR IN RR CALC.
107	KCL	N.D.	1.	FACTOR IN DTH CALC.
108	HT 2	FT	70	ALT THRESH FOR 2ND FLARE
109	GF3	FPS	6	INCREMENTAL G FOR 2ND FLARE
110	RDT3	FPS	-4	ALT RATE AFTER 2ND FLARE
111	KSB	N.D.	.5	SPEED BRAKE GAIN
112	KSBH	1/SEC	.003	FACTOR IN NOM VEL FOR S.B.
113	VR0	FPS	425	NOM VEL IN S.B. CALC
114	KV	N.D.	-.4	GAIN IN FINAL PHASE LAT CONTROL
115	KD	N.D.	-.017	GAIN IN FINAL PHASE LAT CONTROL
116	VLG	FPS	550	VEL TO DEPLOY LANDING GEAR
117	ILG	N.D.	1	IN FOR LANDING GEAR
118	SB	PERCENT	20	SPEED BRAKE SETTING
119	ISB1	N.D.	1	IND FOR SPEED BRAKE
120	ALF7	DEG	7	ALPHA AT END OF PITCH OVER
121	KTR	DEG/FPS	.0075	PITCH OVER RATE
122	VLM2	FPS	4000	VELOCITY TO START PITCH OVER
123	VLM1	FPS	1200	VELOCITY TO END PITCH OVER
124	KTURN	N.D.	1	GAIN ON DTH-DTH1
125	IND12	N.D.	1	IND OF TANR11 IN RR CALC

126	ROL 4	DEG	20	LIMIT ROL TO CHANGE ALPH IN FINAL PHASE
127	IND9	N.D.	1	NOT USED
128	IND8	N.D.	0	INDICATOR FOR USING ROL 4
129	LM3	N.D.	-1.	LIMIT ERROR ON CC CONTROL
130	BIAS1	N.M.	1.8	BIAS ON TARGET IN FINAL PHASE
131	GF2	FPS²	10	INCREMENTAL G FOR FLARE
132	HDT2	FPS	-18	NOMINAL SINK RATE AFTER FLARE
133	HF2	FT	50	FLARE ALTITUDE AFTER FLARE
134	ALF	DEG	8	NOM ALPHA IF PAST
135	DTM4	DEG	45	BIAS TURN ANGLE TO START FINAL PHASE
136	DTHLM1	DEG	90	BIAS TO START STRAIGHT SEGMENT
137	IND6	N.D.	1.	NOT USED INDICATOR FOR DIRECT TO FINAL
138	IND7	N.D.	1.	INDICATOR FOR BIASING ALPHA-FINAL PHASE
139	-	-	-	
140	KDMP1		.02	DAMPING GAIN-FINAL PHASE
141	ALFMN	DEG	4	MIN ALPHA
142	ALFMX	DEG	15	MAX ALPHA
143	RTGLM	FT	50	RANGE TO END OF SET TARGET CALC
144	DTHC	DEG	20	MIN TURN ANGLE FOR CC CONTROL
145	DLDA	1/DEG	1.4	CHANGE OF L/D WITH ALPHA
146	KALF	N.D.	2	GAIN ON DELTA L/D-FINAL PHASE
147	LD0	N.D.	5	NORMINAL L/D-FINAL PHASE
148	RL5	DEG	30	NOMINAL L/D-FINAL PHASE
149	DTBIAS	DEG	20	BIAS ON PREDICTTED TURN ANGLE
150	DEL3	RAD	.75	NOMINAL ROL. IN S-TURN LOGIC
151	D2LIM	FT	2000	MIN ERROR FOR S-TURN
152	DELLIM	FT	2000	MIN ERROR FOR CC CONTROL
153	LM2	N.D.	2	LIMIT ERROR FOR CC CONTROL
154	DTHLM	DEG	30	BIAS TO END STRAIGHT SEGMENT
155	KDMP	N.D.	.01	DAMPING GAIN-PHASE 3
156	ALPH	DEG	29	NOMINAL ALPHA-BEFORE FINAL PHASE
157	TMAG	-	-	NOT USED
158	MDOT	-	-	NOT USED
159	M	SLUGS	4350	VEHICLE MASS
160	LOD	N.D.	7	NOMINAL L/D-BEFORE FINAL PHASE
161	AZR	DEG	75	RUNWAY AZIMUTH
162	RL1	DEG	30	NOMINAL ROLL
163	-	-	-	
164	FTR	N.D.	.9	FACTOR IN DTH CALCULATION
165	HF	FT	10000	ALTITUDE TO START FINAL PHASE

END OF DATA

APPENDIX D

COMPUTER LISTINGS

The Fortran computer listings by which these trajectories were generated are included here. The main program is EQMOT1. It calls in turn:

INIT	The initialization program
A	The input data file
ATMOS	The 1962 U.S. Standard Atmosphere
LNDSTR	The steering program
AERO	The aerodynamic subroutine AERDY4 contains the 040a vehicle

Sub. Fort contains the following subroutines:

DIFEQ	4th Order Range Kutta Gill integratter
ATMOS	The 1962 U.S. Standard Atmosphere
AXB	Vector cross product routine
UNITV	Routine to unitizing a vector
VSUB, VAD	Vector subtraction and addition
VECSCL	Vector times scalar routine

Subl. Fort contains these subroutines:

SIND, COSD	sine cosine of angles in deg.
LALONG	converts unit vector to latitude & longitude
DANG	calculates angle between two vectors by cross product

```
 2.1069056E 07 0.0           0.0          -2.0000000E 02 6.0518750E 03  00000005
 0.0           0.0           7.0710677E-01 7.0710677E-01 1.0000000E 00  00000010
 1.0000000E 00 0.0           0.0           9.9824584E-01 5.9195109E-02  00000015
 2.5972724E-05 2.0000000E 00 0.0           1.0000000E 00 4.5000000E 01  00000020
 6.0000000E 00 1.0000000E 06 0.0           2.0000000E 01 6.0000000E 01  00000025
 1.5000000E 00 5.0000000E 00 3.0000000E 01 1.2000000E 03 1.0000000E 00  00000030
 0.0           1.0000000E 00 1.2000000E 03 1.0000000E 00 1.0000000E 00  00000035
 0.0           1.5000000E 00 6.0000000E 00-2.6999969E 00 1.0000000E 00  00000040
 4.0000000E 00 2.2799988E 01 2.5000000E-01 5.0000000E 00 2.0000000E 00  00000045
 1.2000000E 04 0.0           7.5000000E 01 6.0000000E 00 1.0000000E 01  00000050
 5.0000000E 01 2.0000000E-02 0.0           0.0           1.0000000E 00  00000055
 2.0000000E 03 2.0000000E 03 1.0000000E 00 1.0000000E 00 2.0529000E 04  00000060
 2.3090000E 04 2.3500000E 04 3.5000000E 04 0.0           0.0            00000065
-3.4599990E-02-5.5099996E-02-9.0339959E-02-1.4099962E-01-1.9779927E-01  00000070
-2.3719949E-01-3.3049995E-01-3.6049996E-01-4.9599995E-01-6.4029992E-01  00000075
-2.0209990E 00-3.3539982E 00 1.0000000E 00-2.5000000E-02 2.0000000E-02  00000080
 1.0000000E 00 0.0           0.0           1.0000000E 00 1.0000000E 00  00000085
 1.0000000E 00 5.0000000E-01 4.5000000E 01 3.0000000E 01 1.0000000E 00  00000090
 3.0000000E 01 1.5000000E 01 1.3000000E 01 1.0000000E 03 5.0000000E-01  00000095
-3.0000000E 03-1.2000000E 03-1.5000000E 01-2.5000000E 01 0.0            00000100
 1.2000000E 04 1.5000000E 01 2.9999996E-04 0.0           3.1000000E 04  00000105
 1.0000000E 00 1.0000000E 00 7.0000000E 01 6.0000000E 00-4.0000000E 00  00000110
 5.0000000E-01 2.9999998E-03 4.2500000E 02-3.9999998E-01-1.0977978E-02  00000115
 5.5000000E 02 1.0000000E 00 2.0000000E 01 1.0000000E 00 7.0000000E 00  00000120
 7.4999966E-03 4.0000000E 03 1.2000000E 03 1.0000000E 00 1.0000000E 00  00000125
-2.0000000E 02-1.0000000E 00 0.0          -1.0000000E 00 1.7999983E 00  00000130
 1.0000000E 01-1.6000000E 01 5.0000000E 02 5.0000000E 00 4.5000000E 01  00000135
 9.0000000E 01 1.0000000E 00 1.0000000E 00 3.1552996E 03 2.0000000E-02  00000140
-4.0000000E 00 1.5000000E 01 5.0000000E 04 2.0000000E 02 1.3799997E 00  00000145
 2.0000000E 00 5.0000000E 00 3.0000000E 01 2.0000000E 01 7.5000000E-01  00000150
 2.0000000E 03 0.0           2.0000000E 00 3.6000000E 03 9.9999942E-03  00000155
-2.9000000E-01-0.0           0.0           4.3500000E 05 7.0000000E 00  00000160
 7.5000000E 01 3.0000000E 01 0.0           8.9999998E-01 1.0000000E 04  00000165
```

File A: Input Data for Nominal Case

```
0001        SUBROUTINE LNDSTR(R,V,UEO,VAX,VIX,AZIM,H,ROLL,ALPH,AMAG,
          * V1,V2,DTH,DTH1,S83,INI,LATT,LONST,AZM1,RTOGO,HF1,ALF1,DT,LG,SB)
0002        IMPLICIT REAL (I-N)
0003        INTEGER I,IH,II,IND,ISTART
0004        DATA ISTART,DRL/0,0./
0005        DIMENSION R(3),V(3),A(165),UEO(3),UL(3),AZ(3),TEM(3),UNI1(3)
0006        DIMENSION UET(3),UZ(3),URT(3),UNT(3),UF(3),URT2(3),UR(3),UNI3(3)
0007        DIMENSION URT1(3),UC(3),UC1(3),UC2(3),URT3(3),B(12)
0008        DIMENSION UE1(3),TEM1(3),UE(3)
0009        EQUIVALENCE (A(14),URT),(A(7),UZ),(A(20),RL3),(A(28),PL4),
          * (A(83),KBIASW),(A(82),KBIAST),(A(78),ILI),
          * (A(80),KDYFT),(A(79),RDTRFT),(A(81),IND22),
          * (A(95),DELTR),(A(94),VF),(A(93),ACTR),(A(92),RLZMN),
          * (A(87),DALFLM),(A(86),IND13),(A(85),IH1),(A(84),IREL),
          * (A(91),FLB),(A(90),OMGM),(A(89),BIAST),(A(88),RLT1),
          * (A(99),RDTMN),(A(98),RDTMX),(A(97),BIASFL),(A(96),VLM3),
          * (A(103),KCN),(A(102),RL2MN),(A(101),HSB),(A(100),KSB1),
          * (A(107),KCL),(A(106),FCTR2),(A(105),HS1),(A(104),KBLND),
          * (A(111),KSR),(A(110),RDT3),(A(109),GF3),(A(108),HTT2),
          * (A(115),KDC),(A(114),KVV),(A(113),VF0),(A(112),KSBH),
          * (A(119),TSB1),(A(118),SB1),(A(117),ILG),(A(116),VLG),
          * (A(123),VLM1),(A(122),VLM2),(A(121),KTR),(A(120),ALF7),
          * (A(126),ROLL4),(A(18),LONO),(A(125),IND12),(A(124),KTURN),
          * (A(130),BIAS1),(A(129),LM3),(A(128),IND8),(A(127),IND9),
          * (A(134),ALFF1),(A(133),HF2),(A(132),RDT2),(A(131),GF2),
          * (A(137),IAC6),(A(138),IND7),(A(136),DTHLM1),(A(135),DTMN),
          * (A(161),AZR),(A(162),RL1),(A(160),LOD),(A(164),FTR),(A(165),HF),
          * (A(19),PUTP),(A(21),PCTR),(A(49),ALFC),(A(50),BIAS)
0010        EQUIVALENCE (A(156),ALFC1),
          * (A(154),DTHLM),(A(155),KDMP),(A(153),LM2),(A(152),DELLIM),
          * (A(150),DEL30),(A(151),D2LIM),(A(149),DTBIAS),(A(148),RL5),
          * (A(144),DTHC),(A(145),DLDDA),(A(146),KALF),(A(147),LDO),
          * (A(143),RTGLM),(A(142),ALFMX),(A(141),ALFMN),(A(140),KDMP1)
0011        DATA LC/1.,0.,0./
0012        IF (ISTART.EQ.1) GO TO 111
0013        DTH=361.
0014        DTH1=362.
0015        DTHP=DTH1
0016        ISTART=1
0017        INDT= 0.
0018        PI=3.14159265
0019        RTD=180./PI
0020        GS=32.2
0021        AMAG=GS
0022        HS=25000.
0023        COSRLC= 1.
0024        SF=RTD*60.*6080.
0025        RF=20902900./6080.
0026        IND=1
0027        FCTR1=1.
```

```
              READ (7'1,21) A
              CALL AXB(UZ,URI,TEM)
              CALL UNITV(TEM,UET,X1,X1)
              CALL AXB(URT,UET,UNT)
              TANRL1=SIND(RL4)/COSD(RL4)
              TANR11=TANRL1
              TANRL5=SIND(RL5)/COSD(RL5)
              SAZR=SIND(AZR)
              CRL1=COSD(RL4)
              CAZR=COSD(AZR)
              ASSIGN 1 TO II
              IF(H.LT.HF) ASSIGN 4 TO II
              IF(H.LT.HF) IND=4
              DO 11 I=1,3
       11     UF(I)=(UNT(I)*CAZR+UET(I)*SAZR)
              CALL AXB(UF,URT,URT1)
              DO 1116 I=1,3
     1116     TEM(I)=URT(I)-UF(I)*BIAS/RE
              CALL UNITV(TEM,URT3,X1,X1)
       21     FORMAT (5F14.7)
              DO 1119 I=1,3
     1119     URT2(I)=URT3(I)
              IF(VIX.LT.VLM1) GO TO 111
              DO 1222 I=1,3
     1222     TEM(I)=URT(I)-UF(I)*BIAST/RE
              CALL UNITV(TEM,URT2,X1,X1)
      111     CALL AXB(V,R,TEM)
              CALL UNITV(TEM,UL,X1,X1)
              CALL UNITV(R,UR,X1,X1)
              CALL AXB(UZ,UR,TEM)
              CALL UNITV(TEM,UE,X1,X1)
              CALL ADCTB(UF,UL,X2)
              VA=VIX
              IF(IREL.EQ.1.) VA=VAX
              VA1=VA
              AZIM=ARCOS(X2)*RTD
              CALL ADCTB(V,UE,X1)
              IF(X1.LT.0.) AZIM=360.-AZIM
              IF(IND.EQ.4.AND.IND2.NE.1.) GO TO 4448
     4448     CALL AXB(URT2,R,TEM)
              CALL UNITV(TEM,UNI1,X1,X1)
              CALL AXB(UR,UNI1,UNI3)
              CALL ADCTB(UNI3,UL,ARG)
              TEST =SIGN(1.,ARG)
              CALL ADCTB(V,UR,ROT)
              CALL AXB(URT2,UR,TEM)
              CALL UNITV(TEM,UNI1,X1,X1)
              CALL ADCTB(UNI1,UL,X1)
              IF(X1.GT.1.) X1=1.
              DEL = ARCOS(X1)
```

```
              RTOGO-DANC(UP,URT2)*SF
              GO TO II,(1,2,3,4)
              IF(VIX.GT.VLM1) GO TO 5558
              IF(INDT1.EQ.1.) GO TO 5554
              DO 5553 I=1,3
        5553  TEM(I)=URT3(I)-(KBIAST*(VIX-VAX)/RE)*UF(I)
              CALL UNITV(TEM,URT2,X1,X1)
              CALL UNITV(URT2,URT3,X1,X1)
              INDT1=1.
              GO TO 4448
        5554  ROLL=RL1*TEST
              GM = GS*SIND(RL1)/(COSD(RL1)*VA)
              IF((GM*DT).GT.DEL)  ROLL=ATAN2((DEL*VA),(GS*DT))*RTD*TEST
              IF(DEL.LT..01) ASSIGN 2 TO II
              IF(DEL.LT..01) IND = 2
           2  CALL ADCTR(UNI1,UL,X1)
              IF(IND.EQ.2.AND.RTOGO.LE.RTGLM) IND3=1.
              IF(IND.EQ.1.) GO TO 225
              IF(DTF.LT.180..AND.IND6.EQ.1.) IND=4
              IF(IND.EQ.4) ASSIGN 4 TO II
              IF(IND.EQ.4) GO TO 4446
              ROLL=ATAN2((DEL*VA),(GS*DT))*RTD*TEST
              IF(ABS(ROLL).GT.RL1) ROLL=SIGN(RL1,ROLL)
              IF(X1.LT.0.) IND=3
              IF(RTOGO.LE.(DT*VA)) IND= 3
              IF(IND.EQ.3) ASSIGN 3 TO II
              IF (IND.EQ.3) GO TO 3
         225  DH1=RTOGO/LOD
              IF(IND9.EQ.1.) VA1=VA*SQRT(GS/(CRL1*AMAG))
              HH1=H-DH1
              V1=VA1*EXP(-DH1/(2.*HS))
              V11=V1*FCT*2
              RDT2FF=-VA/LOD
         223  V2=VA1*EXP(-(H-HF)/(2.*HS))
              V22=VA1*EXP(-(H-HF)/(2.*HS1))
         224  RR=V11**2/(GS*TANR11*20902000.)
              RRR=V22**2/(GS*TANR11*20902000.)
              DO 1115 I=1,3
        1115  TEM(I)=URT3(I)+RRR*URT1(I)*ILT
              CALL UNITV(TEM,UC,X1,X1)
              IF(IND3.EQ.1.) GO TO 1114
              CALL ADCTR(URT1,UNI1,CTH)
              IF(CTH.GT.1.)   CTH=1.
              STH=-SQRT(1.-CTH**2)
              CALL ADCTR(UNI1,UF,ARG)
              IF(ARG.LT.0.) STH=-STH
              DO 1113 I=1,3
        1113  TEM(I)=URT3(I)+((RRR-RR*CTH)*URT1(I)+RR*STH*UF(I))*ILT
              CALL UNITV(TEM,URT2,X1,X1)
        1114  IF(V2.GT.V1) GO TO 5
```

```
              DTH=CCD*SIND(RL1)*GS*HS*FTR*(1./V2**2-1./V1**2)*RTD*FCTR1
             +KCL*LCD*SIND(RL1)*(HH1-HF)*RTD/(2.*HS)
              IF(INC.NE.3) DTH=DTH-DTBIAS
              DAZ=(AZP-AZIM)*ILT
              DO 222 IH=1,10
              IF((IH*360.+DAZ).GT.DTH) GO TO 2222
 222          CONTINUE
 2222         DTH1=(IH-1)*360.+DAZ
              IF((DTH-DTH1-180.).GT.0.) DTH1=DTH1+360.
              IF(INC.NE.3..AND.IH1.NE.0.) DTH1=IH1*360.+DAZ
              IF(INC.EQ.1) GO TO 2227
              DTDIF=DTHC-DTH1
              IF((ABS(DTDIF)).GT.180.) DTH1=DTH1+SIGN(360.,DTDIF)
 2227         DTHC=DTH1
              IF(INC.NE.3) DTHI=DTH1
              ARG=ABS(DTH1*SIND(RL1)/DTH)
              IF (ARG.GT.1.) ARG=1.
              RL2=ARSIN(ARG)*RTD
              RL2=RL1+KTURN*(RL2-RL1)
              IF(RL2.GT.RL3) RL2=RL3
              IF(RL2.LT.RL2MN) RL2=RL2MN
              IF(INC12.EQ.1.) TANR11=SIND(RL2)/COSD(RL2)
              IF(INC12.EQ.1.) CRL1=COSD(RL2)
              IF(INC12.EQ.1.) FCTR1=COSD(RL1)/COSD(RL2)
              DO 1118 I=1,3
 1118         TEM(I)=UR(I)+RR*UL(I)
 2228         CALL UNITV(TEM,UC1,X1,X1)
              CALL AXP(UC,UC1,TEM)
              R3=DANG(UP,UC)*SF
              DRL=-KCN*(R3-RR*SF)
              CALL UNITV(TEM,UC2,X1,X1)
              CALL ADOTP(UL,UC2,CTEST)
              DEL2=DANG(UC,UC1)*SF
              IF(INC13.NE.1.) GO TO 1117
              IF(CTEST.EQ.0.) GO TO 1117
              DRL=-KCN*DEL2*SIGN(1.,CTEST)
              IF(CTEST.LT.LM2) GO TO 1117
              IF(DTH1.LT.DTHC) GO TO 1117
              CALL ADOTB(UL,UF,X1)
              IF(ABS(X1).LT.LM3) GO TO 1117
              IF(DEL2.GT.DELLIM) RL2=0.
 1117         IF((DTH-DTHLM).LT.180.) GO TO 4441
              IF(DTH1.LT.360..AND.(DTH-DTH1-DTHLM1).GT.0.) GO TO 6
 4441         IF(INC.EQ.3) ROLL=(RL2+DRL)*ILT
              IF(ABS(ROLL).GT.RL3) ROLL=SIGN(RL3,ROLL)
              ALPH= ALF7+KDMP*(ROTREF-RDT)
              IF(INC22.EQ.1.) ALPH=ALPH*COSRLD/COSD(ROLL)
              COSRLD=COSD(ROLL)
              IF(INC.EQ.3) ALPH=ALPH+KBLND*(1.-DTH1/DTHI)*(ALFC-ALF7)
              GO TO 444
```

```
      3       IF(H.LT.HF) IND=4
              IF(DTH1.LT.DTMN) IND=4
              IF(IND.EQ.4) ASSIGN 4 TO II
              IF(IND.EQ.4) GO TO 4446
              HH1=H
              VA1=VA*SQRT(GS/(CRL1*AMAG))
              V1=VA1
              V11=VA1
              RDTREF=-VA/(LDD*CRL1)
              GO TO 223
      4       CALL ARCTR(UP,URI1,ARG)
              DD=ARG*SF
              D3=(VA**2/(GS*TANRL5))*2.*(SIN(DEL/2.))**2
              CALL ARCTR(V,URI1,VLAT)
              D3=SIGN(D3,VLAT)
              D2=DD+D3
              IF((ABS(D2)).LT.D2LIM) IND4=5.
              LDCC=(RTREF-BIAS1*6080.)/H
              IF(IND4.EQ.5.) GO TO 41
              DEL3=DEL30*(1.-(LDCC-LDD)/2.)
              IF(DEL3.LT.0.) DEL3=0.
              IF(DEL3.GT.(PI/2.)) DEL3=PI/2.
              DDEL=-SIGN(DEL3,DD)
              DEL=DEL*TEST+DDEL
              TEST = 1.
     41       ROLL=ATAN2((DEL*VA),(GS*DT))*RTD*TEST
              IF(KDD.NE.0..AND.IND4.EQ.5.) ROLL=KDD*DD+KVV*VLAT
              IF((ABS(ROLL)).GT.RL5) ROLL=SIGN(RL5,ROLL)
              IF(ILG.EQ.1..AND.VA.LT.VLG) LG=1.
              LDCC=(RTREF-BIAS1*6080.)/H
              IF(LDCC.LE.0.) LDCC=LDD
              RDTREF=-VA/LDD
              IF(INF10.EQ.1.) GO TO 4461
              HTT=HF2+(RDT**2-RDT2**2)/(2.*GF2)
              IF(H.LE.HTT) GO TO 4461
              IF(H.GT.HSP) GO TO 4463
              VRSB=VR0+KSBH*H
              SB=KSB*(VA-VRSB)+SB1+KSB1*(LDD-LDCC)
              IF(SB.GT.100.) SB=100.
              IF(SB.LT.0.) SB=0.
   4463       ALPH=ALF0+KALF*(LDCC-LDD)/DLDDA+KOMP1*(RDTREF-RDT)
              ALPH=ALPH+KBIASW*(VIX-VAX)
              IF(IND7.EQ.1.) ALPH=ALPH/COSD(ROLL)
              IF(IND8.EQ.1..AND.ABS(ROLL).GT.ROLL4) ALPH=ALFF
              IF(IND8.EQ.1..AND.IND4.NE.5.) ALPH=ALFF
C             SIMULATE AUTOPILOT IN ALPHA
              DALF=ALPH-ALFOLD
              IF(ABS(DALF).GT.DALFLM) ALPH=ALFOLD+SIGN(DALFLM,DALF)
              ALFOLD=ALPH
   4462       IF(ALFF.GT.ALFMX) ALPH=ALFMX
```

```
          IF(ALPH.LT.ALFMN) ALPH=ALFMN
          CALL ADCTP(UNI1,URT1,ARG)
          IF(ARG.LT.0.) ROLL=0.
  444     INI=IND
  445     HF1=HF
          AZM1=AZIM
          ALF1=ALPH
          SB3=SP
          IF(IND.GT.2) GO TO 4465
          CALL LALONG(URT2,UZ,UEO,RTD,LONO,LATT,LONGT)
          GO TO 446
  4465    CALL LALONG(UC,UZ,UEO,RTD,LONO,LATT,LONGT)
  446     RETURN
  4461    IF(H.LE.HF2.AND.RDTMN.NE.0.) RDT2=-VA*H/(ATOGO-BIASFL)
          IF(RDT2.LT.RDTMN) RDT2=RDTMN
          IF(RDT2.GT.RDTMX) RDT2=RDTMX
          IF(H.LE.HTT2) RDT2=RDT3
          IF(H.LE.HTT2) GF2=GF3
          GF1=(-RDT+RDT2)/DT
          IF(GF1.GT.GF2) GF1=GF2
          ALPH=ALPH*(GF1+GS)/AMAG
          IND10=1.
          GO TO 4462
  5       WRITE(6,555)
  555     FORMAT(' LANDING-SITE-BEYOND-VEHICLE-CAPABILITY')
          ASSIGN 4 TO II
          IND= 4
          GO TO 4446
  6       IF((DTH1-GS*SIND(RL2)*DT*RTD/(COSD(RL2)*VA)).GT.180.) GO TO 4441
          DEL1=DTH1/RTD-PI
          ROLL=ATAN2((DEL1*VA),(GS*DT))*RTD
          IF(ABS(ROLL).GT.RL1) ROLL=SIGN(RL1,ROLL)
          IF (IND4.EQ.3.) GO TO 66
          H1=H
          IF(IND.EQ.3) IND4=3.
          GO TO 444
  66      HF=HF+H1-H
          H1=H
          GO TO 444
  4446    DO 4447 I=1,3
  4447    TEM(I)=URT(I)
          CALL UNITV(TEM,URT2,X1,X1)
          IND2=1.
          ALFOLD=ALPH
          GO TO 4448
  5558    ALPH=ALFC1+KDMPI*(RDTRFT-RDT)
          IF(VIX.GT.VLM2) GO TO 5557
          ALPH=ALFC1-KTR*(VLM2 -VIX)
          ALPH=ALPH+KDMPT*(RDTRFT-RDT)
          IF(ALPH.LT.ALF7) ALPH=ALF7
```

```
      5557 IF(VIX.LE.VLMS) GO TO 5556
           IF(INPT.EQ.0.) TEST1=TEST
           INPT=1.
           IF(DEL.GE.DELTR) TEST1=TEST
           RTOGON=(VIX**2-VF**2)/(2.*ACTR)
           ARG=RTOGO/RTOGON
           IF(ARG.GE.1.) ARG=1.
           RL7=ARCOS(ARG)*RTD
           IF(RL7.LT.RL7MN) RL7=RL7MN
           IF(RL7.GT.RLT1) RL7=RLT1
           ROLL=RL7*TEST1
           GO TO 444
      5556 OM=GS*SIND(RL8)/(COSD(RL8)*VIX)
           IF(OM.GT.OMLM) OM=OMLM
           IF((OM*DT).GT.DEL) OM=DEL/DT
           ROLL=ATAN2((OM*VIX),GS)*TEST*RTD
           GO TO 444
           END
```

```
FORTRAN IV G LEVEL  20                INIT              DATE = 72158          10/55/38              PAGE 0001

                      SUBROUTINE INIT
                      IMPLICIT REAL (I-N)
                      INTEGER I,M,J,IASS,C
                      DIMENSION R(3),V(3),UZ(3),UR(3),UNI(3),UV(3),A(165),B(5)
                      DIMENSION UE(3),URZ(3),URT(3)
                      EQUIVALENCE (R,A),(V,A(4)),(UZ,A(7)),(UZT,A(10))
                      EQUIVALENCE (UR,A(11)),(URT,A(14)),(URTT,A(17)),(ILON,A(18))
                      DATA YES/4HYES /
                      IF(M.EQ.1) GO TO 11
                      M=1
                      RI=20926043.
                      RP=20855873.
                      ATK=1./60.
                      KH=1.-(RI/RP)**2
          11          WRITE(6,21)
          21          FORMAT(' NEW ENTRY FILE?  ')
                      READ(5,22) C
          22          FORMAT(A3)
                      IF (C.EQ.YES) GO TO 12
                      DEFINE FILE 7(33,80,E,IASS)
                      READ (7' 1,60) A
          12          WRITE(6,600)
          600         FORMAT(' INPUT:')
                      READ(5,100) I
          100         FORMAT(I4)
                      IF(I.EQ.0) GO TO 2
                      IF(I.GE.0) GO TO 101
                      READ(5,200) B(1)
          200         FORMAT(G10.2)
                      GO TO 5
          101         READ(5,200) (B(J),J=1,5)
                      DO 3 J=1,5
          3           A(J+I-1)=B(J)
                      GO TO 12
          5           A(-I)=B(1)
                      GO TO 12
          2           CALL UNITV(R,UR,RL,RLSQ)
                      IF (RL.GT.RP) GO TO 7
                      IF (UZT.EQ.0.) R(2)=UZ(1)
                      RII=R(1)+RI/SQRT(1.-KH*SIND(R(2))**2)
                      R(1)=RII
                      R(2)=0.
                      R(3)=0.
          7           IF(V(1).LT.90000.) GO TO 8
                      V(1)=V(2)*SIND(V(3))
                      V(2)=V(2)*COSD(V(3))
                      V(3)=0.
          8           IF(UZT.EQ.1.) GO TO 4
                      CALL AXB(V,R,TEMP)
                      CALL UNITV(TEMP,UNI,XI,XI)
```

```
               CALL AXB(UR,UNI,UV)
               CL=COSD(UZ(1))
               SL=SIND(UZ(1))
               CAZ=COSD(UZ(2))
               SAZ=SIND(UZ(2))
               UZ(1)=CL*(UV(1)*CAZ-UNI(1)*SAZ)+UR(1)*SL
               UZ(2)=CL*(UV(2)*CAZ-UNI(2)*SAZ)+UR(2)*SL
               UZ(3)=CL*(UV(3)*CAZ-UNI(3)*SAZ)+UR(3)*SL
               UZT=1.
     4         IF(URTT.EQ.1.) GO TO 31
               IF(URTT.EQ.2.) GO TO 40
               CALL AXB(V,R,TEMP)
               CALL UNITV(TEMP,UNI,X1,X1)
               CALL AXB(UR,UNI,UV)
               CDR=CCSD(URT(1)/ATK)
               SDR=SIND(URT(1)/ATK)
               CCR=COSD(URT(2)/ATK)
               SCR=SIND(URT(2)/ATK)
               DO 32 I=1,3
    32         URT(I)=UR(I)*CCR+SDR*(UNI(I)*SCR+UV(I)*CCR)
               URTT=2.
               GO TO 40
    31         CALL AXB(UZ,UR,TEMP)
               CALL UNITV(TEMP,UE,X1,X1)
               CALL AXB(UE,UZ,URZ)
               CLAT=COSD(URT(2))
               SLAT=SIND(URT(2))
               CLON=COSD(URT(3)-ILON)
               SLON=SIND(URT(3)-ILCN)
               DO 33 I=1,3
    33         URT(I)=UZ(I)*SLAT+CLAT*(URZ(I)*CLON+UE(I)*SLON)
               URTT=2.
    40         WRITE (7' 1,6) A
    60         FORMAT (5E14.7)
     6         FORMAT (1P5E14.7)
               RETURN
               END
```

```
0001        IMPLICIT REAL (I-N)
0002        INTEGER T,II,DC,IH
0003        DIMENSION W(3),R(3),V(3),VA(3),UR(3),D(3),L(3),GR(3),
          * TEMP(3),TEMP1(3),UL(3),UVA(3),N3(3),UZ(3),N(3),Z(8),
          * DZ(8),A(165),URO(3),UCR(3),UE1(3),UEO(3)
0004        DIMENSION CC(8),X(8),THRUST(5)
0005        EQUIVALENCE (UZ,A(7)),(UUTP,A(19))
0006        EQUIVALENCE (PCTR1,A(21)),(HMAX,A(22)),(HMIN,A(23)),
          * (ROLL,A(24)),(NOCDA,A(25)),(LCO,A(26)),(DT1,A(27)),(LONO,A(18)),
          * (TMAX,A(29)),(NORUN,A(30)),(NOSTR,A(40)),(A(31),NOPLT),
          * (A(32),DT2),(A(33),HMN2),(A(34),PCTR2)
0007        EQUIVALENCE (Z,V),(Z(4),R),(CLA,A(154)),(CDA,A(155)),
          * (ALPH,A(156)),(IMAG,A(157)),(MDOT,A(158)),(M,A(159)),
          * (KWIF,A(163))
0008        DIMENSION HW(7),VW1(7),UN1(3),VW(3)
0009        DIMENSION B(12)
0010        EQUIVALENCE (A(47),WF),(A(48),AZW),(A(58),KCLA),(A(59),KCDA),
          * (A(56),TW),(A(57),TA),(A(53),VGST),(A(54),WROT),
          * (A(55),KREF)
0011        DATA HW/80.,60.,23.,20.,14.,10.,0./
0012        DATA VW1/150.,150.,40.,40.,97.,97.,28./
0013        DATA CQ/9*0./
0014        DATA X/8*0./
0015       DATA Z,DZ/16*0./
0016        DATA LG,SB/0.,0./
0017        IH=7
0018        IF(M.EQ.1) GO TO 1
0019        GS=32.2
0020        MU=1.407654E16
0021        WIE=.0000729211508
0022        KO=8.849E-6
0023        JO=1623.465E-6
0024        R1=20926043.
0025        RP=20855873.
0026        RE=20925738.
0027        KH=1.-(R1/RP)**2
0028        AREF=7320.
0029        DC=1
0030        RTD=180./3.14159265
0031        ATK=60.*RTD
0032        X1=0.
0033        PCT=-3.
0034        ENDP=0.
0035        T=0.
0036        M=1
0037        CALL INIT
0038        READ (7'1,21) A
0039        DT=DT1
0040        PCTR=PCTR1
0041        CAZW=COSD(AZW)
```

```
0042            SAZW=SIND(AZW)
0043            SWRT=SIND(WROT)
0044            CWRT=COSD(WROT)
0045            DO 27 I=1,3
0046            R(I)=A(I)
0047      27    V(I)=A(I+3)
0048      21    FORMAT(5E14.7)
0049            CROLL=COSD(ROLL)
0050            SROLL=SIND(ROLL)
0051            WIE=KWIE*WIE
0052            CALL UNITV(R,URO,X1,X1)
0053            CALL VECSCL(UZ,WIE,W)
0054            CALL AXB(UZ,URO,TEMP)
0055            CALL UNITV(TEMP,UEO,X1,X1)
0056            CALL AXB(V,URO,TEMP)
0057            CALL UNITV(TEMP,UCR,X1,X1)
0058            WRITE(6,51)
0059      51    FORMAT(1H0,'   TIME          RANGE          ALTITUDE       VELOCITY      RD
               *OT          ACCEL.')
0060            WRITE(6,52)
0061      52    FORMAT('    G               LAT            LONG           LATRANGE     ROLL
               *        MACH')
0062       1    IF(DC.EQ.2) M=M+.5*DT*MDOT
0063            IF(DC.EQ.4) M=M+.5*DT*MDOT
0064            CALL UNITV(R,UR,RL,RLSQ)
0065            CALL AXB(W,R,TEMP)
0066            CALL VSUB(V,TEMP,TEMP1)
0067            CALL AXB(UZ,UR,TEMP)
0068            CALL UNITV(TEMP,UE1,X1,X1)
0069            CALL AXB(UR,UE1,UN1)
0070            CALL ADOTB(UR,UZ,CT)
0071            H=RL-R1/SQRT(1.-KH*CT**2)
0072            IF(INDF.EQ.1.) H=Z(8)
0073            DO 101 II=1,IH
0074            I=IH-II+1
0075            IF((.3048*H).LT.(1000.*HW(I))) GO TO 102
0076     101    CONTINUE
0077     102    GRAD = (.0003048*H-HW(I))/(HW(I)-HW(I+1))
0078            VW2=(VW1(I)+GRAD*(VW1(I)-VW1(I+1)))*(WF/.3048)
0079            IF(T.GT.(TW+TA)) GO TO 203
0080            IF(T.GE.TW) VW2=VGST*(1.-COSD((T-TW)*360./TA))
0081     203    DO 31 I=1,3
0082      31    VW(I)=VW2*((UN1(I)*CAZW+UE1(I)*SAZW)*CWRT+UR(I)*SWRT)
0083            CALL VAD(VW,TEMP1,VA)
0084            CALL UNITV(VA,UVA,VAL,VALSQ)
0085            UE=RE/RL
0086            B1=(1.+((1.-5.*CT**2)*J0+(.5+(10.5*CT**2-7.)*CT**2)*K0*
               *UE**2)*UE**2)*(-MU)/(RLSQ)
0087            B2=(2.*J0+(2.-14.*CT**2/3.)*UE**2*K0)*UE**2*(-MU)*CT/RLSQ
0088            DO 2 I=1,3
```

```
0089          2      GR(I)=B1*UR(I)+B2*UZ(I)
              C      END GRAVITY CALCULATION
0090                 CALL ATMOS(H,RHO,VSOUND)
0091                 MACH=.3048*VAL/VSOUND
0092                 Q=.5*(RHO*KRHO)*VALSQ
0093                 CALL AXB(UVA,UR,TEMP)
0094                 CALL UNITV(TEMP,UL,X1,X1)
0095                 IF(DC.GT.1) GO TO 111
0096                 IF(NOSTR.EQ.0.) GO TO 111
0097                 CALL UNITV(V,TEMP,VMAG,X1)
0098                 CALL LNDSTR(R,V,UEO,VAL,VMAG,AZIM,H,ROLL,ALPH,AMAG,B(1),B(2),
                    * B(3),B(4),B(5),B(6),B(7),B(8),B(9),B(10),B(11),B(12),DT,LG,SB)
0099                 IF(PCT.EQ.0.AND.OUTP.NE.0) WRITE(6,26)B
0100                 CALL AERO(T,AREF,R,V,VA,CLA,CDA,ALPH,ROLL,MACH,LG,SB,H)
0101                 CLA=KCLA*CLA
0102                 CDA=KCDA*CDA
0103                 SROLL=SIND(ROLL)
0104                 CROLL=COSD(ROLL)
0105                 SALPH=SIND(ALPH)
0106                 CALPH=COSD(ALPH)
0107        111      D1=Q*CDA/M
0108                 CALL VECSCL(UVA,-D1,D)
0109                 CALL AXB(UL,UVA,N3)
0110                 DO 3 I=1,3
0111          3      N(I)=N3(I)*CROLL+UL(I)*SROLL
0112                 DLOD=Q*CLA/M
0113                 CALL VECSCL(N,DLOD,L)
0114                 DO 4 I=1,3
0115          4      THRUST(I)=(TMAG/M)*(N(I)*SALPH+UVA(I)*CALPH)
0116                 IF(PCT.LT.0.) GO TO 121
              C
0117                 DZ(1)=L(1)+D(1)+THRUST(1)+GR(1)
0118                 DZ(2)=L(2)+D(2)+THRUST(2)+GR(2)
0119                 DZ(3)=L(3)+D(3)+THRUST(3)+GR(3)
0120                 DZ(4)=Z(1)
0121                 DZ(5)=Z(2)
0122                 DZ(6)=Z(3)
0123                 IF(INDE.NE.1.) GO TO 333
0124                 CALL ADOTB(DZ,UR,AH)
0125                 DZ(7)=AH
0126                 DZ(8)=Z(7)
              C
0127        333      CALL DIFEQ(8,DT,DC,DZ,Z,T,QQ,X)
0128                 IF(DC.LT.5) GO TO 1
0129        303      DC=1
0130                 IF(PCT.LT.0) GO TO 121
0131                 PCT=PCT+1.
0132                 IF(T.GE.TMAX) ENDR=1.
0133                 IF(H.GE.HMAX) ENDR=1.
0134                 IF(H.LE.HMIN) ENDR=1.
```

```
              IF(INDF.EQ.1.) GO TO 121
              IF(H.LE.HMN2) INDF=1.
              IF(H.LE.HMN2) DT=DT2
              IF(H.LE.HMN2) PCTR=PCTR2
              IF(H.LE.HMN2) PCT=PCTR
              IF(H.LE.HMN2) Z(8)=H
                    IF(H.LE.HMN2) CALL ADOTB(V,UR,Z(7))
      121     CALL VAD(L,D,TEMP)
              CALL VAD(TEMP,THRUST,TEMP1)
              CALL UNITV(TEMP1,TEMP,AMAG,X1)
              CALL ADOTB(UR,URO,ARG)
              RANGE=ATK*ARCOS(ARG)
              CALL ADOTB(UR,UCR,ARG)
              LATRNG=ATK*ARG
              CALL UNITV(V,TEMP,VEL,X1)
              CALL ADOTB(V,UR,RDOT)
              LAT=ARSIN(CT)*RTD
              CALL AXB(UZ,UR,TEMP)
              CALL UNITV(TEMP,UE1,X1,X1)
              CALL AXB(UE1,UEO,TEMP)
              CALL UNITV(TEMP,TEMP1,ARG,X1)
              IF(X1.EQ.0.) ARG=0.
              DLON=ARSIN(ARG)
              CALL ADOTB(UZ,TEMP,ARG)
              IF(ARG.GT.0.) DLON=-DLON
              LONG=LONO+(DLON-WIE*T)*RTD
              IF(NOPLT.EQ.1.) GO TO 13
              WRITE(8,501) T,RANGE,H,VAL,RDOT,AMAG,Q,LAT,LONG,LATRNG,ROLL,
             * MACH,B
      501     FORMAT(1P6E12.4)
      13      IF(ENDR.EQ.1.) GO TO 12
              IF(PCT.EQ.PCTR) GO TO 12
              IF(PCT.LT.0) GO TO 12
              GO TO 1
      12      PCT=0.
              WRITE(6,25) T, RANGE,H,VAL,RDOT,AMAG,Q,LAT,LONG,LATRNG,ROLL,
             * MACH
      25      FORMAT(/1P6E12.4/6E12.4)
      26      FORMAT(1P6E12.4/6E12.4)
              IF (ENDR.EQ.1.) GO TO 11
              GO TO 1
      11      STOP
              END
```

```
      SUBROUTINE AERO(T,AREF,V,Q,CLA,CD,ALPH,ROLL,MACH,LG,SB,H)
      IMPLICIT REAL (A-H)
      INTEGER I,J,K,N
      DIMENSION CL(10,8),LD(10,13),MACH1(10),ALCL(8),AL D(13),A(165),
     * DCL1(5,6),ST(9),ROH(5)
      DATA N/0/
      DATA CL/.025,.012,.025,.018,.015,.015, .0  ,-.028,-.028,-.028,
     *   .154, .16 , .173, .15 , .154, .1 3, .09 , .049, .0  , .029,
     *   .254, .30 , .32 , .28 , .23 , .21 , .184, .126, .125, .125,
     *   .375, .4 0, .478, .51 , .425, .31 , .28 , .20 , .125, .125,
     *   .50 , .530, .620, .53 , .500, .419, .382, .2 5, .2 3, .213,
     *   .620, .710, .7 0, .625, .70 , .519, .473, .375, .307, .305,
     *   .620, .715, .760, .625, .70 , .637, .590, .465, .419, .405,
     *   .620, .71 , .700, .625, .70 , .637, .590, .60 , .505, .503/
      DATA LD/.15,.5 ,.7 ,.15,.25,.20,.14,-.45,-.45,-.45,
     *   4.0 , 3.5 , 3.15, 3.35, 1.50,  .65,  .75,  .20,  .20,  .20,
     *   6.25, 5.1 , 4.80, 2.15, 1.93, 1.32, 1.2 ,  .79,  .79,  .79,
     *   7.41, 7.25, 5.10, 2.59, 2.42, 1.70, 1.62, 1.27, 1.27, 1.27,
     *   7.7 , 7.45, 4.5 , 2.70, 2.63, 1.92, 1.99, 1.67, 1.67, 1.57,
     *   7.73, 7.15, 3.98, 2.65, 2.70, 2.03, 2.06, 1.94, 1.94, 1.94,
     *   7.62, 6.2 , 3.52, 2.50, 2.5 , 2.10, 2.16, 2.08, 2.08, 2.08,
     *   7.30, 5.25, 3.10, 2.18, 2.40, 2.10, 2.17, 2.10, 2.10, 2.10,
     *   6.  , 4.32, 2.75, 2.05, 2. 4, 2.07, 2.13, 2.10, 2.15, 2.09,
     *   5.7 , 3.58, 2.18, 1. 3, 2.09, 2.0 , 2.05, 2.03, 2.10, 2.05,
     *   4.30, 2.90, 2. 5, 1.65, 1.90, 1.94, 1.97, 1.95, 2.05, 2.0 ,
     *   4.30, 2.90, 2. 5, 1.65, 1.90, 1.69, 1.71, 1.70, 1.80, 1.73,
     *   4.30, 2.90, 2.25, 1.65, 1.90, 1.45, 1.47, 1.47, 1.50, 1.50/
      DATA  MACH1/.2, .6, .9, 1.2, 1.5, 2.0, 2.4 , 3.93, 10., 30./
      DATA ALCL/0., 4., 8., 12., 16., 20., 25., 30./
      DATA  AL D/0.,2.,4.,6.,8.,10.,12.,14.,16.,18.,20.,25.,30./
      DATA DCL     /-.0  75,.0  1,.3 33/
      DATA  /0.,-.0 ,-.21,-.42,-.59,-.70,-.79,-.8 ,-.97/
      DATA ROH/0.,1.5,3.0,5.0,7.61/
      DATA DCL1/0.    ,0.    ,0.    ,0.    ,0.    ,
     *           0.    ,0.    ,.0 5 ,.050 ,.040 ,
     *           0.    ,.015 ,.048 ,.085 ,.135 ,
     *           0.    ,.020 ,.065 ,.140 ,.2 0 ,
     *           0.    ,.025 ,.093 ,.190 ,.305 ,
     *           0.    ,.03  ,.125 ,.250 ,.390 /
C
      IF(N.EQ.1) GO TO 1
      READ(7'1,60) A
60    FORMAT(5E14.7)
      AREF=A(159)
      B =A(51)
      CD0=A(52)
      N=1
1     DO 1 I=1,10
      I =10-I+1
      IF(MACH.GE.MACH1(I )) GO TO 2
1     CONTINUE
2     GRAD1=(MACH-MACH1(I ))/(MACH1(I +1)-MACH1(I ))
      DO 3 J=1,8
      J =8-J+1
      IF(ALPH.GE.ALCL(J )) GO TO 4
3     CONTINUE
4     GRAD2=(ALPH-ALCL(J ))/(ALCL(J +1)-ALCL(J ))
      DO 5 K=1,13
      K =13-K+1
      IF(ALPH.GE.AL D(K )) GO TO 6
5     CONTINUE
6     GRAD3=(ALPH-AL D(K ))/(AL D(K +1)-AL D(K ))
```

```
      [illegible]
      LD1=LD(I ,K )+GRAD1*(LD(I +1,K )-LD(I ,K ))
      LD2=LD(I ,K +1)+GRAD1*(LD(I +1,K +1)-LD(I ,K +1))
      CL[illegible]=[illegible]+[illegible]2*(C[illegible]-[illegible]1)
      LD[illegible]=LD1+GRAD3*(L[illegible]2-[illegible]1)
      IF([illegible]) [illegible]=1.
      CLA=[illegible]TE[illegible]
      CDA=[illegible]/[illegible]
      [illegible]/[illegible]
      IF([illegible].LT.[illegible]1) GO TO 7
      IF([illegible].GT.7 ) BOH= 7.
      I=[illegible]
      DK=(D[illegible]T(I+1)-DKT(I))*(BOH-I)+DKT(I)
      CDO=(C[illegible]-[illegible]0*[illegible]REF)*(1+DK)+CDO*AREF
      J = AL[illegible]/4.
      GRAD2=[illegible]/4.-J
      DO 8 K=1,5
      K =[illegible] +1
      IF([illegible].GE.BOHT(K )) GO TO 9
8     CONTINUE
9     GRAD1=(BOH-BOHT(K ))/(BOHT(K +1)-BOHT(K ))
      DCL11= DCL1(K ,J )+GRAD1*(DCL1(K +1,J )-DCL1(K ,J ))
      DCL12= DCL1(K ,J +1)+GRAD1*(DCL1(K +1,J +1)-DCL1(K ,J +1))
      DCL= DCL1 +GRAD2*(DCL12-DCL1 )
      CLA=[illegible]A+D[illegible]*[illegible]
7     CLA=CLA+DCL[illegible]3*S[illegible]AREF
      CDA=CDA+(DC[illegible]3*S[illegible]+L[illegible]*CD[illegible]5)*AREF
      RETURN
      END
READY
```

```
SUBROUTINE DIFEQ(N,DT,NA,DZ,Z,Q,X)
DIMENSION Q(1),DZ(1),Z(1),X(1)
DO 4  J=1,N
GO TO (20,21,22,23),NA
20    C0=.5
      C1=1
      C2=.5*DT
      GO TO 20
21    C0=.29289321 3
214   C1=20
      C2=0*DT
      GO TO 20
2     C0=1.70710678 7
      GO TO 214
23    C0=.15
      C1=.5
      C2=.5*DT
20    X(J)=C0*DZ(J)*DT-C1*Q(J)
      Q(J)=Q(J) +3*X(J) - C2*DZ(J)
4     Z(J)=Z(J)+X(J)
      GO TO (30,31,30,31),NA
30    T=T+DT/2
31    NA=NA+1
      RETURN
      END
C
      SUBROUTINE ATMOS(A,RHO,VSOUND)
      DIMENSION BHD(14),BTMP(14),TMPGRD(13),BRHO(14)
      DATA BHD/1.6E5,1.5E5,1.2E5,1.1E5,1.E5,9.E4,7.9E4,
     * 6.1E4,5.2E4,4.7E4,3.2E4,2.E4,1.1E4,0./
      DATA BTMP/1 0.65,9 0.65,3 0.5,2 0.2 5,210.65,180.65,
     * 180.65,2 0.65,270.65,270.65,2 8.65,21 . 5,216. 5,28 .15/
      DATA TMPGRD/.015,.02,.01,.0 5,.0 3,. ,-.0 4,-.0 2,0.,0.28

     * .0 1,0.,-.0 65/
      DATA BRHO/1. 59E-9,1.836E-9,2.436E-8,9.8295-8,4.97 E-7,
     * 3.170E-6,2.0 1E-5,2.5109E-4,7.5943E-4,1.4275E-3,1.52 5E-2,
     * .08 0 5,.6 92,1.2 5/,
      DATA  RE/6356.0  ./
      ATMC=.034163 5
      SRC=401.87/29
      H=.3048*A
      IF (H.GE.BHD(6)) HA=.
      IF (H.LT.BHD(6)) HA=(RE*H)/(RE+H)
      DO 1 I=1,14
      IF (HA.GE.BHD(I)) GO TO 2
1     CONTINUE
2     IF (I.EQ.1) GO TO 3
      HO= A-BHD(I)
      IF (TMPGRD(I-1).EQ.0.) GO TO 4
      TEMP=BTMP(I)+TMPGRD(I-1)*HO
      IF (H.GE.BHD(6)) GO TO 5
      RHO=BRHO(I)*EXP((1+ATMC/TMPGRD(I-1))*ALOG(BTMP(I)/TEMP))
      GO TO 6
4     TEMP=BTMP(I)
      RHO=BRHO(I)*EXP(-ATMC*HO/TEMP)
6     VSOUND=SQRT(SRC*TEMP)
      RHO=.0 19403 2 *RHO
      RETURN
3     RHO=0.
      . 1.
      . .
```

-139-

```
            [illegible]=1./([illegible])*[illegible](I)/[illegible](I-1)[illegible]
            B1=[illegible](I)/[illegible]
            B2=[illegible]/([illegible]A)*([illegible])(I)[illegible]
            RHS=[illegible](I)*[illegible](AT[illegible] 2 [illegible]BU ( 2+[illegible]0*ALOG(B1*(1.+RHO/[illegible]E)[illegible]

            T[illegible]GRD(I-1)+ALOG(B1))
            GO TO 6
            END
C
            SUBROUTINE AXB(A,B,RET)
            DIMENSION A(3),B(3),RET(3)
            RET(1)=A(2)*B(3)-A(3)*B(2)
            RET(2)=A(3)*B(1)-A(1)*B(3)
            RET(3)=A(1)*B(2)-A(2)*B(1)
            RETURN
            END
C
            SUBROUTINE ADOTB(A,B,RET)
            DIMENSION A(3),B(3)
            RET=A(1)*B(1)+A(2)*B(2)+A(3)*B(3)
            RETURN
            END
C
            SUBROUTINE UNITV(A,B,C,D)
            DIMENSION A(3),B(3)
            D=A(1)**2+A(2)**2+A(3)**2
            IF (D.EQ.0.) GO TO 1
            C=SQRT(D)
            B(1)=A(1)/C
            B(2)=A(2)/C
            B(3)=A(3)/C
1           RETURN
            END
C
            SUBROUTINE VSUB(A,B,RET)
            DIMENSION A(3),B(3),RET(3)
            DO 1 I=1,3
1           RET(I)=A(I)-B(I)
            RETURN
            END
C
            SUBROUTINE VAD(A,B,RET)
            DIMENSION A(3),B(3),RET(3)
            DO 1 I=1,3
1           RET(I)=A(I)+B(I)
            RETURN
            END
C
            SUBROUTINE VECSCL(A,B,RET)
            DIMENSION A(3),RET(3)
            DO 1 I=1,3
1           RET(I)=A(I)*B
            RETURN
            END
READY
```

```
SUB1.FORT
          FUNCTION SIND(X)
          SIND=SIN(X*.0174532925)
          RETURN
          END
          FUNCTION DANG(A,B)
          DIMENSION A(3),B(3),C(3),D(3)
          CALL AXB(A,B,C)
          CALL UNITV(C,D,ARG,X1)
          IF (X1.EQ.0.) ARG=0.
          DANG=ARSIN(ARG)
          RETURN
          END
          FUNCTION COSD(X)
          COSD=COS(X*.0174532925)
          RETURN
          END
          SUBROUTINE LATLONG(X,UZ,UE0,RTD,LON0,LATT,LONGT)
          IMPLICIT REAL(J-N)
          DIMENSION X(3),UZ(3),UE0(3),UE1(3),TEM(3)
          CALL AXB(UZ,X,TEM)
          CALL UNITV(TEM,UE1,X1,X1)
          LONGT=LON0+DANG(UE1,UE0)*RTD
          CALL ADOTB(UZ,X,CT)
          LATT=ARSIN(CT)*RTD
          RETURN
          END
          FUNCTION DOTPRO(A,B)
          DIMENSION A(3),B(3)
          DOTPRO=A(1)*B(1)+A(2)*B(2)+A(3)*B(3)
          RETURN
          END
READY
```

APPENDIX E

NAVIGATION FILTER CHARACTERISTICS

The navigation filter of Ref. [12] was used to generate the precision DME results. This is shown in Table E-1. The Triangular Formulation of a Square Root Kalman Filter [16] was used to generate the low precision DME results. This is illustrated in Table E-2. A dramatic increase in computer speed (nearly 4 to 1) resulted in using the Square Root formulation. A nearly 2 to 1 increase in precision characteristic of the square root formulation also resulted.

A thirteen state filter was used. Two states were added to the filter of ref. [12] to estimate the 90 m bias of the low precision DME's. These states are illustrated in Table E-3. The corresponding state transition matrix is in Table E-4, and the driving noise elements are in Table E-5.

The landing aids are located in Fig. E.1. The two DMEs are rather close to the runway and probably should be moved out. But this baseline was chosen to provide results comparable to those of ref. [14].

The DME model, Table E-6, is from both ref. [12] and [14]. The 90 m bias required the addition of two filter states to estimate this bias. Without the estimate, divergence resulted and even with the positive definite guarantee of the Joseph formulation, which was used in early tests, the covariance matrix became negative!

The barometric altimeter model, Table E-7, is from ref. [14]. No bias proportional to altitude is present (scale factor error) and probably should be corrected.

The radar altimeter model is in Table E-8, and the ILS model is in Table E-9.

As in all these studies, correct modelling of the navigation is vital. This is true both in the filter equations and in the error driving model. For example, the filter will drive the altitude close to the .61 m value of the radar altimeter near landing. If terrain effects are greater than this value, the simulation will be over optimistic in the altitude performance near landing.

Finally, the IMU characteristics from ref. [13] as summarized in Table E-10. The 2/3 meru gyro in this unit is a high quality unit placing this system near the front in the state of the art.

$$\underline{\hat{x}}_i = \Phi_{i-1}\, \underline{\hat{x}}_{i-1}$$

$$P_i^- = \Phi_{i-1}\, P_{i-1}^+\, \Phi_{i-1}^T + Q_{i-1}$$

$$\underline{k}_i = P_i^- \underline{h}_i / (\underline{h}_i^T\, P_i^-\, \underline{h}_i + r_i)$$

$$\underline{\hat{x}}_i^+ = \underline{\hat{x}}_i^- + \underline{k}_i (z_i - \underline{h}_i^T\, \underline{\hat{x}}_i^-)$$

$$P_i^+ = (I - \underline{k}_i \underline{h}_i^T)\, P_i^-\, (I - \underline{k}_i \underline{h}_i^T)^T + \underline{k}_i r_i \underline{k}_i^T$$

(See Ref. [12] for notation)

Table E-1: Kalman Estimator (Joseph Form) Used in Precision DME Work

$S^T S = P$ (S = upper triangular root of P)

$\underline{f} = S^T \underline{h}$

$\alpha = r + \underline{f}^T \underline{f}$

$S^+ = S[I - \underline{f}\,\underline{f}^T/\alpha]^{1/2}$

where $[I - \underline{f}\,\underline{f}^T/\alpha]^{1/2}$ is upper triangular root of [ ], derived by Cholesky decomposition.

$\hat{\underline{x}}^+ = \hat{\underline{x}} + S\underline{f}\ \Delta z/\alpha$

Table E-2: Triangular Formulation of Square Root Kalman Estimator Used For Low Precision Navigation Study

Variable		Sign Convention
x_1	Error in east position	Positive if indicated position is east of actual.
x_2	Error in north position	Positive if indicated position is north of actual.
x_3	Error in altitude	Positive if INS indicated altitude is above actual.
x_4	Error in east velocity	Positive if indicated east velocity exceeds actual.
x_5	Error in north velocity	Positive if indicated north velocity exceeds actual.
x_6	Error in altitude rate	Positive if indicated up velocity exceeds actual.
x_7	Platform tip about east axis	Positive if platform is rotated positive about the east axis.
x_8	Platform tip about north axis	Positive if platform is rotated positive about the north axis.
x_9	Platform azimuth error	Positive if platform is rotated positive about the up axis.
x_{10}	Vertical acceleration error	Positive if it induces a positive altitude-rate error.
x_{11}	Altimeter error	Positive if measured altitude exceeds actual.
*x_{12}	DME1 Bias	Positive if bias exceeds actual
*x_{13}	DME2 Bias	Positive if bias exceeds actual

* New

Table E-3: State Variables Estimated by the Kalman Filter

$\Phi_{1,1} = 1,$	$\Phi_{1,4} = T$
$\Phi_{2,2} = 1,$	$\Phi_{2,5} = T$
$\Phi_{3,3} = 1,$	$\Phi_{3,6} = T$
$\Phi_{4,4} = 1,$	
	$\Phi_{4,8} = -\Delta v_z$
	$\Phi_{4,9} = \Delta v_n$
$\Phi_{5,5} = 1,$	
	$\Phi_{5,7} = \Delta v_z$
	$\Phi_{5,9} = -\Delta v_e$
$\Phi_{6,6} = 1,$	$\Phi_{6,3} = 2(g/R)T$
	$\Phi_{6,7} = -\Delta v_n$
	$\Phi_{6,8} = \Delta v_e$
	$\Phi_{6,10} = T$
$\Phi_{7,7} = 1,$	$\Phi_{7,5} = -(1/R)T$
	$\Phi_{7,9} = -\Delta\theta_n$
	$\Phi_{7,3} = -\Delta\theta_e/R$
$\Phi_{8,8} = 1,$	$\Phi_{8,4} = (1/R)T$
	$\Phi_{8,9} = \Delta\theta_e$
	$\Phi_{8,3} = -\Delta\theta_n/R$
$\Phi_{9,9} = 1,$	$\Phi_{9,4} = (\tan L/R)T$
	$\Phi_{9,8} = -\Delta\theta_e$
	$\Phi_{9,7} = \Delta\theta_n$
	$\Phi_{9,3} = -(v_e \tan L/R^2)T$
$\Phi_{10,10} = 1 - (v/d_{gz})T$	$*\Phi_{12,12} = 1 - T/400$
$\Phi_{11,11} = 1 - (v/d_{alt})T$	$*\Phi_{13,13} = 1 - T/400$

* New

TABLE E-4: NON-ZERO ELEMENTS OF THE STATE TRANSITION MATRIX

$$Q_{4,4} = |\Delta v_e| \; v \; \sigma^2_{ASF} + |\Delta v_n| \; v \; \sigma^2_{A\theta}$$

$$Q_{5,5} = |\Delta v_n| \; v \; \sigma^2_{ASF} + |\Delta v_e| \; \dot{v} \; \sigma^2_{A\theta}$$

$$Q_{6,6} = 2|\Delta v_{hor}| v [2\sigma^2_{A\theta} + (\sigma_{ABIAS}/g)^2 + \sigma^2_{\delta e}]$$

$$Q_{7,7} = \Delta t \; T_B(\sigma^2_{GBIAS} + \sigma^2_{ADSRA} \; g^2) + |\Delta v_e| \; v \; \sigma^2_{ADIA}$$
$$+ |\Delta\theta_e| \; \Delta\theta_{total} \; \sigma^2_{GSF} + \Delta t(2v/d_{\delta n})\sigma^2_{\delta n}$$

$$Q_{8,8} = \Delta t \; T_B(\sigma^2_{GBIAS} + \sigma^2_{ADSRA} \; g^2) + |\Delta v_n| \; v \; \sigma^2_{ADIA}$$
$$+ |\Delta\theta_n| \; \Delta\theta_{total} \; \sigma^2_{GSF} + \Delta t(2v/d_{\delta e})\sigma^2_{\delta e}$$

$$Q_{9,9} = \Delta t \; T_B(\sigma^2_{GBIAS} + \sigma^2_{ADIA} \; g^2) + |\Delta v_n| \; v \; \sigma^2_{ADSRA}$$

$$Q_{10,10} = \Delta t(2v/d_{gz})\sigma^2_{gz}$$

$$Q_{11,11} = \Delta t(2v/d_{alt})\sigma^2_{alt} + |\Delta h| h_s \; \sigma^2_{temp} + |\Delta(v^2)| v_s^2 \; \sigma^2_{sp}$$

* $Q_{12,12} = 2 \; GBIASD^2 \; \Delta T/400 = Q$

* $Q_{13,13} = Q_{12,12}$

* New

Table E-5: Non-Zero Elements of the Noise Covariance Matrix

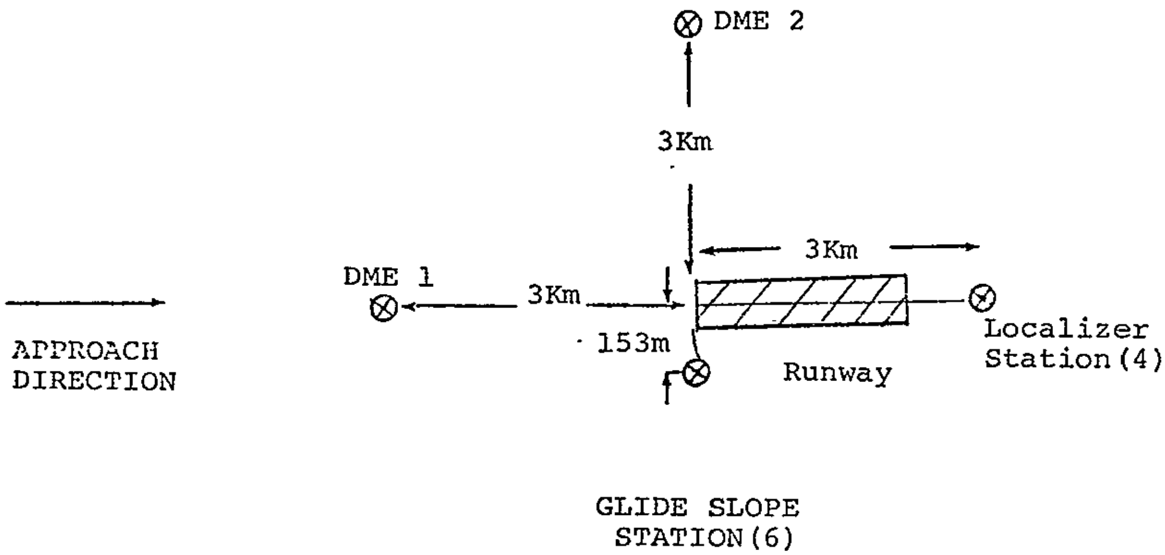

Fig. E.1: Landing Aid Locations

The measurement variance is assumed to be [12]

$$\sigma^2 = \sigma_b^{\,2} + r^2\sigma_p^{\,2} f^2(h) + \sigma_m^{\,2}\cos^2\varepsilon + \sigma_r^{\,2}$$

$$f(h) = (1-e^{-h/h_s})/(h/h_s)$$

$$\cos^2\varepsilon = (1-b_z^{\,2})^{1/2}$$

σ_b =	transponder bias	90m
σ_p =	propagation error	50×10^{-6}
σ_m =	multipath error	.9m
σ_r =	random error	14m
h_s =	scale height	6900m

90 bias is added to DME1, measured range -90 is added to DME2 and a random error of 7m is also added.

The filter estimates these biases in states 12 and 13 assuming an exponentially correlated random variable

σ = 90m	(Ref. 14)
Tc = 400 sec	

Compensation for non-linear elongation of the measured range are made to the actual measurement and assumed variance as in ref.[12].

Table E-6: DME Model

The altimeter has both a bias and a correlated error. The bias variance is:

$$\boxed{\begin{aligned} \sigma^2 &= K_1 h^4 + K_2 V_R{}^4 + 40^2 \\ K_1 &= .43 \times 10^{-12} \\ K_2 &= .25 \times 10^{-6} \end{aligned}}$$

No bias term proportion to altitude (scale factor) is presently added.

The uncorrelated error is also added as:

$$\boxed{\begin{aligned} \sigma^2 &= K_3 h^2 + 3^2 \\ K_3 &= 6.25 \times 10^{-8} \end{aligned}}$$

This bias and uncorrelated error are added to the measurement.

The filter assumes a measurement noise of the uncorrelated value.

Table E-7: Barometric Altimeter Model Ref. [14]

The radar altimeter error is altitude dependent as shown below.

h(m)	σ(m)
$h \geq 152.4$	$\sigma = .05h$
$30.48 < h < 152.4$	$\sigma = .02h$
$h \leq 30.48$	$\sigma = .61$ m

At present this is added to the measurement as an uncorrelated error.

The filter assumes a measurement noise of this value plus an additional 1 m, additive value.

Table E-8: Radar Altimeter Model Ref. [14]

The localizer (azimuth) error is range dependent as shown below:

range ρ (meters)	σ azimuth (mr)
$0 < \rho < 1067$	1.4
$1067 \leq \rho < 8330$	$1.4+4.2(\rho-1067)/7263$
$8330 \leq \rho$	5.6

The range dependence of the glide slope is shown below:

range ρ (m)	σ elevation (mr)
$0 \leq \rho < 1067$	1.4
$1067 \leq \rho < 8330$	$1.4+1.1(\rho-1067)/7263$
$8330 \leq \rho$	2.5

Uncorrelated random numbers of this magnitude are added to the measurement.

The filter also assumes a measurement noise of this value. If measurement is not within 2 degrees of the runway azimuth or elevation angle it is rejected.

Table E-9: ILS Model Ref. [14].

Source	Units	Value
gyros		
Bias	deg/hr	.010
g sensitive	deg/hr/g	.015
IA Misalignment	sec	60
Scale factor	ppm	50
Accelerometer		
Bias	μg	60
Scale Factor	ppm	34
IA Misalignment	sec	40

Table E-10: Inertial Measurement Unit Model, Kearfott KT70 Ref. [11]

APPENDIX F

Aerodynamic Characteristics for the 040a Vehicle

MACH	ALPHA	CL	CD	L/D	S.B(%)	[illegible]
0.30000	0.0	0.02250	0.09000	0.25000	0.0	[illegible]
0.30000	2.00000	0.08162	0.02106	3.87500	0.0	[illegible]
0.30000	4.00000	0.14075	0.02260	6.22750	0.0	[illegible]
0.30000	6.00000	0.20350	0.02761	7.37000	0.0	[illegible]
0.30000	8.00000	0.26525	0.03486	7.63750	0.0	[illegible]
0.30000	10.00000	0.32875	0.04333	7.58750	0.0	[illegible]
0.30000	12.00000	0.39125	0.05382	7.27000	0.0	[illegible]
0.30000	14.00000	0.45562	0.06713	6.78750	0.0	0.0
0.30000	16.00000	0.52000	0.08560	6.07500	0.0	0.0
0.30000	18.00000	0.58200	0.11198	5.19750	0.0	0.0
0.30000	20.00000	0.64400	0.15304	3.95000	0.0	0.0
0.50000	0.0	0.01550	0.03444	0.45000	0.0	0.0
0.50000	2.00000	0.08487	0.02341	3.62500	0.0	0.0
0.50000	4.00000	0.15425	0.02495	6.18250	0.0	0.0
0.50000	6.00000	0.22250	0.03052	7.29000	0.0	0.0
0.50000	8.00000	0.29075	0.03870	7.51250	0.0	0.0
0.50000	10.00000	0.35725	0.04892	7.30250	0.0	0.0
0.50000	12.00000	0.42375	0.06450	6.57000	0.0	0.0
0.50000	14.00000	0.49187	0.08536	5.76250	0.0	0.0
0.50000	16.00000	0.56000	0.11417	4.90500	0.0	0.0
0.50000	18.00000	0.62600	0.15296	4.09250	0.0	0.0
0.50000	20.00000	0.69200	0.21292	3.25000	0.0	0.0
0.70000	0.0	0.01633	0.02649	0.61667	0.0	0.0
0.70000	2.00000	0.09067	0.02680	3.38333	0.0	0.0
0.70000	4.00000	0.16500	0.02891	5.70667	0.0	0.0
0.70000	6.00000	0.23767	0.03638	6.53333	0.0	0.0
0.70000	8.00000	0.31033	0.04787	6.48333	0.0	0.0
0.70000	10.00000	0.38150	0.06254	6.10000	0.0	0.0
0.70000	12.00000	0.45267	0.08509	5.32000	0.0	0.0
0.70000	14.00000	0.52433	0.11566	4.53333	0.0	0.0
0.70000	16.00000	0.59600	0.15698	3.79667	0.0	0.0
0.70000	18.00000	0.66333	0.27156	2.44267	0.0	0.0
0.70000	20.00000	0.73067	0.27230	2.68333	0.0	0.0
0.90000	0.0	0.02500	0.03333	0.75000	0.0	0.0
0.90000	2.00000	0.09900	0.03143	3.15000	0.0	0.0
0.90000	4.00000	0.17300	0.03604	4.80000	0.0	0.0
0.90000	6.00000	0.24900	0.04832	5.10000	0.0	0.0
0.90000	8.00000	0.32500	0.07143	4.55000	0.0	0.0
0.90000	10.00000	0.40150	0.10088	3.98000	0.0	0.0
0.90000	12.00000	0.47800	0.13580	3.52000	0.0	0.0
0.90000	14.00000	0.55300	0.17839	3.10000	0.0	0.0
0.90000	16.00000	0.62800	0.22836	2.75000	0.0	0.0
0.90000	18.00000	0.69400	2.79837	0.24800	0.0	0.0
0.90000	20.00000	0.76000	0.33778	2.25000	0.0	0.0

Table F-1: 040a Aerodynamic Characteristics, Clean vehicle No Landing Gear, No Speed Brake

MACH	ALPHA	CL	CD	L/D	S.B(%)	L.G.
0.30000	0.0	0.02250	0.09380	0.23987	0.0	1.00000
0.30000	2.00000	0.08162	0.02486	3.28279	0.0	1.00000
0.30000	4.00000	0.14075	0.02640	5.33116	0.0	1.00000
0.30000	6.00000	0.20350	0.03141	6.47843	0.0	1.00000
0.30000	8.00000	0.26625	0.03866	6.88681	0.0	1.00000
0.30000	10.00000	0.32875	0.04713	6.97571	0.0	1.00000
0.30000	12.00000	0.39125	0.05762	6.79052	0.0	1.00000
0.30000	14.00000	0.45562	0.07093	6.42385	0.0	1.00000
0.30000	16.00000	0.52000	0.08940	5.81677	0.0	1.00000
0.30000	18.00000	0.58200	0.11578	5.02691	0.0	1.00000
0.30000	20.00000	0.64400	0.16684	3.86003	0.0	1.00000
0.50000	0.0	0.01550	0.03824	0.40529	0.0	1.00000
0.50000	2.00000	0.08487	0.02721	3.11882	0.0	1.00000
0.50000	4.00000	0.15425	0.02875	5.36532	0.0	1.00000
0.50000	6.00000	0.22250	0.03432	6.48286	0.0	1.00000
0.50000	8.00000	0.29075	0.04250	6.84083	0.0	1.00000
0.50000	10.00000	0.35725	0.05272	6.77616	0.0	1.00000
0.50000	12.00000	0.42375	0.06830	6.20446	0.0	1.00000
0.50000	14.00000	0.49187	0.08916	5.51690	0.0	1.00000
0.50000	16.00000	0.56000	0.11797	4.74700	0.0	1.00000
0.50000	18.00000	0.62600	0.15676	3.99330	0.0	1.00000
0.50000	20.00000	0.69200	0.21672	3.19302	0.0	1.00000
0.70000	0.0	0.01633	0.03029	0.53929	0.0	1.00000
0.70000	2.00000	0.09067	0.03060	2.96315	0.0	1.00000
0.70000	4.00000	0.16500	0.03271	5.04378	0.0	1.00000
0.70000	6.00000	0.23767	0.04018	5.91541	0.0	1.00000
0.70000	8.00000	0.31033	0.05167	6.00649	0.0	1.00000
0.70000	10.00000	0.38150	0.06634	5.75060	0.0	1.00000
0.70000	12.00000	0.45267	0.08889	5.09257	0.0	1.00000
0.70000	14.00000	0.52433	0.11946	4.38913	0.0	1.00000
0.70000	16.00000	0.59600	0.16078	3.70693	0.0	1.00000
0.70000	18.00000	0.66333	0.27536	2.40896	0.0	1.00000
0.70000	20.00000	0.73067	0.27610	2.64640	0.0	1.00000
0.90000	0.0	0.02500	0.03713	0.67325	0.0	1.00000
0.90000	2.00000	0.09900	0.03523	2.81022	0.0	1.00000
0.90000	4.00000	0.17300	0.03984	4.34219	0.0	1.00000
0.90000	6.00000	0.24900	0.05262	4.73172	0.0	1.00000
0.90000	8.00000	0.32500	0.07523	4.32017	0.0	1.00000
0.90000	10.00000	0.40150	0.10468	3.83552	0.0	1.00000
0.90000	12.00000	0.47800	0.13960	3.42418	0.0	1.00000
0.90000	14.00000	0.55300	0.18219	3.03534	0.0	1.00000
0.90000	16.00000	0.62800	0.23215	2.70499	0.0	1.00000
0.90000	18.00000	0.69400	2.80217	0.24766	0.0	1.00000
0.90000	20.00000	0.76000	0.34158	2.22497	0.0	1.00000

Table F-2: 040a Aerodynamic Characteristics, Speed Brake = 0%
Landing Gear Extended

MACH	ALPHA	CL	CD	L/D	S.B (%)	L.G.
0.30000	0.0	0.00375	0.09630	0.03894	25.00000	1.00000
0.30000	2.00000	0.06287	0.02736	2.29768	25.00000	1.00000
0.30000	4.00000	0.12200	0.02890	4.22125	25.00000	1.00000
0.30000	6.00000	0.18475	0.03391	5.44793	25.00000	1.00000
0.30000	8.00000	0.24750	0.04116	6.01299	25.00000	1.00000
0.30000	10.00000	0.31000	0.04963	6.24649	25.00000	1.00000
0.30000	12.00000	0.37250	0.06012	6.19624	25.00000	1.00000
0.30000	14.00000	0.43687	0.07343	5.94978	25.00000	1.00000
0.30000	16.00000	0.50125	0.09190	5.45450	25.00000	1.00000
0.30000	18.00000	0.56325	0.11828	4.76213	25.00000	1.00000
0.30000	20.00000	0.62525	0.16934	3.69232	25.00000	1.00000
0.50000	0.0	-0.00325	0.04074	-0.07977	25.00000	1.00000
0.50000	2.00000	0.06612	0.02971	2.22540	25.00000	1.00000
0.50000	4.00000	0.13550	0.03125	4.33607	25.00000	1.00000
0.50000	6.00000	0.20375	0.03682	5.53349	25.00000	1.00000
0.50000	8.00000	0.27200	0.04500	6.04415	25.00000	1.00000
0.50000	10.00000	0.33850	0.05522	6.12985	25.00000	1.00000
0.50000	12.00000	0.40500	0.07080	5.72053	25.00000	1.00000
0.50000	14.00000	0.47312	0.09166	5.16186	25.00000	1.00000
0.50000	16.00000	0.54125	0.12047	4.49285	25.00000	1.00000
0.50000	18.00000	0.60725	0.15926	3.81268	25.00000	1.00000
0.50000	20.00000	0.67325	0.21922	3.07107	25.00000	1.00000
0.70000	0.0	-0.00242	0.03279	-0.07371	25.00000	1.00000
0.70000	2.00000	0.07192	0.03310	2.17284	25.00000	1.00000
0.70000	4.00000	0.14625	0.03521	4.15323	25.00000	1.00000
0.70000	6.00000	0.21892	0.04268	5.12955	25.00000	1.00000
0.70000	8.00000	0.29158	0.05417	5.38311	25.00000	1.00000
0.70000	10.00000	0.36275	0.06884	5.26939	25.00000	1.00000
0.70000	12.00000	0.43392	0.09139	4.74809	25.00000	1.00000
0.70000	14.00000	0.50558	0.12196	4.14543	25.00000	1.00000
0.70000	16.00000	0.57725	0.16328	3.53534	25.00000	1.00000
0.70000	18.00000	0.64458	0.27786	2.31981	25.00000	1.00000
0.70000	20.00000	0.71192	0.27860	2.55535	25.00000	1.00000
0.90000	0.0	0.00625	0.03963	0.15770	25.00000	1.00000
0.90000	2.00000	0.08025	0.03773	2.12703	25.00000	1.00000
0.90000	4.00000	0.15425	0.04234	3.64298	25.00000	1.00000
0.90000	6.00000	0.23025	0.05512	4.17698	25.00000	1.00000
0.90000	8.00000	0.30625	0.07773	3.93999	25.00000	1.00000
0.90000	10.00000	0.38275	0.10718	3.57112	25.00000	1.00000
0.90000	12.00000	0.45925	0.14210	3.23198	25.00000	1.00000
0.90000	14.00000	0.53425	0.18469	2.89273	25.00000	1.00000
0.90000	16.00000	0.60925	0.23466	2.59627	25.00000	1.00000
0.90000	18.00000	0.67525	2.80467	0.24076	25.00000	1.00000
0.90000	20.00000	0.74125	0.34408	2.15431	25.00000	1.00000

Table F-3: 040a Aerodynamic Characteristics, Speed Brake = 25%
Landing Gear Extended

MACH	ALPHA	CL	CD	L/D	S.B(%)	L.G.
0.30000	0.0	-0.01500	0.09880	-0.15182	50.00000	1.00000
0.30000	2.00000	0.04412	0.02986	1.47750	50.00000	1.00000
0.30000	4.00000	0.10325	0.03140	3.28407	50.00000	1.00000
0.30000	6.00000	0.16500	0.03641	4.55894	50.00000	1.00000
0.30000	8.00000	0.22875	0.04365	5.23924	50.00000	1.00000
0.30000	10.00000	0.29125	0.05213	5.58722	50.00000	1.00000
0.30000	12.00000	0.35375	0.06242	5.62942	50.00000	1.00000
0.30000	14.00000	0.41812	0.07593	5.50693	50.00000	1.00000
0.30000	16.00000	0.48250	0.09440	5.11141	50.00000	1.00000
0.30000	18.00000	0.54450	0.12078	4.50831	50.00000	1.00000
0.30000	20.00000	0.60650	0.17184	3.52949	50.00000	1.00000
0.50000	0.0	-0.02200	0.04324	-0.50874	50.00000	1.00000
0.50000	2.00000	0.04737	0.03221	1.47054	50.00000	1.00000
0.50000	4.00000	0.11675	0.03375	3.45931	50.00000	1.00000
0.50000	6.00000	0.18500	0.03932	4.70483	50.00000	1.00000
0.50000	8.00000	0.25325	0.04750	5.33134	50.00000	1.00000
0.50000	10.00000	0.31975	0.05772	5.53952	50.00000	1.00000
0.50000	12.00000	0.38625	0.07330	5.26951	50.00000	1.00000
0.50000	14.00000	0.45437	0.09416	4.82557	50.00000	1.00000
0.50000	16.00000	0.52250	0.12297	4.24903	50.00000	1.00000
0.50000	18.00000	0.58850	0.16176	3.63805	50.00000	1.00000
0.50000	20.00000	0.65450	0.22172	2.95189	50.00000	1.00000
0.70000	0.0	-0.02117	0.03529	-0.59985	50.00000	1.00000
0.70000	2.00000	0.05317	0.03560	1.49353	50.00000	1.00000
0.70000	4.00000	0.12750	0.03771	3.38075	50.00000	1.00000
0.70000	6.00000	0.20017	0.04518	4.43067	50.00000	1.00000
0.70000	8.00000	0.27283	0.05667	4.81473	50.00000	1.00000
0.70000	10.00000	0.34400	0.07134	4.82192	50.00000	1.00000
0.70000	12.00000	0.41517	0.09389	4.42195	50.00000	1.00000
0.70000	14.00000	0.48683	0.12446	3.91151	50.00000	1.00000
0.70000	16.00000	0.55850	0.16578	3.36893	50.00000	1.00000
0.70000	18.00000	0.62583	0.28036	2.23224	50.00000	1.00000
0.70000	20.00000	0.69317	0.28110	2.46592	50.00000	1.00000
0.90000	0.0	-0.01250	0.04213	-0.29668	50.00000	1.00000
0.90000	2.00000	0.06150	0.04023	1.52876	50.00000	1.00000
0.90000	4.00000	0.13550	0.04484	3.02174	50.00000	1.00000
0.90000	6.00000	0.21150	0.05762	3.67037	50.00000	1.00000
0.90000	8.00000	0.28750	0.08023	3.58351	50.00000	1.00000
0.90000	10.00000	0.36400	0.10968	3.31877	50.00000	1.00000
0.90000	12.00000	0.44050	0.14460	3.04643	50.00000	1.00000
0.90000	14.00000	0.51550	0.18719	2.75393	50.00000	1.00000
0.90000	16.00000	0.59050	0.23716	2.48984	50.00000	1.00000
0.90000	18.00000	0.65650	2.80717	0.23387	50.00000	1.00000
0.90000	20.00000	0.72250	0.34658	2.08467	50.00000	1.00000

Table F-4: 040a Aerodynamic Characteristics, Speed Brake = 50%
Landing Gear Extended

MACH	ALPHA	CL	CD	L/D	S.B(%)	L.G.
0.30000	0.0	-0.03375	0.10130	-0.33317	75.00000	1.00000
0.30000	2.00000	0.02537	0.03236	0.78404	75.00000	1.00000
0.30000	4.00000	0.08450	0.03390	2.49252	75.00000	1.00000
0.30000	6.00000	0.14725	0.03891	3.78418	75.00000	1.00000
0.30000	8.00000	0.21000	0.04616	4.54930	75.00000	1.00000
0.30000	10.00000	0.27250	0.05463	4.98830	75.00000	1.00000
0.30000	12.00000	0.33500	0.06512	5.14658	75.00000	1.00000
0.30000	14.00000	0.39937	0.07843	5.09231	75.00000	1.00000
0.30000	16.00000	0.46375	0.09690	4.78603	75.00000	1.00000
0.30000	18.00000	0.52575	0.12328	4.26479	75.00000	1.00000
0.30000	20.00000	0.58775	0.17434	3.37133	75.00000	1.00000
0.50000	0.0	-0.04075	0.04574	-0.89082	75.00000	1.00000
0.50000	2.00000	0.02862	0.03471	0.82450	75.00000	1.00000
0.50000	4.00000	0.09800	0.03625	2.70349	75.00000	1.00000
0.50000	6.00000	0.16625	0.04182	3.97525	75.00000	1.00000
0.50000	8.00000	0.23450	0.05000	4.68980	75.00000	1.00000
0.50000	10.00000	0.30100	0.06022	4.99821	75.00000	1.00000
0.50000	12.00000	0.36750	0.07580	4.84843	75.00000	1.00000
0.50000	14.00000	0.43562	0.09665	4.50683	75.00000	1.00000
0.50000	16.00000	0.50375	0.12547	4.01493	75.00000	1.00000
0.50000	18.00000	0.56975	0.16426	3.46853	75.00000	1.00000
0.50000	20.00000	0.63575	0.22422	2.83535	75.00000	1.00000
0.70000	0.0	-0.03992	0.03779	-1.05637	75.00000	1.00000
0.70000	2.00000	0.03442	0.03810	0.90337	75.00000	1.00000
0.70000	4.00000	0.10875	0.04021	2.70431	75.00000	1.00000
0.70000	6.00000	0.18142	0.04768	3.80507	75.00000	1.00000
0.70000	8.00000	0.25408	0.05917	4.29439	75.00000	1.00000
0.70000	10.00000	0.32525	0.07384	4.40474	75.00000	1.00000
0.70000	12.00000	0.39642	0.09639	4.11273	75.00000	1.00000
0.70000	14.00000	0.46808	0.12696	3.68681	75.00000	1.00000
0.70000	16.00000	0.53975	0.16828	3.20746	75.00000	1.00000
0.70000	18.00000	0.60708	0.28286	2.14622	75.00000	1.00000
0.70000	20.00000	0.67442	0.28360	2.37807	75.00000	1.00000
0.90000	0.0	-0.03125	0.04463	-0.70015	75.00000	1.00000
0.90000	2.00000	0.04275	0.04273	1.00050	75.00000	1.00000
0.90000	4.00000	0.11675	0.04734	2.46611	75.00000	1.00000
0.90000	6.00000	0.19275	0.06012	3.20590	75.00000	1.00000
0.90000	8.00000	0.26875	0.08273	3.24858	75.00000	1.00000
0.90000	10.00000	0.34525	0.11218	3.07765	75.00000	1.00000
0.90000	12.00000	0.42175	0.14710	2.86719	75.00000	1.00000
0.90000	14.00000	0.49675	0.18969	2.61879	75.00000	1.00000
0.90000	16.00000	0.57175	0.23966	2.38564	75.00000	1.00000
0.90000	18.00000	0.63775	2.80967	0.22698	75.00000	1.00000
0.90000	20.00000	0.70375	0.34908	2.01603	75.00000	1.00000

Table F-5: 040a Aerodynamic Characteristics, Speed Brake = 75% Landing Gear Extended

MACH	ALPHA	CL	CD	L/D	S.B(%)	L.G.
0.30000	0.0	-0.05250	0.10380	-0.50578	100.00000	1.00000
0.30000	2.00000	0.00662	0.03486	0.19002	100.00000	1.00000
0.30000	4.00000	0.06575	0.03640	1.80625	100.00000	1.00000
0.30000	6.00000	0.12850	0.04141	3.10297	100.00000	1.00000
0.30000	8.00000	0.19125	0.04866	3.93026	100.00000	1.00000
0.30000	10.00000	0.25375	0.05713	4.44179	100.00000	1.00000
0.30000	12.00000	0.31625	0.06762	4.67708	100.00000	1.00000
0.30000	14.00000	0.38062	0.08093	4.70351	100.00000	1.00000
0.30000	16.00000	0.44500	0.09940	4.47701	100.00000	1.00000
0.30000	18.00000	0.50700	0.12578	4.03095	100.00000	1.00000
0.30000	20.00000	0.56900	0.17684	3.21764	100.00000	1.00000
0.50000	0.0	-0.05950	0.04824	-1.23330	100.00000	1.00000
0.50000	2.00000	0.00987	0.03721	0.26536	100.00000	1.00000
0.50000	4.00000	0.07925	0.03875	2.04519	100.00000	1.00000
0.50000	6.00000	0.14750	0.04432	3.32797	100.00000	1.00000
0.50000	8.00000	0.21575	0.05250	4.10935	100.00000	1.00000
0.50000	10.00000	0.28225	0.06272	4.50065	100.00000	1.00000
0.50000	12.00000	0.34875	0.07830	4.45415	100.00000	1.00000
0.50000	14.00000	0.41687	0.09916	4.20416	100.00000	1.00000
0.50000	16.00000	0.48500	0.12797	3.78948	100.00000	1.00000
0.50000	18.00000	0.55100	0.16676	3.30410	100.00000	1.00000
0.50000	20.00000	0.61700	0.22672	2.72138	100.00000	1.00000
0.70000	0.0	-0.05867	0.04029	-1.45624	100.00000	1.00000
0.70000	2.00000	0.01567	0.04069	0.38509	100.00000	1.00000
0.70000	4.00000	0.09000	0.04271	2.10706	100.00000	1.00000
0.70000	6.00000	0.16267	0.05018	3.24182	100.00000	1.00000
0.70000	8.00000	0.23533	0.06167	3.81624	100.00000	1.00000
0.70000	10.00000	0.30650	0.07634	4.01483	100.00000	1.00000
0.70000	12.00000	0.37767	0.09889	3.81915	100.00000	1.00000
0.70000	14.00000	0.44933	0.12946	3.47078	100.00000	1.00000
0.70000	16.00000	0.52100	0.17078	3.05071	100.00000	1.00000
0.70000	18.00000	0.58833	0.28536	2.06172	100.00000	1.00000
0.70000	20.00000	0.65567	0.28610	2.29175	100.00000	1.00000
0.90000	0.0	-0.05000	0.04713	-1.06082	100.00000	1.00000
0.90000	2.00000	0.02400	0.04523	0.53064	100.00000	1.00000
0.90000	4.00000	0.09800	0.04984	1.96623	100.00000	1.00000
0.90000	6.00000	0.17400	0.06262	2.77851	100.00000	1.00000
0.90000	8.00000	0.25600	0.08523	2.93529	100.00000	1.00000
0.90000	10.00000	0.32650	0.11468	2.84707	100.00000	1.00000
0.90000	12.00000	0.40300	0.14960	2.69393	100.00000	1.00000
0.90000	14.00000	0.47800	0.19219	2.48716	100.00000	1.00000
0.90000	16.00000	0.55300	0.24216	2.28358	100.00000	1.00000
0.90000	18.00000	0.61900	2.81217	0.22011	100.00000	1.00000
0.90000	20.00000	0.68500	0.35158	1.94836	100.00000	1.00000

Table F-6: 040a Aerodynamic Characteristics, Speed Brake = 100%
Landing Gear Extended

REFERENCES

1. Morth, R., & Widnall, W.S., "Space Guidance Development, Approach and Landing Study Results", Contract Final Report, Intermetrics, March 26, 1971.

2. Sullivan, N., & Cockayne, W.G., "Space Shuttle Automatic Terminal Guidance, Approach and Landing", AIAA Guidance and Control Conference, Santa Barbara, California, August 1970.

3. Elias, A., "New Approach Guidance Concept for Shuttle", 234 STS Memo No. 58-72, Draper Laboratory, Cambridge, Mass., Dec. 4, 1972.

4. Moore, T., "Terminal Area Subsonic Guidance", presented at the Guidance & Control Division Space Shuttle Task Review Meeting, NASA/MSC, April 15, 1971.

5. Griggs, D., Tuntline, R., "Flight Tests With A Pilot Oriented Energy Management System", Presented at NASA/MSC, Houston, Texas, March 20, 1971.

6. Stoner, E.E., "Spiral Descent Terminal Guidance", AIAA Guidance and Control Conference paper 72-834, Stanford, California, Aug. 1972.

7. Osder, S., & Keller, R., "Study of Automatic and Manual Terminal Guidance and Control Systems for Space Shuttle Vehicles", Final Report for NASA/Ames by Sperry Rand, #710225-00-01, Phoenix, Arizona, Dec. 1971.

8. Elson, B.M., "NASA Gets Shuttle 'Landing' Data", Aviation Week & Space Technology, Sept. 25, 1972.

9. Graves, C., "An Analytical Examination of Constant Equivalent Air Speed Gliding Subsonic Flight", MSC Internal Note No. 72 FM-183 NASA/MSC, Houston, Texas, July 18, 1972.

10. Hill, O., "040a Aerodynamics", Informal Communication, NASA/MSC, Houston, Texas, May 11, 1972.

11. Clark, C.M., & Mitchell, R.H., "Internal Measurement Unit Performance Comparison for a Shuttle One-Rev Mission", MSC Internal Note No. 72-FM-172, NASA/MSC, Houston, Texas, July 5, 1972.

12. Morth, R., & Widnall, W.S., "Space Shuttle Landing Navigation Using Precision Distance Measuring Equipment", Intermetrics Final Report for NASA/MSC under Contract NAS9-11593, Cambridge, Mass., Aug. 2, 1971.

13. Boudreuti, R., et al, "Shuttle Program Navigation Systems Characteristics", MSC Internal Note No. 72-FM-190, NASA/MSC Aug. 15, 1972, Houston, Texas.

14. Lear, W.S., "Navigation Errors Using Various Navigation Aids During A Space Shuttle Reentry and Landing", MSC Internal Note No. 72-FM-213, NASA/MSC, Houston, Texas, Sept. 12, 1972.

15. Vaughn, N.W., "Natural Environment Criteria For The NASA Space Shuttle Program", NASA TMX-53973, Marshall Space Flight Center, Feb. 9, 1970.

16. Carlson, N.A., "A Fast Triangular Formulation of the Square Root Filter", Intermetrics Report to be published, September 1972.

U.S. DEPARTMENT OF COMMERCE
Technology Administration
National Technical Information Service
Springfield, VA 22161 (703) 487-4650